Università degli Studi di Pavia

Facoltà di Ingegneria

Dipartimento di Ingegneria Civile e Architettura

Finite element analysis of Transcatheter Aortic Valve Implantation: a clinical case

Analisi agli elementi finiti di Impianto Transcatetere di Valvola Aortica: un caso clinico

Supervisor: Professor
SIMONE MORGANTI

Author:
ALICE FINOTELLO
UIN **420535**

Academic year 2014/2015

"Graduation is only a concept. In real life every day you graduate.
Graduation is a process that goes on until the last day of your life.
If you can grasp that, you'll make a difference."
A.P.

Acknowledgments

At the end of my thesis I would like to thank all those people who made this thesis possible and an unforgettable experience for me.
First of all, I would like to express my gratitude to my supervisor Professor Simone Morganti for the continuous support of my research, for his patience, motivation, enthusiasm and knowledge. I want to thank Prof. Ferdinando Auricchio for supervising my activities. I would also like to acknowledge Dott. Michele Conti, Dott. Anna Ferrara and Dott. Mauro Ferraro for their interest in my work and for the help they give me.
Many thanks to Valentina, Rodrigo, Gianluca, Marco, Xi and Alberto: working in the "Lampedusa Laboratory" has been an exiting experience. A special thanks to Margherita: I am indebted to you!
Many friends have helped me stay sane through these difficult years. Their support and care helped me overcome setbacks and stay focused on my graduate study. I greatly value their friendship and I deeply appreciate their belief in me.
Finally, none of this would have been possible without the support of my family. To you I dedicate this thesis.

Pavia, October 2015

Contents

List of Tables

List of Figures

Abstract

Transcatheter aortic valve implantation (TAVI) has recently become the new standard medical treatment for patients affected by severe aortic stenosis who are not eligible for open heart surgery. Different factors such as amount and location of calcium deposits, valve positioning, valve type, and prosthesis size could severely impact the post-operative performance. Given such considerations, computer-based simulations may represent a valid approach to predict surgical outcomes and assist clinicians in the decision making improving the outcome of the intervention. This thesis concerns the implementation and validation of a systematic approach to perform patient-specific finite element analyses with the aim of virtually (and realistically) reproduce the TAVI procedure and predict post-intervention outcomes. In particular, in the present work we investigated a 76 year-old patient with severe symptomatic aortic stenosis whose valvular geometry was extracted from pre-operative and post-operative CT-scans performed at ICSA Sant'Ambrogio Clinical Institute, Milano. The finite element program Abaqus was used to perform explixit analysis to simulate the deployments of a self-expanding Nitinol prosthesis in the patient-specific model of the aortic root. Calcifications have accurately been introduced in the model to evaluate their impact on the stent expansion and, consequently, on post-operative performance. The obtained simulation results have been compared with post-operative CT data to validate the computational procedure. Sensitivity analyses have also been performed to evaluate the impact of finite element mesh size and aortic wall material properties on simulation results. We conclude that finite element analysis could be a valid method to investigate several aspects of TAVI procedures. Although limited to only one patient, this study represents a further step towards the use of realistic computer-based simulations for virtual planning of TAVI procedures.

Sommario

La tecnica TAVI (Trascatheter Aortic Valve Implantation) è diventata negli ultimi anni il trattamento medico standard per la cura di quei pazienti affetti da stenosi aortica che non sono eligibili per l'intervento chirurgico tradizionale. Il successo dell'intervento può essere fortemente influenzato da differenti fattori quali la presenza di calcificazioni, sia in termini di posizione che di quantità, la posizione dell'impianto, la scelta della tipologia di protesi e la dimensione ottimale della valvola. Alla luce di queste considerazioni, le simulazioni al computer possono rappresentare un valido approccio per predire tutti questi effetti e guidare il chirurgo nel compiere scelte ottimali, aumentando in tal modo le probabilità di riuscita dell'intervento. Questo lavoro di tesi riguarda l'implementazione e la validazione di un approccio sistematico per effettuare analisi agli elementi finiti specifiche per paziente con l'obiettivo di riprodurre virtualmente (e in modo realistico) la procedura TAVI e di predire in questo modo i risultati post-intervento. In particolare, nel presente studio ci siamo focalizzati su un paziente di 76 anni, affetto da stenosi aortica severa sintomatica, la cui geometria valvolare è stata estratta da scansioni TAC pre-operatorie e post-operatorie effettuate presso l'Instituto Clinico Sant'Ambrogio di Milano. Abaqus è il programma agli elementi finiti usato per effettuare analisi esplicite al fine di simulare l'impianto della protesi di Nitinol auto-espandibile all'interno del modello di radice aortica paziente specifico. Le calcificazioni sono state introdotte in modo accurato nel modello al fine di valutare il loro impatto sull'espansione dello stent e, di conseguenza, sulla performance post-operatoria. Per validare la procedura computazionale i risultati ottenuti dalla simulazione sono stati comparati con i dati della TAC post-operatoria. Analisi di sensitività sono state effettuate per valutare l'impatto del numero degli elementi della mesh e delle proprietà del materiale costituente la parete aortica sui risultati della simulazione. Possiamo concludere dicendo che l'analisi agli elementi finiti può essere un valido metodo per investigare diversi aspetti delle procedure TAVI. Sebbene limitato ad un solo paziente, questo studio rappresenta un ulteriore passo avanti verso l'utilizzo di simulazioni realistiche al computer che consentano di pianificare in modo virtuale le procedure TAVI.

Chapter 1

Overview

In the first part of this chapter, an introduction to the problem under investigation is given. Some literature data regarding the transcatheter aortic valve implantation are reported. In particular the focus is on the role that numerical simulations have in the study of the diseases affecting the aortic valve. In the second part, the collaboration with the ICSA Sant'Ambrogio Clinical Institute is introduced. The aim of this thesis work and the organization of the dissertation are reported in the last sections.

1.1 Background

Aortic Stenosis (AS) is the most common form of valvular heart disease in Europe and America, constituting approximately 40% of all valvular lesions [Nkomo et al., 2006]. It is a degenerative disease of the aortic valve, compromising its function of regulating blood flow from the left ventricle to the aorta. This pathology has profound effects on morbidity and mortality of patients, representing a significant clinical problem.
Conventional surgery is nowadays considered the gold standard treatment for heart valve replacement [Chiam and Ruiz, 2009]. In spite of that, in clinical practice, nearly 30% of all elderly patients with severe AS are not suitable candidates for such an invasive procedure, because of their advanced age or to the possible presence of left ventricular dysfunction or multiple coexisting conditions [Iung et al., 2005]. Since these patients are at high surgical risk, a less invasive treatment may be a worthwhile alternative.
Transcatheter aortic-valve implantation (TAVI) represents a minimally-invasive procedure, where the pathologically altered valve is not replaced surgically but crushed against the aortic wall by a self-expandable or balloon-expandable stent containing a prosthetic aortic valve. Compared to standard aortic valve replacement interventions, the TAVI technique limits surgical access to small incisions causing minimal tissue trauma and can be performed on the beating heart without cardiopulmonary bypass support [Walther et al., 2009].
It is estimated that, since the first TAVI was performed in 2002 [Cribier et al., 2002], more than 100 000 patients worldwide have benefited from this revolutionary procedure [Bax et al., 2014]. Despite the clinical success, there are still many complications associated with TAVI, e.g., post-operative paravalvular leakages and aortic root rupture. Typically these postoperative complications are related to the mutual interaction between the device and the native aortic root. Moreover, they are hard to predict due to the variability in the geometry of

the aortic root as well as in the distribution of calcific plaques. Given such considerations, patient-specific computational simulations, based on pre-operative imaging, may help to obtain predictive information about the behavior of the device during transcatheter delivery in order to improve the success of percutaneous valve implantation.
The earliest 3D finite element aortic valve (FE) models date back to the early 1990s when Huang et al. [1990] and Black et al. [1990] investigated the stress distribution, respectively, on a bileaflet and a trileaflet tissue valve with non-linear isotropic material properties. Grande et al. [1998] created a 3D FE model of the aortic valve in order to assess the effect of the valve root asymmetry on the overall functional and stress state. Hereafter, they extended their model to study the effect of aortic root dilation on valve competence.
Later computational analyses have been performed to evaluate the interactions between aortic root and TAVI procedure from an engineering perspective. In the last decades an increase of computer-based simulations concerning TAVI was observed. To the author's knowledge, the first study regarding finite element TAVI simulation was made by Dwyer et al. [2009] only seven years later the first surgical implantation was performed. Sun et al. [2010] conducted a finite element analysis of the prosthetic valve deformation applying a diastolic pressure to the TAV leaflets and reporting the axial force. In the same year, Capelli et al. [2010] and Schievano et al. [2010] proposed a finite element guideline to provide information and help clinicians by focusing on the percutaneous pulmonary valve implantation. In a more recent study [Capelli et al., 2012], the same research group investigated the deployment of the SAPIEN device (Edwards Lifesciences, Irvine, California) within patient specific aortic root models of five patients, four of which with failed bioprosthetic aortic valves. In addition, predictions of TAVI by means of mechanical simulations have been investigated by Russ et al. [2013] and Wang et al. [2012].
Marom et al. [2012], Sturla et al. [2013] and Sun et al. [2014] focused on fluid structure interactions (FSI) simulations and explained the benefit of using these simulations compared to finite element models. Moreover Tan et al. investigated the effects of TAVI on flow patterns in the thoracic aorta using computational fluid dynamics analyses.
Auricchio et al. and Morganti et al. have proposed a patient-specific finite element simulation of TAVI procedure focusing on the Edwards SAPIEN device. However, to our knowledge, little has been done about the CoreValve bioprosthesis (Medtronic Inc., Minneapolis, MN, USA) [Russ et al., 2014, Gessat et al., 2013]. Starting from [Morganti et al., 2014] the goal of the thesis is to properly define an approach that allows the simulation of the CoreValve self-deployment into a patient-specific aortic root using finite element analysis.

1.2 Aim of the thesis work

This work has been developed within the Compmech -Computational Mechanics & Advanced Materials- Research Group, Department of Civil Engineering and Architecture, Università degli studi of Pavia.
The main goal of this thesis work is to define the set-up of simulation strategy for the CoreValve device able to predict the mechanical behavior and the interactions between the device and the patient-specific aortic root and help surgeons evaluate complicated, high-risk cases as well as improve the success of percutaneous valve implantation. In particular, starting from medical image elaboration, a patient-specific model of the aortic valve is created: aortic root, native

leaflets and calcifications are accurately included into the model. Moreover, the CoreValve stent is modeled. The surgical intervention is then simulated by means of the finite element method that discretizes the geometry into a finite number of elements. Loads and boundary conditions, soft tissues and device material properties need to be accurately characterized and calibrate, depending the accuracy of results of the finite element model. A validation procedure is required to ascertain the credibility of the proposed simulation framework: obtained simulation results have been compared with post-operative CT data.
A successful program requires close collaboration between cardiac surgeons, radiologists and engineers where computational models offer clinical input to help steering the developments into a direction where they may solve real clinical problems.

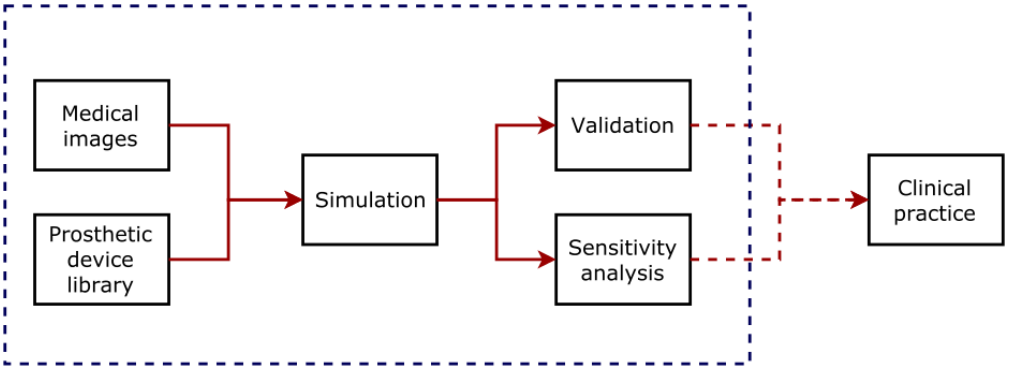

Figure 1.1: Work-flow of the computational framework to evaluate TAVI post-procedural outcomes. Starting from medical images, a patient-specific model of the aortic valve is created. The percutaneous device is modeled and inserted into a library for future uses. Surgical intervention is simulated by means of the finite element method. Validation of the method and sensitivity analysis are performed to ensure the validity of the proposed simulation framework. With the present study a further step toward the use in the clinical practice of realistic computer-based simulations for virtual planning of TAVI procedures is done. An interdisciplinary team where clinicians and engineers will work closely together integrating these simulation technologies to increase the reliability of clinical decisions is strongly demanded.

1.3 Collaboration with ICSA Sant'Ambrogio Clinical Institute

This thesis work is done in close collaboration with the ICSA Sant'Ambrogio Clinical Institute, located in Milano. Periodically meeting to openly discuss clinical needs, progresses and problems encountered are organized.
"We Were Among the First in Italy to Perform Carotid Angioplasty and to Implement Transcatheter Aortic Valve Replacement and Mitraclip Procedures" are the words of the Professor Francesco Bedogni, head of the Cardiothoracic Department and physician responsible for this collaboration [Ozkan, 2013]. Effectively the ICSA started its TAVI programme in 2008. Since then, more than 450 cases have been performed, resulting in one of the first centers in Italy.

The validation of the simulation framework involves the simulation of TAVI cases prospectively and the comparison between in-silico results and the actual intervention outcomes that can be extracted from post-operative Computed Tomography (CT) scans. CT requires a special iodinated contrast dye to be delivered into the body before the test starts to help the visualization of vascular structures, but contrast agents can be harmful due to impaired renal function. It is clear that not all patient types can be included in this work but that a focus is required on patients with no renal impairment. In particular, this thesis focuses on the case of a 76 year-old man who underwent TAVI procedure, referred to the ICSA center for severe aortic stenosis. Clinical data, such as intra-operative angiographic images, CT scans, and angiographic data have been provided. Therefore, even though the post-operative CT is not usually included in the routine protocol of TAVI, CT scan has been also performed after the surgical intervention.

1.4 Organization of the dissertation

This dissertation is divided into six main chapters where the first one is the introduction and the last one is the conclusion. In the following, a brief overview regarding the topics treated for each Chapter is presented.

Chapter 2: Background

In this chapter key concepts regarding the physiology of the heart, the background of TAVI technique, including the procedures and types of valves, are introduced together with the main imaging techniques and image processing software. Subsequently, the core idea of the finite element discretization method as well as a general description of the most relevant features of the software Abaqus CAE ®(Dassault Systemes, Providence, RI, USA) are presented.

Chapter 3: Simulation strategy

This chapter concerns the implementation of a finite element analysis to accurately reproduce the TAVI procedure. First of all, a patient specific aortic root model is constructed. Native leaflets are modeled starting from the patient specific valve anatomy and calcifications are included. The CoreValve stent-frame is designed and the crimping procedure precedes the stent deployment into the aortic valve geometry. At the end, simulation results are presented. In this context, the influence of stent positioning on the actual deployment and the final simulation is investigated. The influence of annular calcifications located close to annulus is also studied.

Chapter 4: Validation of the patient specific finite element analysis

This chapter describes in detail the validation approach. The attempt to validate the proposed finite element simulation method using the post-operative CT data is discussed. Different implantation sites are considered and the simulated stent shapes are compared to the morphology assumed by the implanted stent. Intra-operative angiographic images are then analyzed to get information about the real implantation and compared with the position achieved by the simulated device in the best configuration.

Chapter 5: Sensitivity analysis: mesh size and material model

In this chapter a sensitivity study referring to the aortic root is performed to assess the reliability of the different results obtained by finite elements modeling since they could severely impact on the accuracy of the characterization. Mesh convergence studies allow to reach a balance between accuracy and computational time. Moreover, an analysis based on a hyperelastic material model for the soft tissue of the aortic root is proposed to assess if simulation outcomes may be relate to the material properties.

Chapter 2

Introduction

In this chapter, the heart, its components and their related pathologies are presented. The TAVI technique is introduced as a serious alternative to open-heart surgery: aims, implantation procedure and types of bioprosthetic valves are debated. Moreover, an outlook of the main techniques for medical imaging and the main software used in literature to work them is provided.

2.1 The Heart and the Aortic Valve

The heart is the vital part of the cardiovascular system and provides continuous blood circulation to the body. It is composed of two receiving chambers, the right and the left atria that receive returning blood, and two main pumping chambers, the right and the left ventricles that have thick muscular walls that cyclically contract and relax to create pressure gradients to pump blood throughout the circulatory system. Starting from the left ventricle, which is the largest chamber of the heart, the oxygen-rich blood is pumped through the aortic valve into the aorta which supplies oxygenated blood to the organ systems of the body. Deoxygenated blood is then returned through veins, emptied into the right atrium, and then pumped through the tricuspid valve into the right ventricle. Subsequently, it enters through the pulmonary valve into the pulmonary circuit. Once the blood is in the pulmonary circuit, it becomes oxygenated as it passes the alveoli of the lungs and returns to the left atrium. Oxygenated blood from the left atrium is pumped through the mitral valve into the left ventricle to complete the circuit. Figure 2.1 provides visual information about the function of heart and heart valves.
A heart beat occurs when the heart muscle contracts in a single rhythmic motion, starting at the atria and finishing with the contraction and relaxation of the ventricles. This motion occurs during the first 40% of the cardiac cycle with the heart at rest during the remaining time. Systole describes the phase of the cardiac cycle when the heart is in contraction, and diastole occurs when the heart is at rest. All four heart valves open and close during each heart beat approximately 80 million times a year, but the aortic one is subjected to the highest pressure of the circulatory system. Because of this, the aortic valve is often the first one to deteriorate and develop diseases with age.

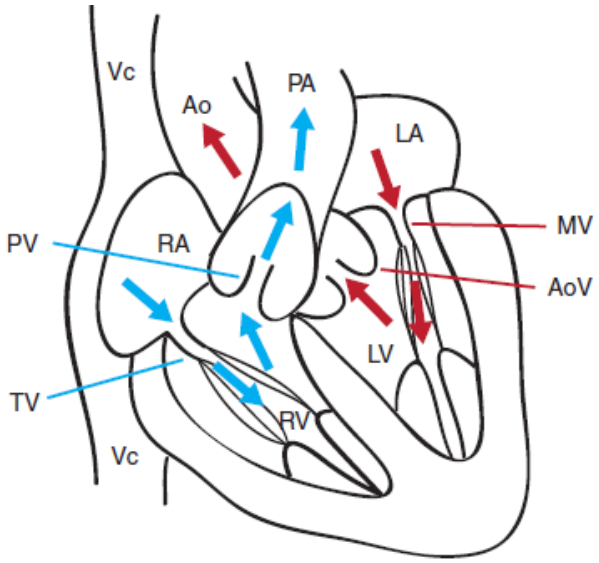

Figure 2.1: Heart valve structure and function. Oxygen-depleted blood (blue) enters the heart from the vena cava (Vc) through the right atrium (RA) and transits via the tricuspid valve (TV) into the right ventricle (RV). From there, it passes through the pulmonary valve (PV) and reaches the lungs via the pulmonary artery (PA). The oxygenated blood from the lungs (red) enters the left atrium (LA) and empties into the left ventricle (LV) by passing through the mitral valve (MV). From the LV, the blood is pumped through the aortic valve (AoV) to the aorta (Ao), and from there it distributes to the rest of the body.

2.2 Aortic valve anatomy and physiology

The aortic valve consists of three semi-lunar leaflets (that is why it is often called tricuspid) that are attached to a ring of fibrous tissue called annulus. The annulus provides support and maintains the proper shape of the valve. This trileaflet structure opens during cardiac systole and closes during diastole. The aortic leaflets are different in size and are approximately cylindrical in shape when closed [Gould et al., 1976]. The root contains sinuses, one behind each leaflet. Two out of three sinuses serve as origin of the coronary arteries. The leaflets are named from the coronary artery that originates in its adjacent sinus. In fact, they are designated as the right-, left-, and non-coronary leaflets. These valvular sheets are connected to the aortic wall by the semilunar attachment lines and the commissures which are formed by two portions of attachment lines of adjacent leaflets running side by side. Between the commissures the leaflets contain a free edge which can seal the leaflets together. In Figure 2.2 the anatomical position of the valve and all its components are depicted.
During the valve loading, adjacent leaflets come in contact with each other over the coaptation area and create a seal against back-flow from the aorta into the left ventricle. The aortic leaflets are pliable and thin in young people but tend to thicken with age, especially at the leaflet free edge.

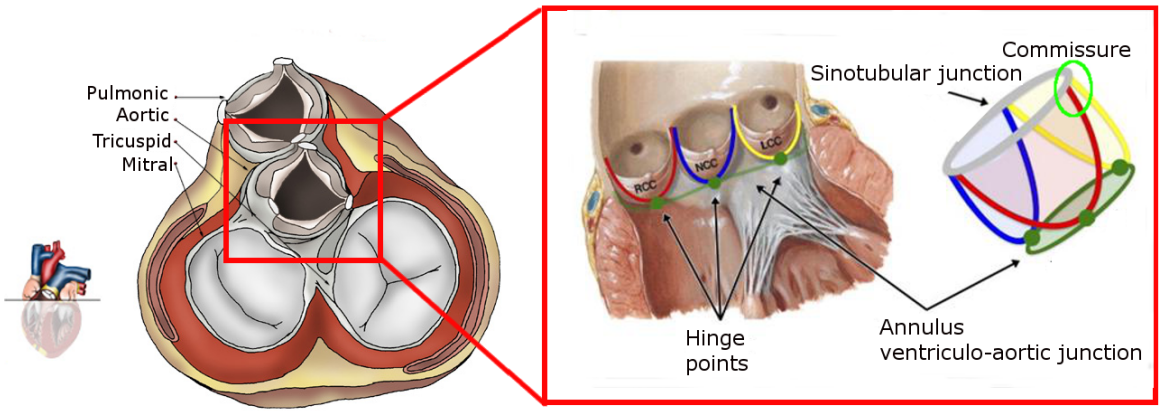

Figure 2.2: Position of the aortic valve in the heart and its anatomy. The aortic annulus (or ventriculo-aortic junction) accounts for the tightest part of the aortic root and is defined as a virtual ring (green line) with three anatomical anchor points at the nadir (green points) of each of the attachments of the three aortic leaflets. Grey-line refers to the sinotubular junction while green circle highlights the commissure. The three cusps (or sinuses) are differently colored: LCC = left coronary cusp (yellow), NCC = noncoronary cusp (blu), RCC = right coronary cusp (red.

2.3 Aortic valve stenosis

Aortic stenosis (AS) is the most common form of valvular heart disease in developed countries, affecting 2% to 4% of adults older than 65 years in the United States. It is also found that the AS constitutes 43% of all valve diseases in Europe with a prevalence of 4.6% in adults older than 75 years of age.
Under normal conditions the aortic valve allows blood to flow forwards out of the heart and prevents back flow. In case of AS, the aortic valve is narrowed thus the valve is unable to open properly (see Figure 2.3). This means that the blood cannot flow effortlessly out of the heart. This puts a strain on the heart, as it must work harder and, over the time, the heart muscle in the left ventricle walls may become thicker and dilate to support this extra load.
Without any intervention, the increased pressure on the left ventricle results in symptoms of congestive cardiac failure increasing the risk of sudden death.

The most common causes of the valvular AS include:

- Degeneration and calcification: the aortic valve leaflets undergo an active disease process, with lipid deposition, inflammation, and osteo-calcific changes. This form of aortic stenosis progresses slowly over 10 to 15 years in patients between 70 and 90 years.
- Congenital aortic stenosis: bicuspid valve is an example of congenital aortic diseases. In this particular kind of stenosis the aortic valve has only two leaflets instead of three.

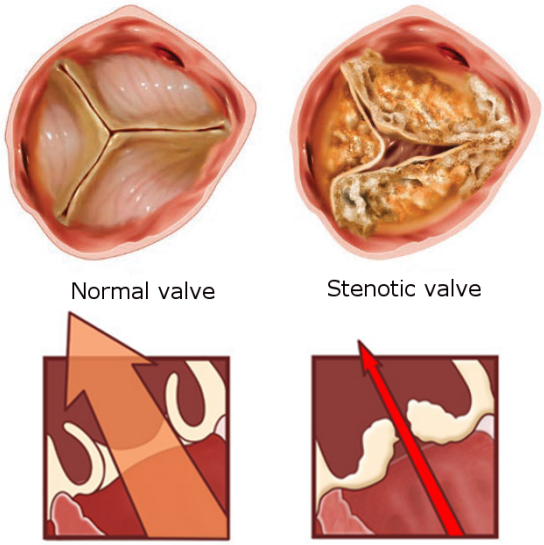

Figure 2.3: Aortic valves can become thickened and calcified over time inhibiting their ability to open properly. That narrow opening will make the heart struggle to push blood flow through it.

About 10% of bicuspid valves become significantly narrowed, resulting in symptoms and heart problems of AS.

- Rheumatic heart disease: it is less common in the developed countries. It can occur in people who have, or have had, strep throat and results in rigid stenotic or steno-incompetent orifice.

The classic triad of symptoms in patients with AS comprises chest pain, heart failure and syncope. Patients with symptomatic AS can benefit from valve replacement; however, the management of that patients with asymptomatic severe AS is more controversial.

2.4 Conventional heart valve replacement

When stenotic heart valves are not repairable, due to extensive calcification, infection, or congenital malformation, surgical valve replacement with heart valve prosthesis is required. Standard valvular heart surgery traditionally requires open cardiac surgery. During this procedure the breastbone is divided, the heart is stopped, and blood is sent through a heart-lung machine. In Figure 2.4a an illustration of the operation is given. The stenotic valve is then removed and replaced with an artificial valve.
In Figure 2.4b the two kinds of prostheses that can be used for replacement are shown. Mechanical valves are usually made of materials such as plastic, pyrolite carbon, or metal with the sewing ring (which is like the annulus of the native valve) from various fabrics. Since the mid-1980s, mechanical bi-leaflet valves are still the most frequently implanted valves to treat aortic valve pathologies. An example is given by the St. Jude Medical valve. These devices are

strong, and they last a long time. Since blood tends to stick to mechanical valves and create blood clots, patients with these implanted valves need to take anticoagulants for the rest of their life. Mechanical valves are frequently favored in younger patients due to their better durability. However, in the last years an increasing trend to a greater usage of bioprosthetic valves can be observed, even in individuals younger than 65 years.
Bioprosthetic valves are made of biological tissues derived from animals (these valves are named xenografts) for example pig tissue, cow tissue pericardial or pericardial tissue from other species. They may also have some artificial parts to provide additional support and to allow the valve to be sewn in place. There are alternatives to animal tissue valves: in some cases, a human aortic valve can be implanted; these are called homografts. Homograft valves are donated by patients and recovered after the patient expires. On one hand the advantage of biological valves is that they do not require formal anticoagulation; on the other hand, the disadvantage is that they generally wear out after 12-15 years and another operation is required to replace the worn out valve.
Another procedure for aortic valve replacement is the Ross procedure (or pulmonary autograft). This procedure involves the replacement of the patient diseased aortic valve with its pulmonary valve. A pulmonary homograft or a valvular prosthesis are then used to replace the patient's own pulmonary valve.

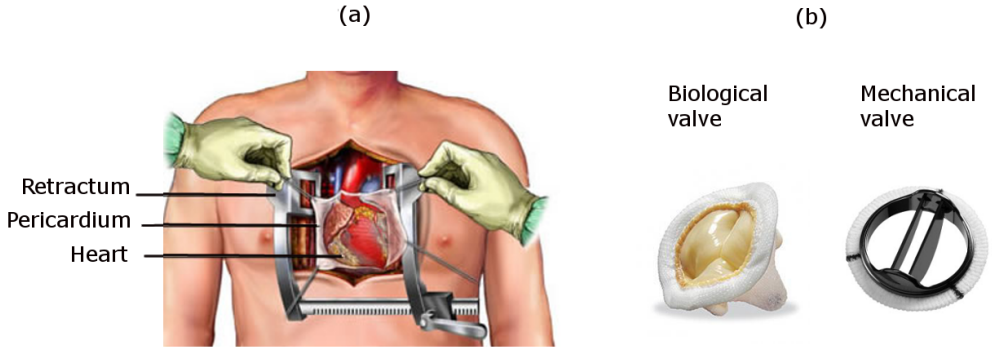

Figure 2.4: Valve replacement through open-heart-surgery (a) : an incision is made into the chest over the sternum and heart, sternum and pericardial sac are opened exposing the heart. The old diseased valve is excised and the new prosthetic valve (b) (biological or mechanical) is seated into the vessel.

During or post the aortic valve replacement there is still a risk of death and complications. Operative mortality for AS patients receiving open-heart operation varies between 2% and 30%. Strokes are a major concern owing to hemorrhage, aortic cannulation at the site, hypoperfusion and emboli from the calcified valve. Other possible complications among these patients include wound infection, pleural effusion, endocarditis (i.e. an infection of the endocardium) and hemolysis due to mechanical valve.

2.5 TAVI

Aortic valve replacement is yet considered the mainstay of treatment for symptomatic AS. However, this kind of surgery entails substantial risks for elderly patients with severe comorbilities. Since these patients are too high risk for surgery, therapeutic options are limited and neither medical therapy nor valvuloplasty could offer survival benefits.
Transcatheter aortic-valve implantation (TAVI) represents a recent minimally invasive procedure developed as a worthwhile alternative for this cohort of patients. A bioprosthetic valve, mounted within a metal stent, is inserted through a catheter and implanted within the diseased native aortic valve forcing the native valve cusps against the annulus wall.
Compared to the standard aortic valve replacement interventions, the TAVI limits the surgical access to small incisions causing minimal tissue trauma. This technique can be performed on the beating heart without cardiopulmonary bypass support; for this reason the recovery time may be reduced and the patient can return to normal activity more quickly.
Since 2002, when the procedure was first performed, a rapid growth in its use throughout the world for the treatment of severe AS in patients who are at high surgical risk has been observed. Recent clinical studies reported 30-day mortality ranges between 5 and 15% and is acceptable when compared to the risk predicted by the logistic EuroSCORE (varying between 20 and 35%) [Vahanian et al., 2012].
As reported in Figure 2.5 the access to the native valve can occur using different approaches:

- **Transfemoral Approach** is the first choice of approach in the vast majority of centers performing TAVI procedures. The delivery system is introduced, making a small incision in the groin, through the femoral artery which leads back to the heart. This strategy makes it possible to avoid the use of general anesthesia.
- **Transapical Approach** has been first reported as an alternative to the transfemoral approach by Lichtenstein et al. [2006]. Such approach requires a small left lateral thoracotomy to obtain access to the left ventricular apex of the heart. Potential advantages of the transapical approach include the avoidance of using large catheters throughout the iliofemoral system, aortic arch, ascending aorta and aortic valve and the possibility of obtaining very accurate transesophageal echocardiographic images for valve positioning, which might lead to a reduction in the amount of contrast agent used during the procedure. The main disadvantage is represented by the need for a thoracotomy.
- **Transsubclavian Approach** is a procedure that can be used as an alternative to the transapical procedure, in case the anatomy of the femoral vessels is inconvenient. Possible problems that can occur are: peripheral vessels too small due to atherosclerosis or too angulated, a previous performed aorto-iliac bypass surgery. In this case access is gained through the subclavian artery below the clavicle.
- **Transaortic Approach** is rarely used. Here the delivery system is advanced through the ascending aorta.

In some cases, before the actual positioning of the stent a balloon valvuloplasty is performed: the aortic valves is reformed with a balloon catheter resulting in an increased opening size of the valve in order to improve the blood flow.

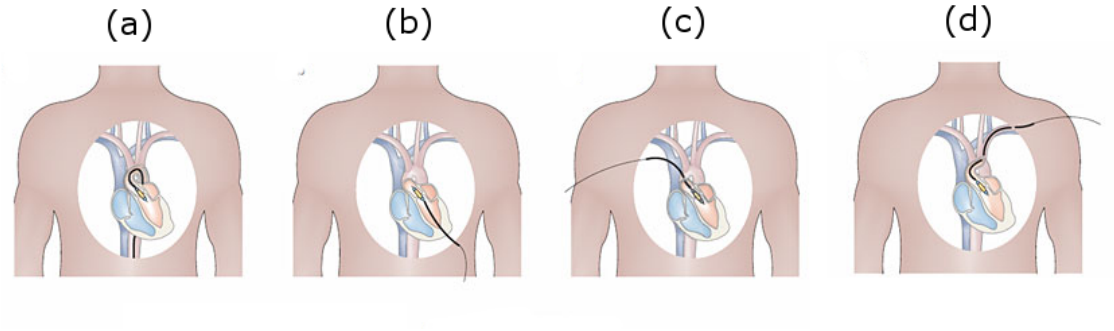

Figure 2.5: Different approaches to valve access. (a) transfemoral TAVI; (b) transapical TAVI; (c) transaortic TAVI and (d) transsubclavian TAVI.

2.6 Bioprosthetic valves for TAVI

The first TAVI procedure was successfully executed almost ten years ago. Currently, there are different prosthesis designs for TAVI whereas the stents housing the bioprosthetic valves can be divided in two main groups depending on the different procedure required for their deployment:

- **Balloon-expandable stents** are manufactured of stainless steel or cobalt chromium and the deployment is due to plastic deformation, inflating a balloon;
- **Self-expandable stents** are created with shape memory alloys, like Nitinol, which allow them to be crimped and constrained to smaller diameter and, when released, to expand themselves to a predetermined size.

The two leading devices for TAVI are the Edwards-SAPIEN (Edwards Lifesciences Inc, Irvine, CA, USA) and the CoreValve ReValving System (Medtronic Inc., Minneapolis, MN, USA) , which use different types of bioprosthetic valves and stent design.

2.6.1 The CoreValve prosthesis

The Medtronic CoreValve ReValving System consists of a self-expanding Nitinol frame, which is implanted in a sutureless fashion using oversizing to anchor the prosthesis at the level of the aortic annulus. The structure has the function of substituting the native aortic valve and is designed to be compatible with the native anatomy of the aortic root. The Nitinol stent frame holds a trileaflet porcine pericardial tissue valve. As depicted in Figure 2.6, the third generation of the CoreValve is available in four sizes (23, 26, 29 and 31 mm) for annulus diameters which ranges from 18 to 29 mm. This device is delivered using an 18 French catheter delivery system, predominantly via transfemoral access.

The non-cylindrical frame design of the device incorporates three regions characterized by different radial force. The lower part, called inflow portion, exerts a high radial force to anchor the prosthesis in the annulus of the native aortic valve and to mitigate paravalvular aortic

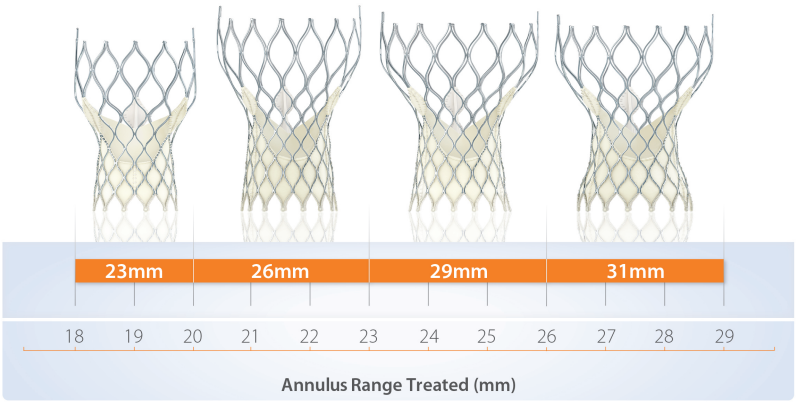

Figure 2.6: Medtronic CoreValve Revalving System in four different sizes covering an aortic annulus diameter from 18 to 29 mm.

regurgitation. The middle part of the CoreValve, named as constrained center, holds the valve leaflets in a supra-annular position to ensure proper valve functioning even if the valve inflow part is non-circular. The concave, hourglass-like shape of the frame avoids the coronary artery ostia and allows unimpeded coronary blood flow. The upper region of the stent, the outflow portion, sits with low radial force in the ascending aorta and ensures an optimal alignment of the prosthesis during the deployment. In Figure 2.7 the different parts of the CoreValve prosthesis are highlighted.

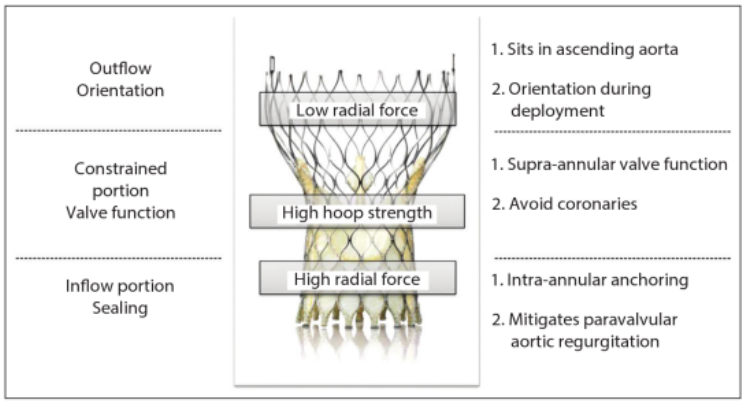

Figure 2.7: Different parts of the CoreValve system.

On February 2015 Medtronic has announced CE mark for the 26mm and 29mm sizes of the CoreValve Evolut R System, a self-expanding valve that advances performance and deliverability during transcatheter aortic valve implantation (TAVI), while providing the option to recapture and reposition the valve during such procedures. At present, also the CoreValve Evolut R 23 mm is available. This new device is not approved for commercial use in the USA, where it is currently undergoing clinical trials.

Implantation procedure

In this section some details of the TAV implantation procedure are provided.
Prior to TAVI intervention the use of multiple modalities of imaging technique is required to define inclusion criteria and assess the cardiac anatomy. During the procedure, two teams worked simultaneously: one team prepares the CoreValve to be ready for the implantation while the second team indulges in obtaining vascular access, in valvuloplasty and finally in the valve deployment. Depending on the individual patient situation, the procedure is carried out under local or general anesthesia. The self expandable Medtronic CoreValve device, thanks to its stent-frame, is mounted ex-vivo onto its delivery catheter on ice-cold water in order to be compressed. The deployment steps include the balloon aortic valvuloplasty to dilate the native valve. The positioning of valve prosthesis is a very crucial issue and it is done under fluoroscopy. The calcifications present on the native aortic valve serve as a guide in defining the level at which the deployment has to be performed. Frequent injections by a pigtail catheter placed in the aortic root are used to determine the position of the valve and the plane of alignment of the aortic annulus. Once the correct position is achieved, the prosthesis is released and can expand on its own anchoring to the damaged valve. In detail, firstly the CoreValve is released, for the first third, from the end of the catheter. At body temperature, it self expands spontaneously to its original size. Then, the stent-frame must be expanded rapidly until the two thirds open, at which point the bioprosthetic valve is fully functional. Doing so, the peripheral circulation is restored.

2.6.2 Other devices

The Sapien valve

The Edwards Sapien valve (see Figure 2.8a) consists of a balloon-expandable stainless steel frame and three bovine pericardium cusps (leaflets) mounted onto a polyethylene terephthalate (PET) skirt.
The current state-of-the-art Edwards SAPIEN XT valve (see Figure 2.8b) utilizes a balloon-expandable cobalt chromium alloy tubular frame within which are sewn leaflets that are constructed from bovine pericardium. The inflow of the frame is covered with fabric to provide an annular seal. For transarterial implantation the device is compressed onto a delivery catheter and introduced into the body by cutting a small opening in the femoral artery. Alternatively a sheath can be placed surgically in the left ventricular apex or ascending aorta. In either case the Sapien valve is balloon-expanded within the diseased native valve displacing the diseased native leaflets. Both valves are available in 23 mm and 26 mm sizes, although more recently, the Sapien XT has been introduced in a 29 mm size.
The Sapien 3 valve is the most recent version of the transcatheter heart valve system.

Newer devices

Nowadays a great number of newer transcatheter valves are available. In general these valves incorporate some peculiar features to reduce the delivery catheter diameter, to improve ease of positioning and sealing, or to facilitate the repositioning or the removal phase. For the most part these next generation valves are constructed of self-expanding Nitinol. Some of

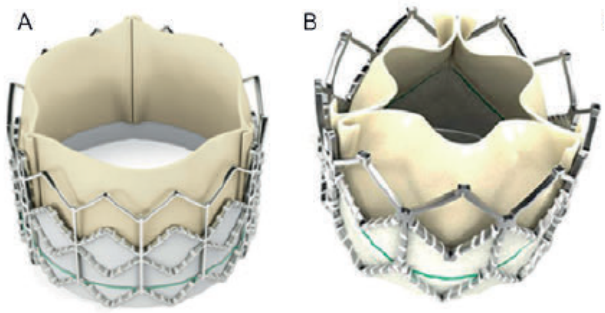

Figure 2.8: The Edwards Sapien (A) and Sapien XT (B) .

them have unique expansion mechanisms: the Lotus valve (Boston Scientific Inc., Natick, Massachusetts) is designed to expand laterally as longitudinal Nitinol wires are retracted, while the Direct Flow valve (Direct Flow Medical Inc., Santa Rosa, California) has a tubular fabric frame, which is inflated with a rapid setting polymerizing agent. The Acurate (Symetis Inc., Ecublens, Switzerland) and the Portico (St. Jude Medical Inc., St. Paul, Minnesota) devices extend from the annulus to the supracoronary aorta to assist in the coaxial alignment and the fixation. The Engager (Medtronic), the JenaClip (JenaValve Inc., Munich, Germany), and the Acurate valves incorporate features that facilitate positioning and anatomical orientation in relation to the native valve commissures and coronaries. Other valves incorporate new sealing mechanisms to reduce paravalvular leakage. In Figure 2.9 an overview of the available devices is presented.

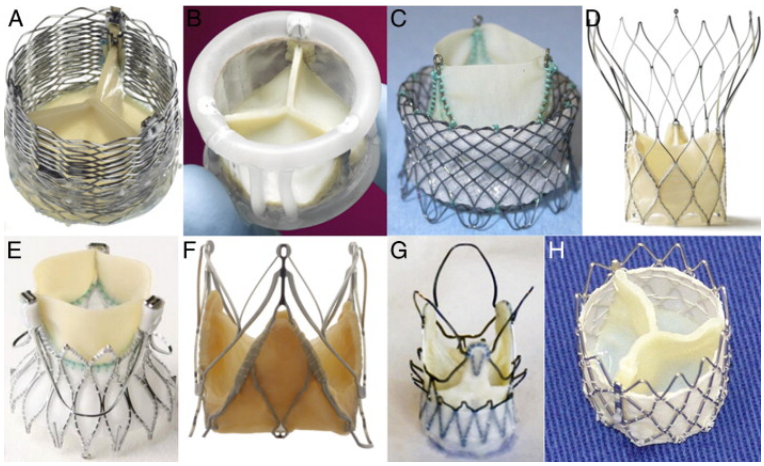

Figure 2.9: Newer devices are nowadays available. (A) Lotus (Boston Scientific Inc., Natick, Massachusetts), (B) Direct Flow (Direct Flow Medical Inc., Santa Rosa, California), (C) HLT (Bracco Inc., Princeton, New Jersey), (D) Portico (St. Jude Medical Inc., St. Paul, Minnesota), (E) Engager (Medtronic Inc., Minneapolis Minnesota), (F) JenaClip (JenaValve Inc., Munich, Germany), (G) Acurate valve (Symetis Inc., Ecublens, Switzerland), and (H) Inovare (Braile Biomedica Inc., São José do Rio Preto, Brazil) valves.

2.7 Diagnostic tools for TAVI procedure

A fundamental characteristic of percutaneous interventions is the lack of direct visualization. Consequently, interventional cardiology is greatly related to and depending on imaging. Especially in TAVI, which is entering the field of traditional valve surgery, the greatest possible amount of information must be obtained before performing the technique. Before the procedure, in fact, the patient need to undergo routine investigations to evaluate whether TAVI is possible and which is the best surgical approach. Echocardiography, Multi Slice Computed Tomography, Magnetic Resonance Imaging and Angiography are the major techniques used to provide a detailed characterization of the vascular and cardiac anatomy and to determine the anatomical suitability for the procedure. The use of these techniques provides invaluable insight to confirm the severity of the aortic stenosis, for patient selection and for the planning of the procedure: imaging assists in the selection of bioprosthesis type, prosthetic sizing and in the decision of the best vascular access. The aortic root has specific anatomic characteristics, which affect device design, selection, and clinical outcome. For example, female sex is associated with smaller annular. The degree of ellipticity as well as a significant mismatch between annular and left ventricular outflow tract dimensions in selected patients deserve careful evaluation.
In addition, some imaging techniques can be used during the operation to guide the implantation, as well as after the procedure to evaluate the positioning and functionality of the implanted prosthesis. In this section the principal imaging techniques and the use of medical images in the clinical practice are described.

2.7.1 Echocardiography

Echocardiography has an established role in the morphological and hemodynamical assessment of the disorders of the aortic root and it is the first imaging modality to help diagnose and evaluate the canditates for TAVI [Nieman et al., 2015]. Echocardiography, also known as cardiac ultrasound, uses standard ultrasound techniques to figure two-dimensional slices of the heart. Ultrasound allows for a dynamic analysis of the heart functionality and for an assessment of aortic stenosis. The contrast in the images is reconstructed from the strength of the reflected waves which are captured by a transducers array. The depth of the reflection is then obtained by timing the arrival of the reflected wave at the probe. For a better visualization of the cardiac valves, trans-esophageal echocardiography (TEE) should be performed if transthoracic echocardiography (TTE) is of insufficient quality. The patient does not feel the sound waves and the entire procedure is painless. The main limitation of echocardiography relates to its intrinsic two-dimensional nature. Two-dimensional echocardiography discloses the morphology of the aortic valve and can often delineate if it is trileaflet or bicuspid. In Figure 2.10 the planimetry of a tricuspid valve is highlighted. This technique also permits the measurement of the aortic annulus and the left ventricular outflow tract. In particular maximum and minimum diameters of the annulus, area, perimeter and ellipticity index are parameters of the outmost importance for the success of the TAVI, because the size of the annulus will determine the size of the prosthesis that should be used. Mismeasurement of the annulus is the most common reason for complications such as aortic regurgitation.

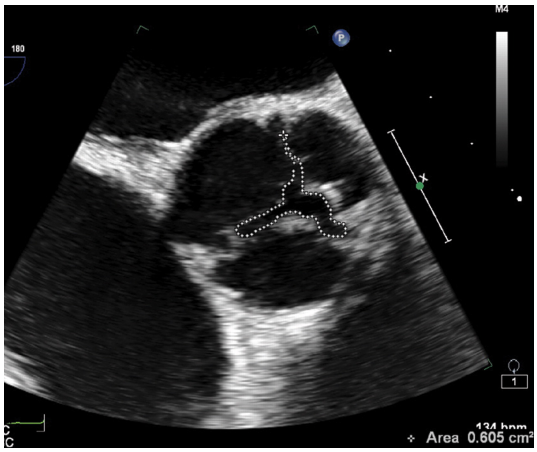

Figure 2.10: Bidimensional echocardiography at the level of the leaflet tips in mid-systole. Planimetry of valve paravalvular area is highlighted by means of a dotted line.

2.7.2 Multi Slice Computed Tomography

Multi Slice Computed Tomography (MSCT) is the method of choice in pre-TAVI assessment of aortic annulus, aortic root and ascending aorta showing superiority over other modalities. In Figure 2.11 a CT image of the heart is reported. In detail, it provides information on important aspects such as the distance between the valve plane and the origin of the coronary arteries, the dimensions of the aortic root, and the presence, severity and quantitative extent of valve calcification. These data define the inclusion and exclusion criteria for each of the different types and sizes of valves, and identify patients at higher risk for complications such as annulus rupture or the need for pacemaker placement in patients with severe calcification. Moreover, 3-dimensional reconstruction of tomographic images gives unique viewing and measuring options and allows determination of the angulation of the valve plane. Furthermore, MSCT of the abdominal aorta and ilio-femoral vessels provides detailed visualization of the vascular and cardiac structures to aid selection of the best access site for valve implantation. This technique allows the diameter and degree of calcification of peripheral vascular tissues to be determined, as well as their course and tortuosity.
It is important to consider that MSCT is associated with the administration of iodinated contrast and exposure to ionizing radiation. Contrast is necessary for precise luminal diameter measurements and the amount depends on the specific protocol. According to this, the use of MSCT should be considered for individual patients based on risks and benefits of contrast administration.

2.7.3 Magnetic Resonance Imaging

Also Magnetic Resonance (MR) imaging can be useful to detect and reliably measure the anatomic valve area. Velocity-encoded Cardiac MR (CMR) is currently being investigated for assessment of the velocity across the stenotic aortic valves. It provides a detailed anatomic assessment of the aortic valve (see Figure 2.12), which can be used to describe valvular morphology and to obtain a direct planimetry of the aortic valve area and precise aortic annulus

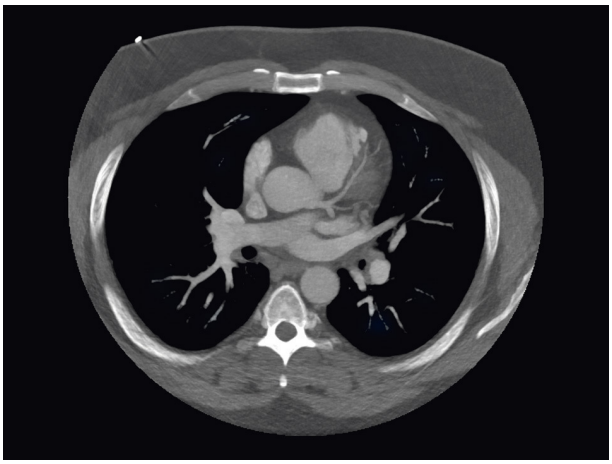

Figure 2.11: Example of Angio-CT axial slice.

measurements. It can be important to exclude associated aortic valvular regurgitation or significant mitral regurgitation. As with cardiac CT, the role of this modality in the management of AS is currently not well defined but it has an established role in evaluating aortic root and ascending aortic anatomy. The main difference between CT and MR is that the latter uses non-ionizing radio frequency signals for images acquisition and, therefore, does not require iodinate contrast procedure.
In the most recent studies of MR imaging of the aortic valve, steady-state free precession acquisitions with ECG gating have been used to evaluate the valve structure and the valve orifice area. Typically, phased-array coils are used. MR is best suited for soft tissues, although it can also be used to acquire images of bones, and other calcium-based body components. MR imaging parameters vary with the MR imaging system vendor but are usually designed to maximize spatial resolution.

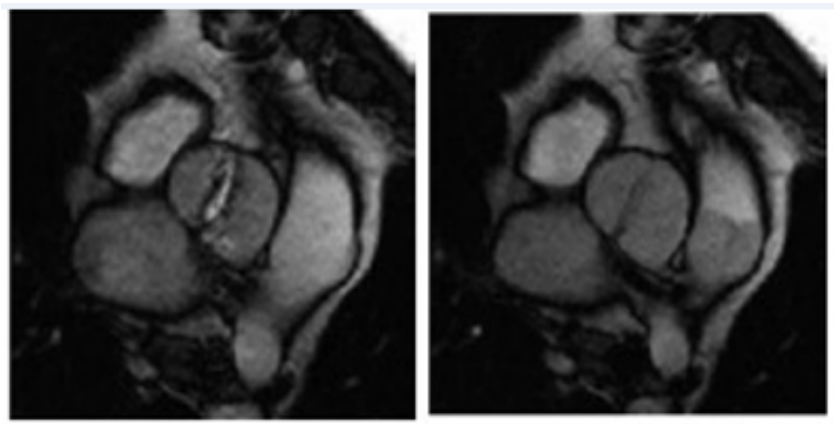

Figure 2.12: Assessment of aortic stenosis when the valve is in the open (a) or close (b) configuration. Cardiac MR was used for this scope.

2.7.4 Intraoperative angiography

Optimal positioning of the transcatheter aortic prosthesis represents a major challenge to the procedural success of TAVI procedure. 2D X-ray angiography is a medical imaging technique employed to visualize the inside of blood vessels, i.e. the lumen of arteries and organs as the heart chambers. Therefore it allows to determine proper valve positioning and the plane of alignment of the aortic valve. Once anaesthetized, the patients are prepared for intraoperative angiography following cannulation of the femoral artery. Using a system of guide wires and catheters, a type of radio-opaque contrast agent is often added to the blood to make it visible on the x-ray images. The angiographic image (see Figure 2.13) is the projection of 3D objects on a 2D plane and results from the interaction of a X-rays beam with the body of the patient. When the radiation travels through the tissues, it is in some part absorbed and the beam exiting from the patient is detected by a receptor, forming the image: two adjacent structures can be identify on the resulting image if they have a X-ray absorbance adequately different.

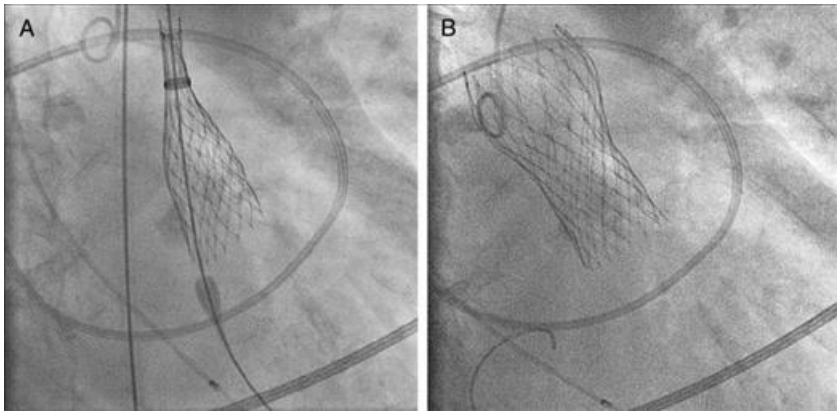

Figure 2.13: Implantation of the CoreValve Prosthesis. On the left side the prosthesis is partially released and is still possible to retrieve the valve (A); on the right (B) the completely released prosthesis is shown.

2.7.5 Follow-up Imaging

Post-procedural imaging relies primarily on echocardiography, which allows assessment of the valve and the evaluation of possible valvular dysfunctions. MSCT and MR can also be used for follow-up examination to evaluate the position of the stent-valve and its relationship to the annulus and the coronary artery.

2.8 Medical imaging pre-processing

In this study the focus is on patient-specific simulations. Thus, appropriate tools to extract the patient geometry from the diagnostic images are required.

The image processing allows to obtain clear and detailed images in order to capture information and the principal features for the analysis. For the 3D reconstruction of the anatomical structures of interest, the study of the images acquisition and the geometrical information that can be obtained from the segmentation are necessary.
The DICOM (Digital Imaging and Communication in Medicine) format describes how to compose messages to send between imaging modalities (for example CT, MR and ultrasound devices) and defines a standard for handling, storing, printing, and transmitting information. DICOM-formatted messages combine images and metadata to create a rich description of a medical imaging procedure.

2.8.1 OsiriX Software

OsiriX is a free and open-source image processing application for Machintosh (Apple, Apple Inc.) dedicated to visualize anatomical DICOM data sets. This software has been developed using open-source libraries such as Papyrus Toolkit for DICOM files, PixelMed and DICOM Offis for DICOM network, the Visualization Toolkit for 3D rendering, and the Insight Toolkit for registration and segmentation. OsiriX has been specifically designed for navigation and visualization of multimodality and multidimensional images: 2D Viewer, 3D Viewer, 4D Viewer (3D series with temporal dimension, for example Cardiac-CT) and 5D Viewer (3D series with temporal and functional dimensions, for example Cardiac-PET-CT). The 3D Viewer offers all modern rendering modes: Multiplanar reconstruction (MPR), Surface Rendering, Volume Rendering and Maximum Intensity Projection (MIP).
Through the OsiriX user interface, using the scissor tool on a 3D volume rendering, it is possible to isolate patient-specific aortic roots, stents and calcifications. Once satisfied with the work, through the creation of a Surface Model, the segmented objects are extracted as STL files. In Figure 2.14 a representative of the heart, in the 3D volume rendering modality, is shown

Figure 2.14: 3D volume rendering from OsiriX.

2.8.2 Itk-Snap software

ITK-Snap is an open source tool that allows to view medical images and to delineate and extract anatomical structures. Image segmentation is typically used to locate objects and boundaries in images and segmentation should end when the object of interest has been found.
This software can be used in two different modes: manual segmentation and semi-automatic segmentation. The interest is focused on the semi-automatic mode in which a powerful level-set based segmentation algorithm is used to segment anatomical structures in three dimensions. Within the region to be segmented, once the mapping between the grey-scale image intensities and the values of the feature image is performed, the user must place one or more seeds that are the starting point of the evolution of the segmentation algorithm. The algorithm evolves in the three dimensions without a stopping criterion; when satisfied the user has to stop the process manually. In Figure 2.15 the result of the aortic valve segmentation is provided.

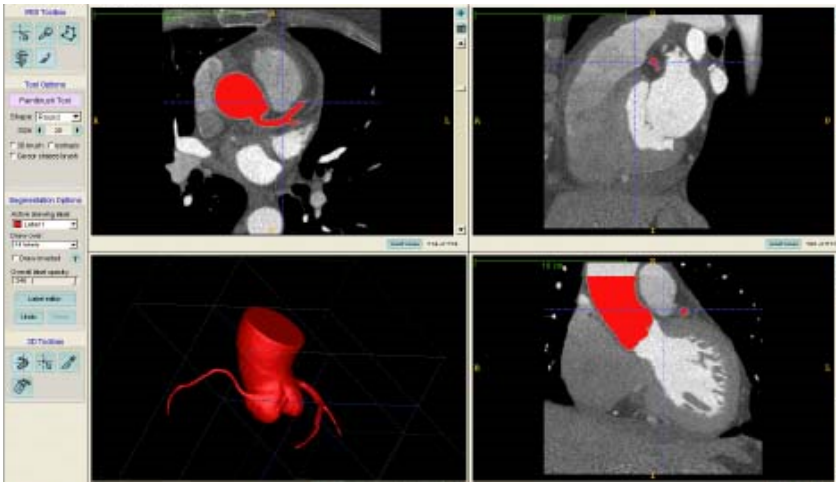

Figure 2.15: ITK Snap software interface. Segmented aortic valve is shown.

2.8.3 Synedra View Personal Software

Synedra View Personal 3.4 is a free software designed to display the DICOM images using a video player and to manipulate them using helpful accessory tools. A view of the main user interface is provided in Figure 2.16. This tool is well suited to analyze the intra-operative angiographic images performed during the intervention.

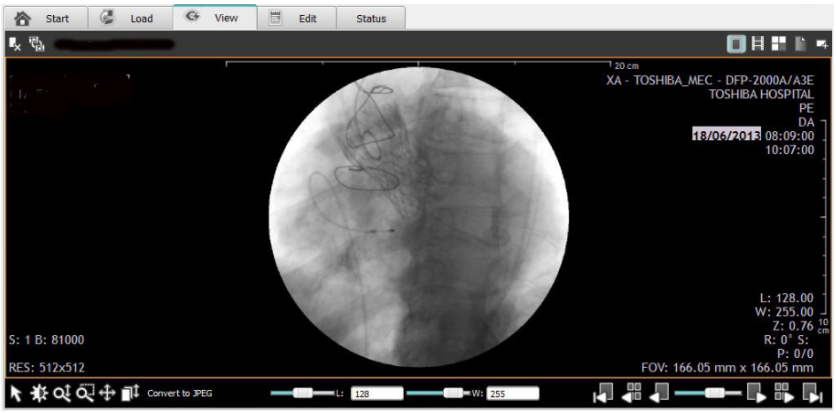

Figure 2.16: Synedra Software user interface.

2.9 3-D Computational simulation

Over the last decades, increasingly refined computational methods have been proposed in order to get better insight into the mechanical behavior of heart valves. Computational modelling has been acknowledged by the Food and Drug Administration (FDA) as being beneficial and, as a consequence, computational simulations are becoming a significant part of medical device evaluation.
If patient-specific considerations are taken into account, computational analysis could help to enhance the optimization of the mechanical performances of devices and patient-specific cardiovascular modelling. The combination of computational and advanced cardiovascular imaging techniques, as well as clinical data, can be a resourceful tool to improve operational planning and procedural outcomes and, ultimately, broaden the range of patients who could benefit from these procedures.

Nowadays, computational methods, Finite Element Analisis (FEA) methods, Computational Fluid Dynamic (CFD) methods and Fluid Structure Interaction (FSI) methods, form an integral part of heart valve dynamics analysis.

2.9.1 Finite element formulation of the aortic valve

Finite element analysis coupled with engineering and design began as early as the 1960s with its first major applications in the field of aerospace engineering [Clough, 1990].
Finite elements methods (FEM) are numerical methods for approximating the solutions of mathematical problems where analytical solutions can not be obtained. Many engineering phenomena and mechanical systems can be expressed by governing equations and boundary conditions. FEM relies on a discrete representation of a physical continuum. A discretization strategy consists in the subdivision of the whole domain into a generally large number of non-overlapping subdomains (elements). Elements are interconnected at points (nodes) common to two or more elements and all together they should cover the entire domain as accurately

as possible. The set of nodes and finite elements is called the mesh. Each of these elements is represented by a set of nodal equations. The response of each element is expressed in terms of a finite number of degrees of freedom, characterized as the value of an unknown function at a set of nodal points. The overall response of the mathematical model is approximated by that of the discrete model obtained by assembling the collection of all elements of the mesh. In mechanical problems, the nodal displacements are the fundamental variables that the solver has to calculate. Subsequently, after solution of the global equation system, strain and stress in individual elements can be found.
Implicit and Explicit are two types of approaches that can be used to solve the finite element problem. Implicit formulation requires to solve simultaneously the equilibrium equations to obtain the displacements of all the nodes. The equations system needs to be solved at the end of each solution increment. In contrast to implicit methods, the explicit formulation does not require the simultaneous solving of an equation system; instead the displacement is approximated to the next increment using the acceleration of the current time step. Solution method selection depends on the specifics of the problem. On one hand, the implicit formulation is ideal for problems where the response of the dynamical system depends mainly upon lower frequencies. On the other hand, explicit methods are advantageous to treat high frequency parts and traveling waves. There are, however, certain static or quasi-static problems that can be simulated well with either methods. Several reasons can guide the choice between explicit and implicit approach. The implicit formulation yields results of high accuracy and no stability issues but can result in an high number of iterations and in an excessive computation cost. From the opposing point of view, the explicit method does not require the solution of the whole model at each increment resulting in a more rapid analysis. For many models the number of degrees of freedom is so high that an explicit approach is the only real alternative to get results in a relatively short time. In general, a FEM is defined by its geometry, material properties, and some appropriate loading and boundary conditions. FE models allow quantification of the effects of changes in one or more of the parameters characterizing the system, including geometric dimensions, mechanical properties and fluid dynamics.
The Finite Element Analysis (FEA) of the aortic valve essentially transforms the unknowns from the continuum (e.g. the aortic root) into equations of discrete nodal quantities. By assuming that certain basic numerical requirements and standards of practice are satisfied, the solution obtained from the FEA can estimate the physical solution (e.g. the aortic valve behavior). Quantitative characterization of the anatomy, structure and material properties form the foundation for FEA of the aortic valve and the implanted device. The reliability of the results obtained through FE modeling depends on the accuracy of the characterization and translation of those parameters into the FE model. Important parameters include:

- aortic root and device geometry;
- tissue and device mechanical properties;
- boundary conditions created by the interaction of the anatomy and the implanted devices.

In the following Chapter all these prerequisites, needed to set up a proper finite element model of the aortic valve, are discussed.
In this thesis, the commercial finite element solver Abaqus CAE 6.13 ®by Dassault Systemes (Providence, RI, USA) is used to perform all the simulations.

Abaqus software

To create an aortic root finite element model and to perform simulations of the prosthesis implantation in the native root the Abaqus program is used. It is a software conceived for finite element analysis and computer-aided engineering that consists of five core software products (Abaqus/CAE, Abaqus/Standard, Abaqus/Explicit, Abaqus/CFD and Abaqus/ Electromagnetic). Abaqus is able to compute FE solutions via implicit (Abaqus/Standard) or explicit (Abaqus/ Explicit) numerical methods.
Abaqus contains an extensive library of elements that can virtually model any geometrical frame. It also provides an extensive list of material models that can simulate the behavior of the most typical engineering materials. UMAT and VUMAT are user subroutines that allow to define a material mechanical behavior when none of the existing models included in the Abaqus library accurately represents the behavior of the material of interest.
Abaqus/CAE is divided into functional units called modules. Each module contains only those tools that are relevant to a specific portion of the modeling task. The order of the modules in the menu corresponds to the logical sequence the has to be followed to create a model. The modules are the following:

1. Part: creates individual parts by sketching or importing their geometry.
2. Property: creates material definitions and assign them to regions of parts.
3. Assembly: creates and assembles part instances.
4. Step: creates and defines the analysis steps and associated analysis procedure.
5. Interaction: specifies the interactions, such as contact, between regions of a model.
6. Load: specifies loads, boundary conditions, and fields.
7. Mesh: creates a finite element mesh.
8. Job: submits a job for analysis and monitors its progress.
9. Visualization: watches analysis results.
10. Sketch: creates two-dimensional sketches.

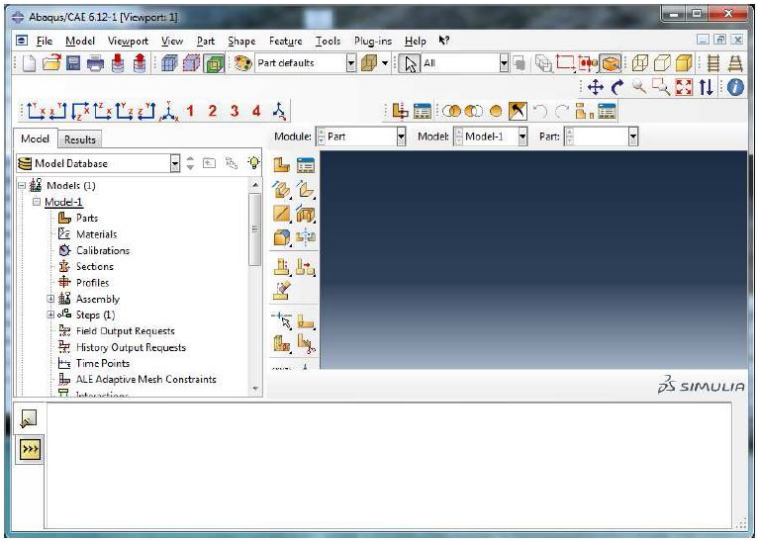

Figure 2.17: Abaqus main window. The appearance of the window changes with the modeling process.

Chapter 3

Simulation strategy

This chapter is dedicated to the explanation of the workflow that has been followed to create a fully patient specific model of the aortic valve and to simulate the TAVI procedure. Firstly, the geometrical model of the aortic root is extracted from pre-operative CT DICOM images, then a computational model of the implantation sites is reconstructed. To obtain a complete model, native leaflets and calcific plaques are also to be taken into account. In effect, the inclusion of the calcifications, or, at least, their most relevant blocks and their location at the leaflet region is important because they affect the dynamic of the stent expansion and its final shape. Afterwards, the CoreValve stent and the catheter are reconstructed and crimped. FE analysis is set and TAVI simulation performed. At the end, the important role calcium has in the prediction of the optimal position of placement to minimize the onset of complications is stated.
In the Figure 3.1 the workflow summarizing all the topics of the entire procedure is depicted. In the following subchapters all the steps involved in this procedure will be discussed in more details.

The construction of the patient model requires the utilization of four different programs: OsiriX, Matlab®(Mathworks Inc, Natick, MA), Rhinoceros 5.0®(McNeel & associates, Seattle, WA, USA) and Abaqus 6.13®.

3.1 Clinical and technical data

In this paragraph we are going to summarize the principal diagnostic aspects of the patient under exam. Moreover some technical data characterizing the CT scans are reported.
The CT images belong to a 76 year-old male patient undergoing TAVI at the ICSA Sant' Ambrogio Clinical Institute, Milano. Echocardiography revealed severe AS and, from the anamnesis informations, the patient is known suffering from arterial hypertension. There was evidence of preserving renal function from contrast agent. The procedure was carried out under general anesthesia and the surgical outcome resulted successful. A size 29 CoreValve bioprosthesis has been implanted. Even though post-operative CT is not included in the routine protocol of TAVI, post-intervention CT images are available for the patient under examination. The MSCT examinations have been performed on a Siemens MedCom volume computer tomography. Technical aspects of the CT scan are reported in Table 3.1. The

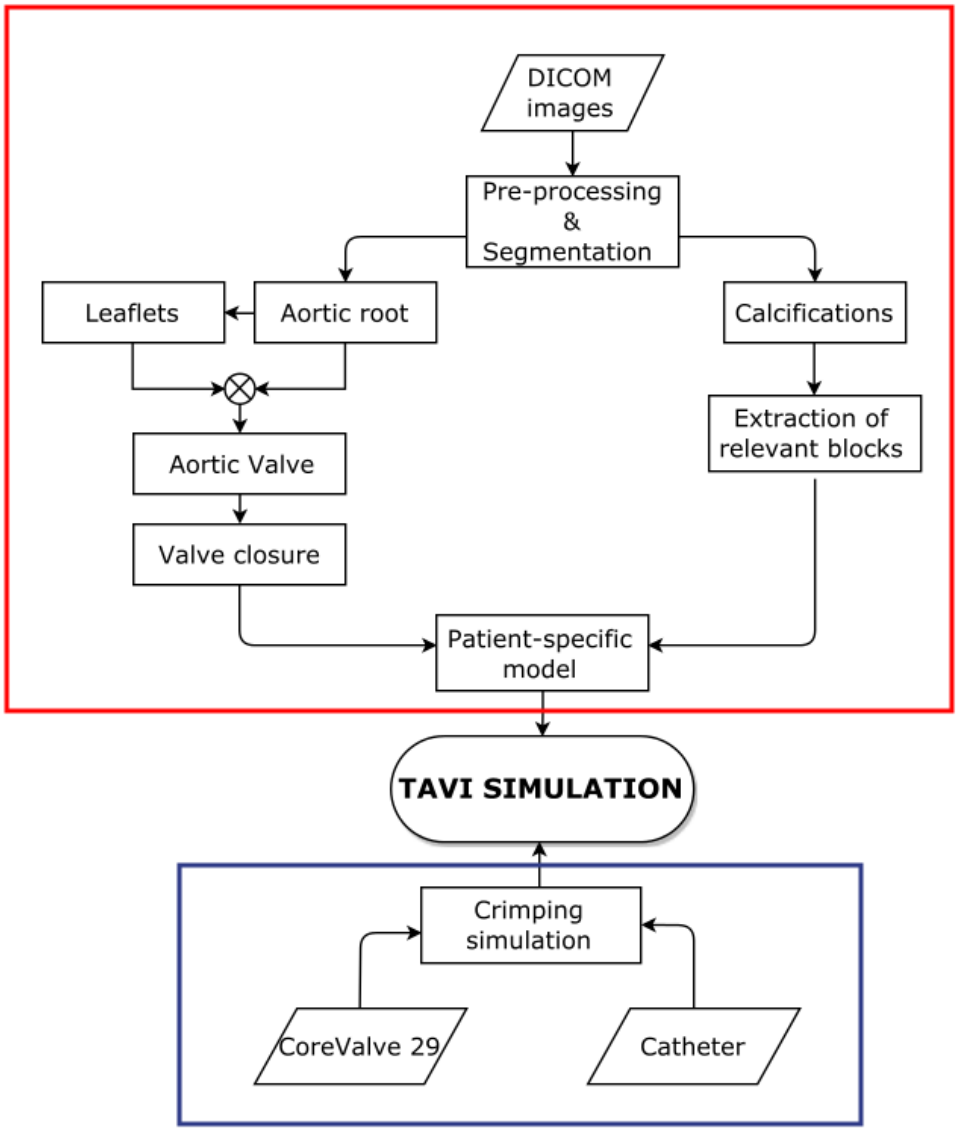

Figure 3.1: Analysis workflow. From CT images, Corevalve 29 stent and catheter geometries to the simulation of TAVI procedure. Red box encloses all the steps required to fulfill the first part, i.e. the creation of the patient specific model. The blue box refers to the second part in which the crimping simulation is achieved.

pixel spacing specifies the physical distance in the patient between the center of each pixel. Distances from the source to the patient and from the source to the detector are also reported.

Technical data	
CT scan	Siemens MedCom
Hospital	ICSA, Milano
Format images	DICOM 512x512
Pixel spacing	2/2
Distance source to patient	595 mm
Distance source to detector	1085.6 mm

Table 3.1: CT technical data.

3.2 Patient-specific aortic valve model

Starting from DICOM images, a patient specific aortic valve model is constructed. The required actions are emphasized in red in Figure 3.1.

3.2.1 Aortic root: from DICOM images to computational model

In this section all the steps required to obtain the computational model of the aortic root starting from DICOM images are detailed. Figure 3.2 summarizes the adopted framework.

Figure 3.2: From DICOM images to computational model. List of the adopted programs.

The first step consists in the acquisition and elaboration of the medical images.

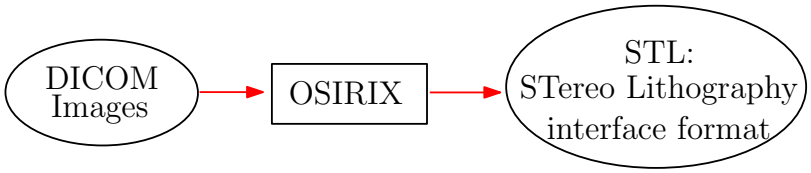

Figure 3.3: Detail of the first step.

In particular pre-operative CT data are considered. The outcome of the CT examination consists of DICOM images. The DICOM files are processed, by means of the software OsiriX, to extract a three-dimensional model of the aortic root wall. As previously reported in Chapter 2,

OsiriX is a very powerful tool that can help performing operations such as segmentation, contrast enhancement and filtering. Through OsiriX user interface, using a 3D Volume Rendering selection, it is possible to separate organs and the anatomical parts of interest. In particular the Crop Volume tool is available. It has a wire frame allowing to create a box around the object in order to crop it. This is the followed procedure that allows the separation of the aortic root from the heart and the entire thorax; then the extraction procedure is manually refined by "scissors". Later the 3D surface model is exported (see Figure 3.4) and used to extract a stereolithographic representation of the patient aortic root. The STL is an engineering file format created by 3D Systems for use with Computer Aided Design software (CAD). It represents a very fine triangular mesh, which is not analysis-suitable due to overlapping and distorted elements; the file contains a list of triangles vertex coordinates that has to be subjected to several transformations.
Moreover, the use of different thresholds and Hounsfield units, describing the radiodensity of the materials, gives the possibility to discern the calcific components from the aortic root material.

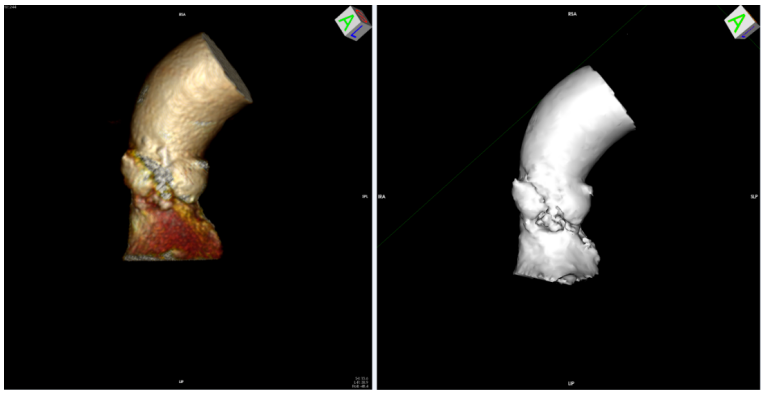

Figure 3.4: On the left, the model resulting from the 3D Volume Rendering is shown. Result of the 3D surface model of the aortic root is reported on the right site.

The STL file of the aortic root is used as input for a in-house Matlab code that allows the generation of a more suitable mesh.

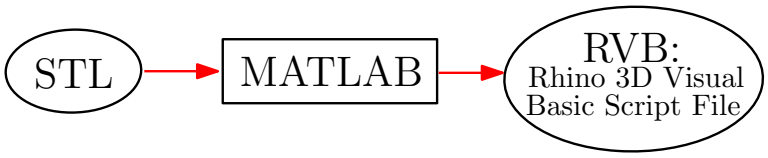

Figure 3.5: Detail of the second step.

This code first loads the input STL file, then computes the centerline of the aortic root; it also normalizes and regularizes the nodes coordinates. Outer profile of the wall is also recreated by considering a thickness of 2.5 mm. The output is a text file containing Rhinoceros commands. Using the nodes produced by this elaboration is possible to build a geometrical model.
Then the commercial software package Rhinoceros 5.0 is used to get an IGES file representing the final 3D model geometry of the aortic root.

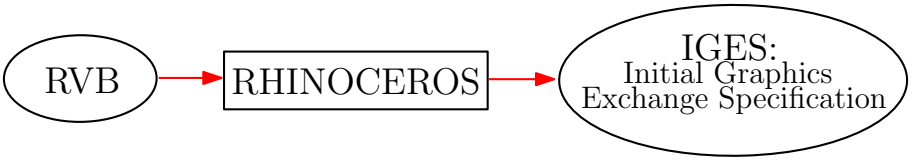

Figure 3.6: Detail of the third step.

The IGES is a file format compatible with finite element software. Thus, the meshing procedure will be then performed within the finite element program Abaqus once importing the IGES file from Rhinoceros to Abaqus.
Once the RVB file is imported in Rhinoceros, the model of the aortic root is automatically built (see Figure 3.8). Through the creation of two surfaces, the inner and the outer one, the solid root is then created. A Rhino solid consists of a closed-loop NURBS (Non-Uniform Rational Basis Spline) surface or poly-surface that encloses a volume with no gaps or openings. The lines and curves delineated with the Matlab procedure are here used to compose NURBS surfaces and then these surfaces joined to construct a solid. The final step consists in exporting the selection as an IGES file. Afterwards, the obtained volume model of the aortic root is imported in Abaqus CAE 6.13 software for the finite element analysis.

Figure 3.7: Detail of the last step.

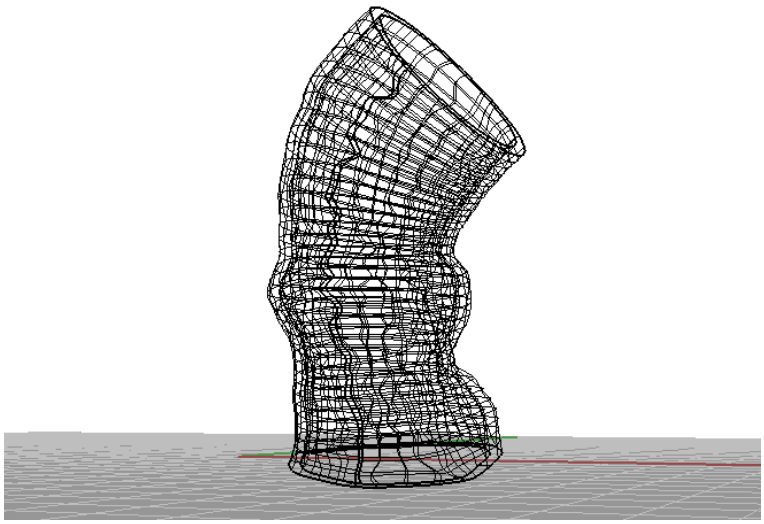

Figure 3.8: Rhinoceros software: creation of a computational model of the patient aortic root. Internal and external surfaces are used to build the solid.

3.2.2 Generation of the native leaflets geometry

The leaflets, in their functional position, have a complex shape which is difficult to both construct and mesh. However the aim of this project is to perform a full TAVI model deployment simulation. For this reason, also native leaflets have to be included in the model. Now the development strategy followed in this work is explained.
Abaqus is used for the definition of the attachment lines and Rhinoceros software is then employed to defined the free margin of the leaflets in order to reconstruct the leaflet surface in the open configuration. The attachment lines represent the junction curves between the leaflets and the root. The development is performed step by step: first of all the IGES file referring to the aortic root is imported in Abaqus. Then a preliminary meshing operation of the part is computed. Tetrahedral elements, with an approximate global size of 2 mm, are adopted to discretize the aortic root. As aid for the identification of leaflets attachment lines, on the internal wall of the root, the calcifications of the patient are also introduced in the CAE model. Calcific plaques are imported from the STL file referred to the diastolic phase, which is routinely performed being the optimal phase for reconstruction according to heart rate.
The main steps for the leaflets reconstruction are reported in the list below:

- Selection on the aortic root wall of nine datum points. Point are selected to represent the attachment lines. As shown in Figure 3.9, the three lowest point (black points) are picked to represent three anatomical anchor points at the base of each of the attachments to the aortic leaflets; these points constitute the aortic annulus. The three highest points (green points) identify the sinotubular junction while middle points (red points) are related to the commissures. It is important to remember that the commissures are the curve segments where the leaflet attachments run parallel, distally upstream towards the ascending aorta.

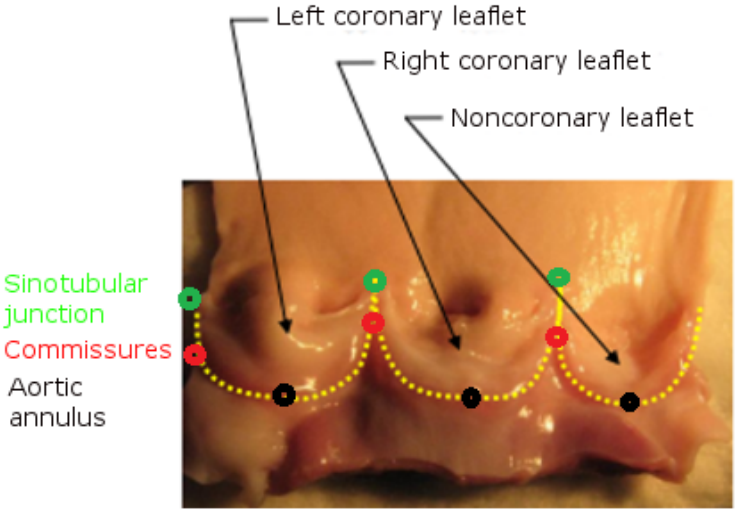

Figure 3.9: Datum points are selected on the computational model of the aortic root to represent the aortic annulus (black points), the commissures (red points) and the sinotubular junction (green points).

- Selection on the aortic root wall of seven datum planes, passing through the nine datum points, in order to cut the aortic root. Each of these planes is defined by three points. The horizontal plane depicted in Figure 3.10 is used to identify the sinotubular junction, three vertical planes refer to the commissures. Three oblique planes are created to represent the native line of attachment. Each of these three planes pass through three points: two points refer to the commissures and the third to the aortic annulus.

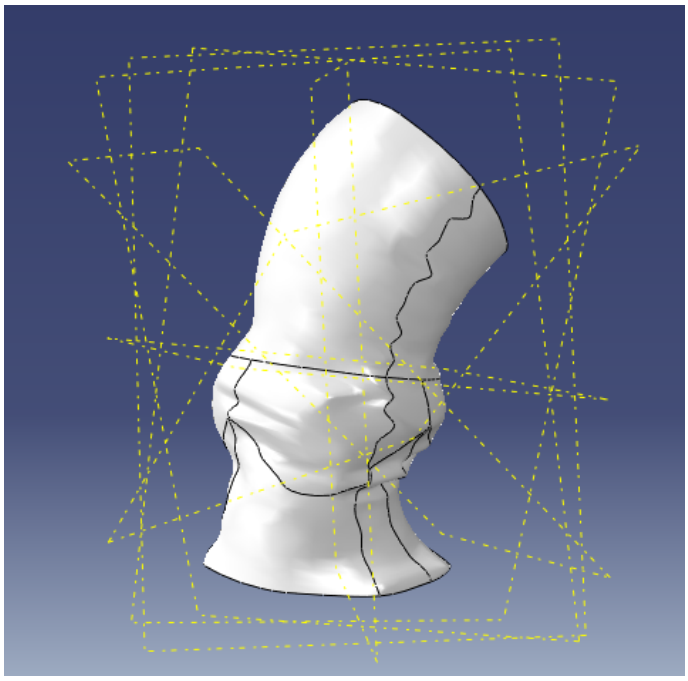

Figure 3.10: Selection of seven datum planes. Each plane passes through three datum points.

- Once the planes are generated, parabolic hinges of the leaflets are defined as intersections between the root surface and the computed planes. Now the implemented strategy proceeds with the exportation of such edge curves as an IGS file, that is the Rhinoceros compatible format. This tool allows to select, from the whole set of partition lines, only the desired leaflets lines: contours extraction, explosion and re-joining lead to the desired result. More in detail, with the feature Explode is possible to split curves, look for and eliminate undesired segments. This operation is followed by the re-joining phase.

- After the definition of the attachment lines, the creation of the free margin of the leaflets in order to reconstruct the leaflets surface in the open configuration has to be done. Rhinoceros allows the user to insert the length of the radius for each of the three corresponding arcs, which is deduced from pre-operative investigations.
  Echocardiography is the key pre-operative imaging modality to assess AV leaflets providing visualization of their morphology. In particular, for the purposes of this work, through OsiriX software accurate measurement of the leaflets free-edge length is per-

formed, then radius can be calculated according to these measures. Free margins are clearly visible in Figure 3.11.

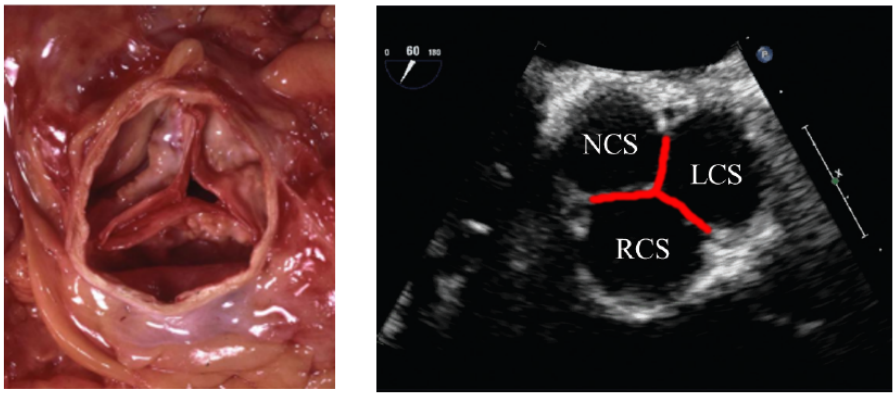

Figure 3.11: On the left free boundaries of the leaflets visible from the aortic root are depicted. On the right measurements of the leaflets free margins taken from TTE are highlighted in red. NCS=noncoronary sinus; LCS=left-coronary sinus; RCS= right-coronary sinus.

In table 3.2 measurements pertinent to the reconstructed leaflets are reported. In particular measurements on the commissures and on inferior margin of the attachment to the aortic valve are carried out. Rhinoceros allows to take directly these parameters. Also the radius chosen for each leaflet is reported.
In Figure 3.12 the result of the creation of the leaflets surface is shown.

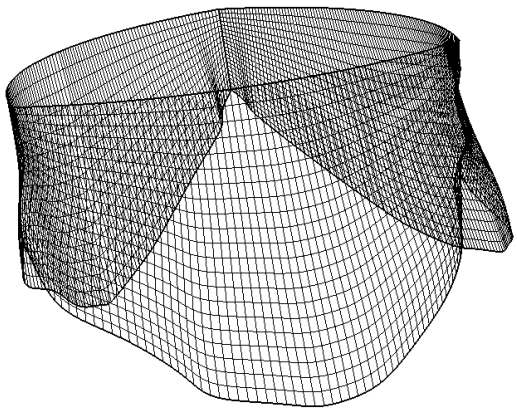

Figure 3.12: Result of the Rhinoceros software. Reconstructed leaflets surface.

Leaflets measurements			
	left coronary	right coronary	non-coronary
Commissures	7.644	7.129	7.859
Inferior margin	51.589	44.164	39.441
Radius	21	22	24

Table 3.2: Measurement on the reconstructed leaflets. Each column refers to a leaflet: left coronary, right coronary and noncoronary.

3.2.3 Creation of the aortic valve: the merging process

The IGES file referring to the leaflets is imported in the Abaqus Model as a new 'Part'. This Model also contains the previously created 'Part' of aortic root of the patient under exam. Now the problem needed to be solved is how to integrate aortic root and leaflets to obtain a single part. The nodes lying on the attachment lines should belong both to the aortic root mesh and to the leaflets mesh. To achieve this result the mesh seeding in the junctions they have in common needs to be the same. Only in this way the merging operation could be performed. Moreover, these lines are composed by several segments and it is necessary to control that the number and the length of each segment on the leaflets is coincident with that lying on the internal surface of the root. Once checked this assumption, the seeding of the edges of the leaflets to be compliant with the seeding of root edges is done. Essentially Abaqus allows to control the seed density by specifying the number of elements desired along an edge. This operation, for each edge on both leaflets and root, is performed.
Then the following step consists in the choice of the elements shape to mesh both the parts. Tetrahedral elements are adopted for the aortic root while quadratic shell elements (2.5 mm) are used for the native aortic leaflets. A shell can be defined as a three-dimensional elastic body occupying a thin neighborhood of a two-dimensional manifold of R^3. A uniform thickness of 0.5 mm is assigned to the leaflet
For each part (root and leaflets) a set containing all nodes lying on the curve junction is created. After that, the merging of the selected nodes belonging to the two different part instances is computed. Abaqus, allows to directly perform the nodes merging: an implemented tool, in the Abaqus Assembly module, deletes nodes that are closer than the specified tolerance and replaces them with a single new node. The merge operation creates both a new part instance in the Assembly module both a new part in the Part module.
In Figure 3.13a the new instance of the patient specific aortic valve is shown. Figure 3.13b offers a view of the leaflets with nodes representing the set of merging nodes highlighted in red.

3.2.4 Simulation of valve closure

The aortic valve opens during systole when the ventricle is contracting and then closes during diastole as the ventricle relaxes. As mentioned at the beginning of this chapter, CT data adopted to generate the geometrical model of the aortic root have been obtained at the diastolic phase of the cardiac cycle while the created instance refers to the systolic phase.
In vivo, the pressure on the leaflets varies from systole to diastole. Under normal physiological conditions, the closed valve supports a transvalvular pressure of 80–120 mmHg acting perpen-

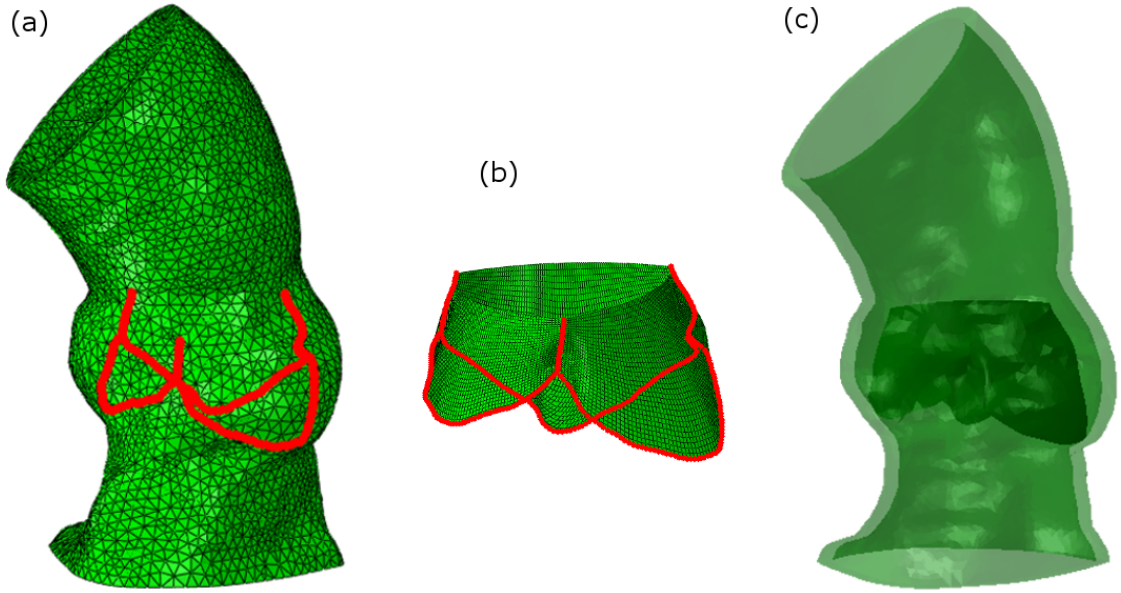

Figure 3.13: In (a) and (b) elements set referring to the aortic root and the leaflets are reported. Nodes used for the merging operation are depicted in red. Instance created (c) from the merging of the aortic root part with the native leaflets part.

dicular to the leaflet area. To simulate the diastolic phase of the cardiac cycle a uniform pressure, with magnitude p=80 mmHg, is gradually applied only on the external surface of the leaflets. The computed simulation considers only the aortic valve portion but, in reality, it is known that the native valve is connected to the circulatory system. For this reason it is necessary to define boundary conditions to fix in space the model. Therefore, a nodes set comprising nodes belonging to the upper extremity of the aortic root is created and, for each of these nodes, the movement of all the translational degrees of freedom is constrained to zero. In the same way nodes at the lower extremity are constrained.
A general contact algorithm is defined to allow interactions between the leaflets. The friction is neglected [Morganti et al., 2014]. It is also specified that the leaflets are free to separate after the contact.
Abaqus Explicit solver is used to perform large deformation analyses.

3.2.5 Inclusion of calcifications

Another geometrical detail that is difficult to treat in the simulations but that possess crucial importance refers to the aortic valve calcifications. As said before, the impact of valve calcified tissue on stent expansion needs to be taken into account because large stent deformation depends on plaques location. In particular the presence of calcifications may lead to an asymmetric configuration of the stent in the implanted configuration. Such a malapposition should be revealed in the pre-operative planning to improve the feasibility of the intervention and to

help surgeons in the decision making phase.
From preoperative CT images, using a threshold of 400 Hounsfield units, also calcific plaques of the patient under study are segmented. In particular, only the calcifications located in close proximity to the aortic valve are considered and, for the sake of simplicity, only the most relevant blocks that have to be taken into account in the subsequent analyses are extracted. In the following paragraphs the performed steps to gain these results are explained. Special focus is given to the problems that are encountered with the attachment of the calcifications to the leaflets. To solve this problem the available solutions are tested performing analyses on simple geometries.

3.2.6 Extraction of the most significant calcifications

In a previous study [Morganti et al., 2014], calcifications were treated as zones projected onto the reconstructed geometry of the native leaflets. It was assumed that calcified tissue intersecting the valve gives the position of calcific shell elements. Now, the aim is to treat calcifications as solid elements since, as it is known from literature [Russ et al., 2013], more accurate simulation results can be gained.

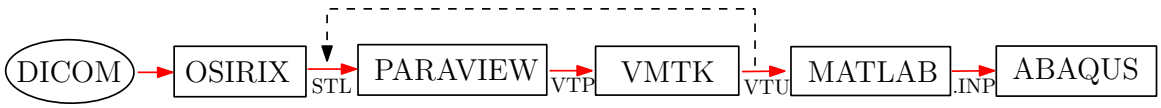

Figure 3.14: Workflow employed to extract the most significant calcifications. Reverse arrow means that the VTU file needs to be processed in ParaView two times. The second time after being elaborated in VMTK.

For this purpose, in the list below, the computed steps are reported:

- DICOM images of the pre-operative CT to extract the calcified tissue are firstly elaborated. Also in this case the software Oririx is used.
- The STL file containing the extracted calcific plaques is then imported in a software called ParaView where preliminary elaborations are performed. ParaView is an open source multiple-platform application for scientific visualization that allows users to build visualizations, modify their geometries and analyze their data using qualitative and quantitative techniques. The 'Filters' Menu provides a list of available filters to process data sets. First of all a filter called 'Clip' that allows to cut away a desired portion of the data set using an implicit plane is apply. Thorough this computational instrument only the calcific blocks that are considered to be the most relevant, in terms of location and dimensions, are conserved. After that, the filter 'Extract Surface' gives the possibility to extract the polygons forming the outer surface of the blocks that are conserved for subsequent analyses.
- At this step the software Vascular Modeling Toolkit (VMTK) is used to get a volume mesh. VMTK is a software that collects many algorithms from the open source Image

Processing Toolkit (ITK) and the Visualization Toolkit (VTK) and assembles them into cohesive functions that can be pipelined into elaborate processes. Principal fields are 3D reconstruction, geometric analysis, mesh generation and surface data analysis for image-based modeling of blood vessels.
To improve the quality of the surface mesh, a surface remeshing is performed. After that the volume is filled with a combination of tetrahedral and prismatic elements.
The used instructions are reported in the line below:

```
vmtkmeshgenerator -ifile inputfile.vtp -ofile outfile.vtu
```

Here the input *inputfile.vtp* represents the surface extracted from the software ParaView while the file named *outfile.vtu* refers to the solid object.

- The output file generated from the VMTK tool is imported another time in ParaView. Using the 'Clip' filter it is possible to cut and remove corners to smooth the external surfaces. At this time the extraction of surfaces is computed by splitting the different calcific blocks. One different output file is exported for each single entity.
- The last step, performed with the VMTK software, considered the following scripts:

  ```
  vmtksurfacecapper -ifile surface_to_cap.vtp -ofile surface_capped.vtp
  vmtkmeshgenerator -ifile surface_capped.vtp -ofile solid_output.vtk
  ```

  With the *vmtksurfacecapper* script the holes on the external surface, that have been created by removing the corners, are capped. These passages are accomplished for each of the input files.

- At the end Matlab is used to open the VTK file in order to redraft an Abaqus-compatibile text editor.

Calcium deposits, considered to be relevant (for dimension and for position), are selected. For each of them the external surface is smoothed and a solid is created. In Figure 3.15 differences between the original calcified aortic valve and the post-processed calcium deposits are shown. In the next step the aggregation of the obtained plaques with the native leaflets will be performed.

3.2.7 Assembly between leaflets and calcific blocks

Once the most relevant calcium blocks are extracted, following step involves the assembly between each block and the aortic valve model. VMTK and ParaView allow to obtain blocks of great dimension, located only in close proximity of the aortic valve. Thanks to the *vmtkmeshgenerator* script, the native mesh appears regular and of good quality. Each calcific block obtained at the end of the procedure explained in Section 3.2.6 is treated as a single entity and imported as a new Part in the Abaqus model. For the case under examination, four different parts, referring to the number of the relevant blocks, are imported in the model. Figure

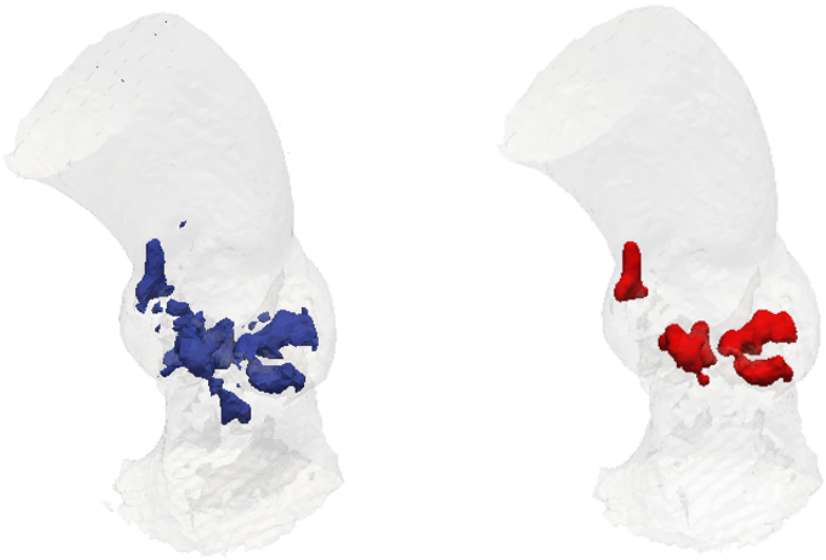

Figure 3.15: A geometrical model of the aortic root is presented. On the left red calcifications refers to the pre-processing phase while the figure on the right highlights only the calcium deposits that are considered to be the most relevant. External surfaces appear more regular and smoothed.

3.16 shows the assembly between leaflets and the most significant, smoothed, calficic blocks. The assembly operation between aortic valve (including the aortic root and the leaflets) and calcifications is delineated. At this point calcium is in the proper position to intersect valvular sheets. If a pressure is applied to the closed leaflets with calcium, since they are not constrained together, they do not react as a single entity to the stimulus.

3.2.8 Preliminary tests for the calcium constraint

The purpose that has to be achieved consists in the fusion, for the duration of the simulation, of leaflets and calcified deposits to allow the latter complying with leaflets during the simulation of valve opening. The atrial systolic phase has to be simulated.
Major problem occurred in this step regards how to bound shell elements, i.e. leaflets, and solid entities i.e. calcifications.
In particular, to solve the problem, in this section test samples based on simple geometries are presented: a 3D deformable, extruded solid, that represents a simplified geometry for the calficic plaque, is considered. This block intersects a rectangular sheet representing the leaflet (see Figure 3.17). In the assembly another rectangular sheet entity is included assuming the role of the aortic wall internal surface. These simulations tests are performed in order to find the best way to embed a region of the model within another region of the same model.
For these tests simplified material properties are used. The module 'Interaction' allows to

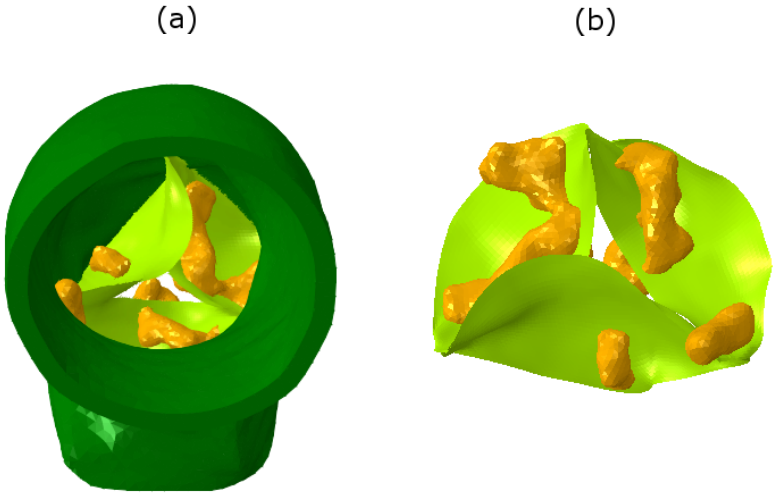

Figure 3.16: Assembly between leaflets and the most significant calficic blocks. For the patient under examination the most significant plaques are considered to be four. Each part appears smoothed, without corners.

create interactions and constraints between different parts of the same model. Constraints partially or fully eliminate degrees of freedom of a group of nodes and couple their motion to the motion of a master node (or nodes). Attention is paid on two different constraint methods that seem to fit with our requests: the shell-to-solid coupling constrain method and the kinematic coupling constrain method.

Shell-to-solid Coupling constraint

The shell-to-solid coupling constraint is used to couple the motion of a shell edge to the motion of an adjacent solid face by specifying a shell edge surface and a solid face region. The shell edge surface and the solid face region must belong to different part instances. The coupling occurs along a shell-to-solid interface defined by the two user-specified surfaces: an edge-based shell surface and an element- or node-based solid surface. The shell-to-solid coupling is enforced by the automatic creation of an internal set of distributing coupling constraints between nodes on the shell edge and nodes on the solid surface. Abaqus uses default or user-defined distance and tolerance parameters to determine which nodes on the shell edge are to be coupled to which nodes on the solid surface. At first glance this method seems to fit perfectly with the needs. However, it does not work very well when the solid surface intersects with shell surface. Indeed, this coupling technique provides for the definition of an edge belonging to the shell surface that has to be in contact with the solid surface. Differently from the sample under consideration, in the reality calcium deposits does not have a regular shape. Therefore the extraction of an edge that exactly surrounds the solid block is quite impossible to find.

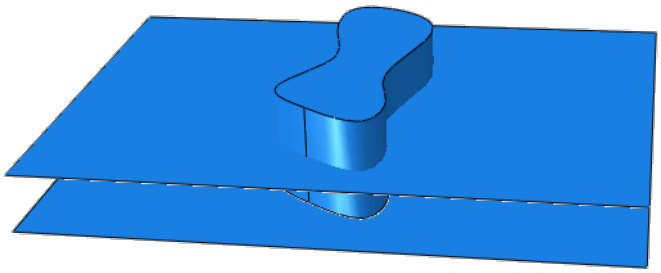

Figure 3.17: Simplified geometry used to compute preliminary tests.

For this reason this coupling method has to be rejected.

Kinematic Coupling constraint

The second considered constraint method is called 'Kinematic coupling constraint'.
More in general terms, the Coupling constraint allows user to constrain the motion of a large number of nodes to the motion a reference node. Defining a coupling constraint requires the specification of the reference node or nodes set, the coupling nodes, and the constraint type. The coupling constraint associates the reference node with the coupling nodes. The reference node has both translational and rotational degrees of freedom. The surface on which the coupling nodes are located can be both node-based or element-based and, automatically, coupling nodes belonging to the entire surface are selected for the coupling definition. Two types of coupling constraints are available: Kinematic Coupling constraint and Distributing Coupling constraint which differ in the nature of the constraint enforcement. Distributing Coupling is enforced in an average sense and degrees of freedom at the coupling nodes are not eliminated. This method could lead to inaccurate results. On the other hand, the Kinematic Coupling technique allows to constrain the motion of the coupling nodes to the rigid body motion of the reference node by eliminating degrees of freedom at the coupling nodes. Abaqus gives also the possibility to choose which are the degrees of freedom that have to be eliminate. When all translational and rotational degrees of freedom are constrained, the coupling nodes follow the rigid body motion of the reference node.
In the performed test a set of nodes belonging to the portion of shell surface that is immersed in the solid block is considered as reference nodes set. The whole external surface of the solid entity is chosen to be coupled with.
The contact between the solid entity and the second shell entity, i.e. the external surface of the aortic root, is introduced to perform the simulation. Also this operation is implemented in the module 'Interaction'. Allowing general contact between the two parts, it must be ensured that the solid does not intersect the shell surface during the analysis. A uniform pressure load is then applied on the leaflet surface shell to which the solid block is tied with the kinematic coupling.

By means of the Kinematic Coupling technique the desired simulation result is achieved (see Figure 3.18). To ensure the realibility we perform a second test, in which a sphere substituted the extruded solid. The result agreed with the precedent.
Therefore, a way to ensure the wanted constraint can be fulfilled: this allows calcium deposit to move together with the native leaflet during the valve opening.

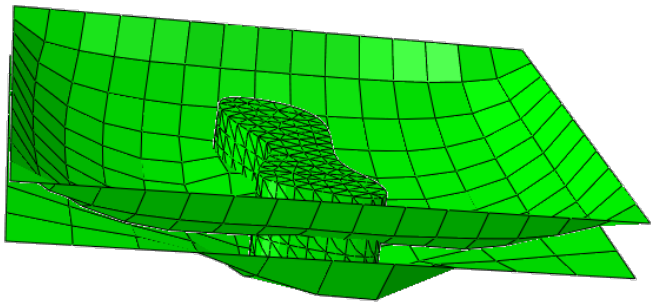

Figure 3.18: Result of simulation test using the Kinematic coupling constraint. The solid block follows the movements of the shell surface during the pressure load. The simulation shows that the solid block successfully moves together with the shell surface.

3.2.9 Opening valve simulation

The last step of the procedure prior to TAVI implantation consists in the simulation of valve opening. The aortic valve must be opened in order to represent the systolic cycle phase avoiding volumetric intersections with the TAV device.
By means of the Kinematic coupling constraint technique, interactions between each calcific block and the leaflets are defined. A frictionless general contact is used to handle the interactions between calcifications and the aortic root inner surface. A uniform pressure of 80 mmHg, acting perpendicular to each element, is applied to the internal surface of the leaflets to represent the pressure experienced during the cardiac cycle. The nodes belonging to both the upper extremity of the aortic root and to the lower one are constrained to avoid root movements. Contact definitions are applied between root and leaflets and self-contact is applied to the leaflets. Also this time the Abaqus/ Explicit solver is used to perform the simulation.

3.2.10 Fully patient specific model

Finally, by following this complex procedure, an accurate, patient specific model of the aortic root is achieved. Native leaflets are modeled starting from the specific valve anatomy of the patient into consideration. Also calcifications are included as solid elements: they are located

in the same positions, relative to the root, of those in the CT images.
The ability of generating, from CT data, patient-specific geometrical models enables patient-specific computer-based simulations reproducing the aortic behavior when effected by pathological conditions such as AS. Patient-specific finite element analysis, including native leaflets and calcifications and considering realistic prosthetic models, may give useful clinical information to guide the surgeons towards an optimal operation choice.
The numerical simulation of TAV implantation is performed assembling the components of the delivery system and the patient-specific aortic valve model. The whole simulation representing the stenting procedure is composed of two main analyses:

- stent crimping simulation: the diameter of the stent is decreased simulating the loading phase of the stent into the delivery system;
- simulation of the TAV implantation procedure: the stent inside its delivery catheter is placed into the patient-specific aortic valve model and there the catheter is gradually removed to allow the stent deployment.

3.3 Stent crimping simulation

Recalling the schema of Figure 3.1, in particular focusing on the actions included by the blue box, the CoreValve bioprosthesis and its crimping into a catheter are detailed.
The simulation procedure of the crimping aims at reproducing the crimping process necessary to the insertion of the catheter. This means that, prior to implantation, the stent needs to be carefully compressed to a size that fits inside the femoral artery. This operation considers the use of a specifically designed crimping device.
In the model TAV leaflets made of pericardial tissue are not included because is supposed they did not affect the mechanical stent behavior and its interactions with the aortic root wall.

3.3.1 CoreValve 29 mm

A geometrical model of the CoreValve bioprosthesis, size 26 mm, has been created in a previous in-house work based on a high-resolution micro-CT scan of a real device sample. The achieved data contain only the metallic stent frame structure, not the soft tissue of the bioprosthesis. Unfortunately, for the CoreValve 29 *mm* no real device is available as sample. To solve this problem the authentic dimensions of both CoreValve 26 *mm* and 29 *mm* are investigated. Measurements are reported in Table 3.3.
In Figure 3.19 the measured zones of the CoreValve stent are highlighted.

It is important to point out that the number of elementary units, both for the CoreValve 29 *mm* stent and for the CoreValve 26 *mm*, is the same. On account of this, starting from the construction process of the 26 *mm* geometry, a geometrical nodal remapping process is implemented to obtain the dimensions of the device of size 29 *mm*.

Nitinol

Nitinol is the stent frame material used in self-expandable valves. It is a metal alloy composed by Nickel and Titanium that exhibits what is known as martensitic transformation,

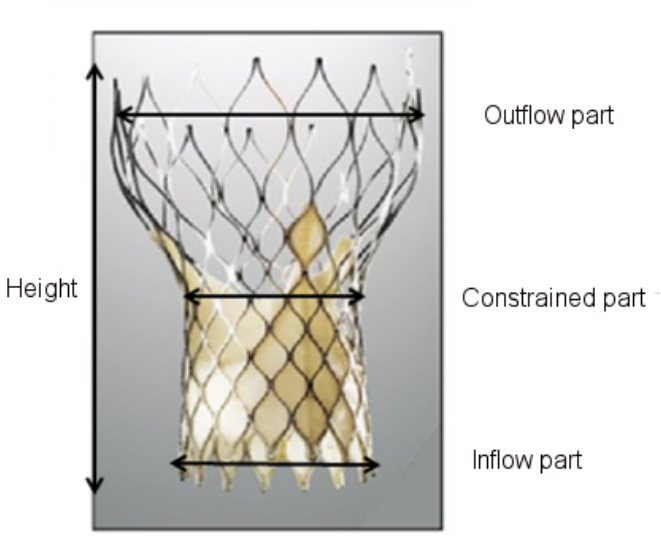

Figure 3.19: Inflow part, outflow part and constrained part diameters are highlighted on the CoreValve stent.

which allows it to undergo a reversible, solid state transformation. As a result, at warmer temperatures, Nitinol forms a very strong, primitive cubic crystal structure. On the contrary, when it is exposed to colder temperatures Nitinol transforms into a complex monoclinic crystal structure. At this lower temperature, Nitinol exhibits the property of superelasticity enabling the CoreValve stent frame to be tightly compressed within its delivery system. The term superelastic is used to describe materials with the ability to undergo large deformations in loading-unloading cycles without showing permanent deformations. In fact, during these cycles, the material shows a hysteretic response. A typical stress-strain response is reported in Figure 3.20. Due to the shape memory property the Nitinol stent remembers its original and undeformed shape of the higher temperature and can recover it. This can occur when the device is exposed to the physiological temperature of the body; here with the deployment phase the stent can regain its original configuration.
The choice of Nitinol as building material for CoreValve bioprosthesis allows the stents to be loaded onto a catheter delivery system that does not require a balloon expandable system and enables the valve to be gradually deployed.

3.3.2 Crimping phase

Abaqus explicit is used to compute a finite element simulation of the crimping technique. The creation of a new 'Model' consists of two parts: the CoreValve stent and the catheter (see Figure 3.21a).
The stent frame model, obtained with the remapping process, is imported and meshed using 71820 solid brick elements with reduced integration ('C3D8R'). The reduced integration elements use fewer elements than the fully integrated ones thus reducing the computational cost. To reproduce the Nitinol material properties a material that is included in the Abaqus UMAT

Measurements: CoreValve 26 mm vs CoreValve 29 mm		
Measurements	26 mm	29 mm
Inflow part diameter [mm]	26	29
Constrained part diameter [mm]	22	24
Outflow part [mm]	40	43
Height [mm]	55	53

Table 3.3: Measurements for the CoreValve 26 mm and CoreValve 29 mm bioprosthesis.

subroutine, a user subroutine to define a material's mechanical behavior, is considered. The constitutive model of this material is based on Auricchio and Taylor (1997). To accurately represent the behavior of Nitinol materials fourteen constants have to been defined. Different elastic constants are related to the austenite and martensite phases; also temperature effects and the control of the volumetric transformation strains are allowed. Material constants are reported in Table 3.4. The material density is set at $6.5 \cdot e^{-09}\ Mg\,mm^{-3}$.
Although in the clinical practice the delivery system is composed of several components, for the sake of simulation strategy it is simplified to its basis component: a cylindrical rigid surface, in the following labelled as the catheter, is built around the CoreValve stent. This 'tube' is used in the numerical analysis to position the stent within the aortic valve and reproduce crimping technique. The catheter is defined through a surface obtained by sweeping a cylindrical section having a radius length equal to 22 mm and meshed using 11040 'SFM3D4R' surface elements with reduced integration. It is modeled as a rigid material with a density equal to $6.7 \cdot e^{-09}\ Mg\,mm^{-3}$.
General contact allows to define contact between the outer CoreValve surface and the inner surface of the catheter. Contact is also used to handle interaction between the stent and itself as it is likely that the cells would come into contact at smaller diameters; it is important to specify that the stent has to be able to separate after the contact. A penalty technique is employed: 'Normal behavior constraint method' is left as default and pressure-over closure set as 'Hard contact'. The penalty contact method is employed in a general contact schema where all surfaces make rigid contact to approximate hard pressure-overclosure behavior.
In the simulation process the catheter is gradually crimped by imposing a displacement set as -19 mm on the radial direction. The crimping is performed defining a cylindrical reference system. In Figure 3.21b the final result of this operation is shown. The time period of the analysis is 0.1 s and a semi-automatic mass scaling strategy is defined. The mass scaling can be defined as an artificial increase of the mass of the model. It improves the computational efficiency while retaining the necessary degree of accuracy required for this particular problem class. In this analysis mass scaling is applied only on the CoreValve stent elements. Then, a quasi-static simulation is performed using Abaqus/Explicit.
Once this analysis is terminated, the deformed parts of the catheter and the CoreValve are exported to be used in a second step of the TAVI simulation procedure: the prosthetic frame will be expanded within the patient-specific aortic root to reproduce the implantation procedure. Thus, a new Abaqus 'Model' is built and the crimped device imported. Moreover, for the CoreValve model, the stress state of the previous analysis is update as initial state with

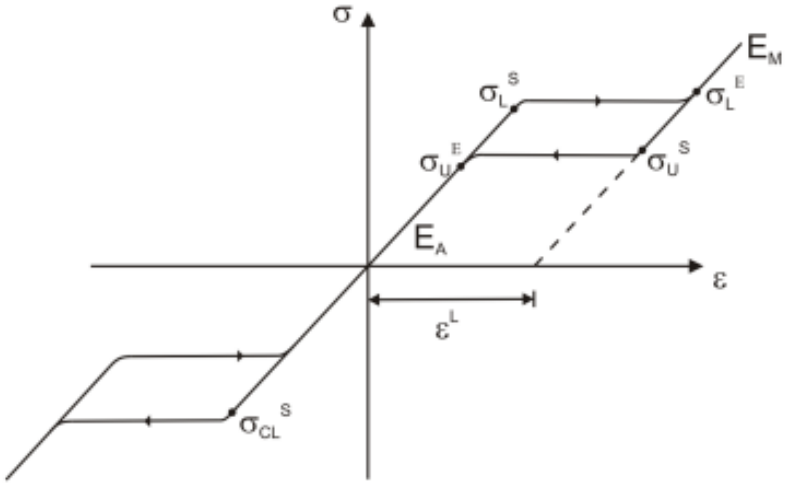

Figure 3.20: Typical stress-strain response for a Nitinol bar.

Nitinol material parameters	
Austenite Young's modulus	51700 MPa
Austenite Poisson's Ratio	0.3
Martensite Young's modulus	47800 MPa
Martensite Poisson's Ratio	0.3
Transformation strain	0.063
Loading	6.527
Loading start of transformation stress	600 MPa
Loading end of transformation stress	670 MPa
Temperature	37 °C
Unloading	6.527
Unloading start of transformation stress	288 MPa
Unloading end of transformation stress	254 MPa
Start of transformation stress (loading in compression)	900 MPa
Volumetric transformation strain	0.063

Table 3.4: Fourteen parameters are used to accurately reproduce the Nitinol behavior.

the option Predefined Field presented in Abaqus Manager. This topic will be discussed in great depth in the next sections of this chapter.

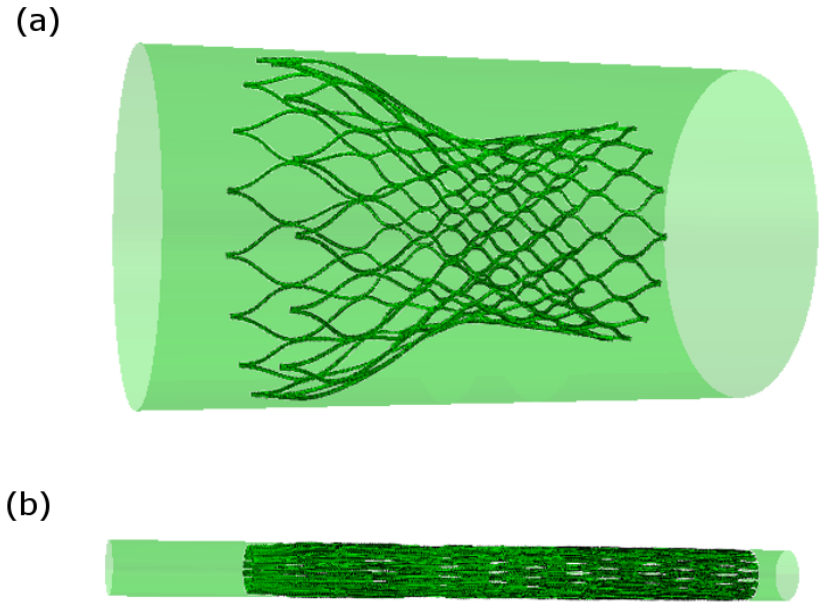

Figure 3.21: On the top of the figure (a) the undeformed stent is depicted. The lower object (b) represents the crimped CoreValve stent inside its catheter.

3.4 Simulation of the TAV implantation procedure

Once obtained a fully patient specific aortic valve and once the crimping is accomplished, TAVI simulation can be finally done. This section is dedicated to the explanation of the main procedural steps that are followed to perform the TAVI simulation. Recalling Figure 3.1 the focus is now in how to link the results of the two sets of procedures, patient specific model and crimping simulation, in order to virtually simulate TAVI.
In the successive paragraphs of this chapter the followed procedure will be explained in detail. The Abaqus program is used. Thanks to this software, very complex geometries, boundary conditions and contact properties can be implemented. In Figure 3.22 all the followed steps are summarized. The order of the 'Modules' in the Abaqus menu traces the logical order of these steps. For this reason, following paragraphs will assume 'Modules' names.

3.4.1 Part and Assembly

First of all a new 'Model' is created. Now, in this model all the outcomes previously computed in the different analyses are introduced.
The model is composed of several parts: the patient specific aortic valve (see Section 3.2.3), the calcium (see Section 3.2.6), the CoreValve stent and the catheter (see Section 3.3). The ODB file resulting at the end of the crimping simulation is considered and metallic frame and catheter are imported in their deformed configuration. As stated before, the aortic valve consists of the aortic root to which the leaflets are merged.

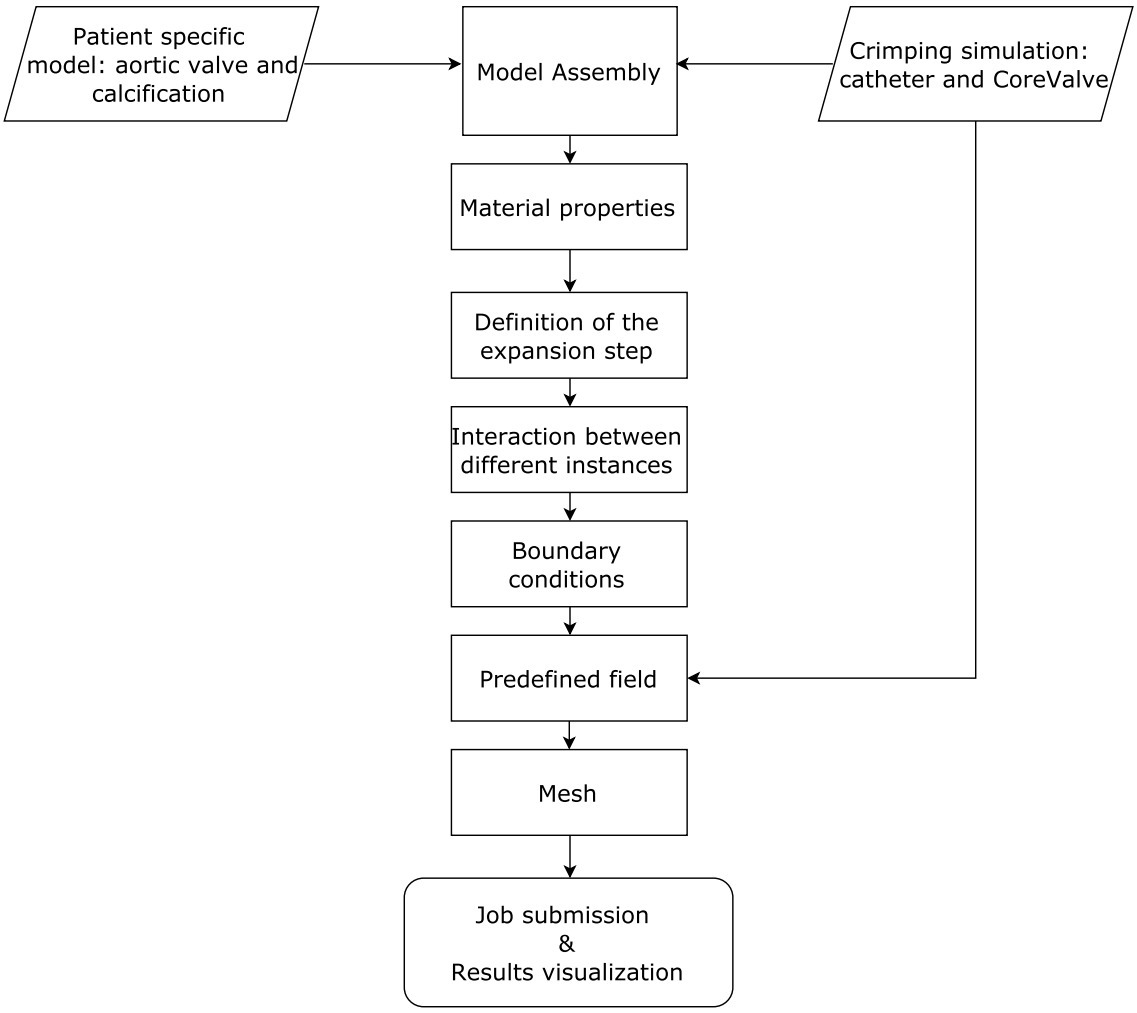

Figure 3.22: Tavi simulation steps. The logical order for the construction of the analysis is the same of the Abaqus menu 'Modules'.

The 'Assembly' module allows to assemble the multiple parts by creating an instance for each of these parts. In this step the creation of the nodes sets, elements sets and surfaces that will be used in the subsequent phases is done.

3.4.2 Property

Afterwards, this step allows the definition of the materials with their desired properties and, at the same time, the creation of the sections that are related with those material properties. It is then necessary to assign one of these sections to each part.
In particular, to characterize the aortic root a simple isotropic St.Venant-Kirchhoff material is considered. The St.Venant-Kirchhoff model is valid for large deformations, but small strains and coincides approximately with the isotropic linear elastic material model for small deformations. For the sake of simplicity, in this thesis and also in largest part of the literature articles, this material is simply referred as linear elastic.
The aortic root material model is characterized by a Young's modulus E of 2 MPa and a Poisson's ratio of 0.45 to represent the nearly incompressible behavior of the cardiac tissue. A density equal to $1.1 \cdot e^{-09}\ Mg\,mm^{-3}$ is assumed.
The leaflets main tissue component is assumed to be elastin. Therefore, it is possible to model the material as an elastic linear isotropic material defined by the same two parameters chosen for the aortic root. The density value, also in this case, is $1.1 \cdot e^{-09}\ Mg\,mm^{-3}$. According to Loree et al. [1994], the calcified tissues are assigned a linear-elastic and isotropic material model with a Poisson's ratio of 0.35 and a Young's modulus equal to 10 MPa ; the density is set to $2 \cdot e^{-09}\ Mg\,mm^{-3}$. Stent frame material and catheter material are defined as previously reported in Table 3.4.

3.4.3 Step

Automatically Abaqus creates a special initial step at the beginning of the 'Model' step sequence. The initial step allows to define boundary conditions, predefined fields and interactions that are applicable when the analysis starts. In addition, a new step is defined to simulate the delivering phase which represents the time when the stent is released from the catheter inside the aortic root of the patient undergoing TAVI. The time period for the step is set as 0.4 seconds. Also in this step a mass scaling on the CoreValve elements set is defined to reduce analysis computational cost.

3.4.4 Interaction

Since different parts are assembled together, there is the need to define the contact acting between these different instances. This is performed using the 'Interaction' Module.
A contact interaction property can define tangential behavior and normal behavior. For the tangential behavior the friction formulation that has been chosen is the penalty method, the fraction of characteristic surface dimension is 0.005 and the friction coefficient is imposed to 0. For the normal behavior the pressure-overclosure is set to hard contact. It is also specified that all the different instances are free to separate after the contact.
General contact interactions allow to define contact between different regions of the model.

It is possible to define the contact interactions acting, at the specified step in the model, including specific surface pairs. During the expansion step general contact is defined between the elements of the stent and the catheter surface. Self-contact is defined for the CoreValve stent elements. Contact between the internal surface of the root and the calcifications, between internal surface of the root and the stent has to be defined. The stent surface is also chosen as the master surface with the internal leaflets surface and the calcifications surface being the slave surfaces.
In the Table 3.5 individual contact surface pairings are summarized.

Interaction properties	
First surface	Second surface
Internal aortic root	CoreValve
Internal aortic root	Calcifications
CoreValve	Catheter
CoreValve	Calcifications
CoreValve	Internal leaflets
CoreValve	self

Table 3.5: Pair surfaces for which general contact is defined.

With regard to the performed preliminary tests (see Section 3.2.8) a kinematic constraint is used to connect the calcium deposits to the valvular sheets. In this way, the relative motion of the calcification is constrained in all rotational and translational degrees of freedom. As stated before, calcifications are attached to the valve leaflets and can move together during the leaflets movements. In such a way, this process allows the reliable reproduction of the in-vivo conditions.

3.4.5 Load

The Section 'Load' involves, for each time step, the definition and the assignation of the boundary conditions acting on the model.

Boundary Conditions

It has to take into account that boundary conditions are important model parameters to get to reliable simulation outcomes. To effectively capture the in-vivo conditions of the aortic root, preliminary boundary conditions are applied to both the extremities which are constrained to a plan normal to the axis of the stent: the lowest boundary of the root is fixed from moving longitudinally, and, to prevent excessive movements, the nodes belonging to the upper boundary are blocked in all the three translational degrees of freedom. Displacement constraints are used to prevent the CoreValve from moving in the longitudinal direction. Only the nodes of the stent base are tied.
All the boundary conditions described here above are applied in the initial step of the analysis and propagated in the consecutive step.

Displacement/rotation constraints with cylindrical coordinates are also set, in the expansion step, to all the catheter nodes to allow the catheter displacement during the simulation. In detail, in this deployment phase, a displacement, set as -85 *mm* in the longitudinal configuration, is imposed allowing for the gradual stent deployment, while the other translational degrees of freedom are constrained to zero.

Predefined Field Manager

When importing the models from an analysis to the other, all the solicitation levels, i.e. the stress and the strain values, can be applied back to the parts imported and taken into account for the next steps through the Predefined Field Manager tool. Precisely, when the entire simulation is divided in two or more "sub-simulations" (also called steps), in the step next to the first one, the Predefined field tool can be used to consider the stress and the strain values in the successful step to get continuity at the all numerical procedures of the simulation. It is important to take into account that an initial state field can be created only during the initial step.
As previously mentioned, to reduce the computational time when multiple expansion simulations are performed, the entire simulation has been divided into two analysis. In the first one only the crimping phase is modelled (see Section 3.3.2) while the second one concerns the stent expansion. As stated before, the stent is here imported from the previous step in its crimped condition and also its tensional state is imported. Referring to the Nitinol shape-memory properties, the tensional state gives to the metallic frame the opportunity to remember the original un-crimped configuration. To fulfill this procedure it is necessary to select the job name corresponding to the analysis from which the initial state field is imported and to update reference configuration allowing to be the imported one. If no initial conditions are specified, Abaqus will assume that the all parts are in unloaded state. In this way displacements and strains can be calculated relative to the new imported configuration.

3.4.6 Mesh

The aortic valve can differentiate two anatomical regions: the aortic root and the leaflets. The orphan mesh created from the previous simulations consists of more than 70000 volumetric elements 'C3D4' (4-node linear tetrahedron elements) for the aortic root and, for the leaflets, approximately 7000 shell-elements 'S4R' are used. 'S4R' defines a 4-node, quadrilateral, stress/displacement shell element with reduced integration and a large-strain formulation. Volumetric elements 'C3D4' are also used to mesh the calcifications. In Table 3.6 a summary of the number and the type of elements assigned to each part involved in the model is reported. The deformed orphan mesh of the catheter and the CoreValve part is imported from the previous analysis.

3.4.7 Job and Visualization

Once the construction of the finite element analysis is finished, the 'Job' module is necessary. In this module, it is possible to create a job which includes all the information of the created FE model. Abaqus first generates an input file representing the model, later this file will be

Mesh: types and number		
Part	Element type	Number of elements
Aortic root	C3D4	76559
Leaflets	S4R	7700
Calficic plaque n.1	C3D4	25013
Calficic plaque n.2	C3D4	17255
Calficic plaque n.3	C3D4	4241
Calficic plaque n.4	C3D4	6095
CoreValve stent	C3D8R	71820
Catheter	SFM3D4R	11040

Table 3.6: Mesh number and type of elements of the parts involved in the FE simulation.

submitted to the solver which performs the analysis using the contents of this file. All the performed simulations run across 12 CPUs, in double precision, on a dedicated server. Crimping analysis complete in about 38 hours while the deployment simulation required approximately 80 hours. The use of additional CPUs does not provide significant elapsed time speed-up. During the simulations, kinetic energy is monitored to ensure that the ratio of kinetic energy to internal energy remains less than 10% since the stent deployment is considered as a quasi-static phenomenon where inertial forces are negligible.
The Abaqus post-processor is called 'Visualization' module and provides a graphical display of the finite element models and results. It obtains these model and information about the results from the output database which is imported at the end of the analysis processing. Figure 3.23 shows four different phases of the expansion simulation.

Accurate patient-specific finite element models including the vessel wall thickness, native leaflets and calcification deposits may represent a useful tool to guide TAVI procedure and to optimize the aortic valve positioning during the deployment. Key role assumes the apposition of the stent against the aortic root wall. By adapting the position of the stent, i.e. placing it more upwards or downwards, and by choosing the appropriate stent size, a good apposition can be achieved. Starting from the outcome of the simulations many different aspects can be examined. A principal role assumes the impact of calcium on the stent configuration. In the next section this topic will be analyzed.

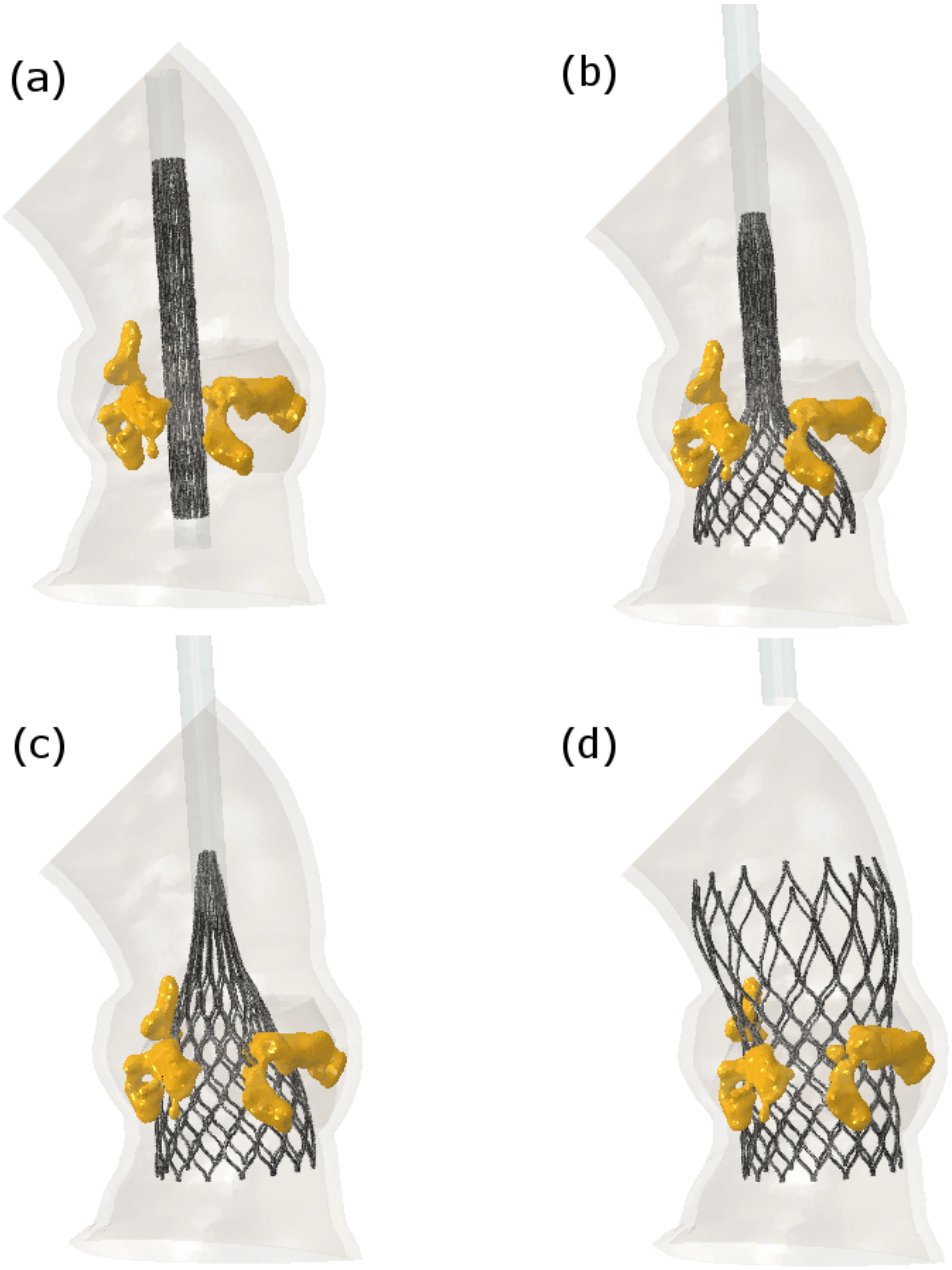

Figure 3.23: Four different phases of the simulated implantation procedure are shown.(a) refers to the initial step, in (b) and (c) is possible to see the progressive expansion of the CoreValve stent. In (d) the stent in the expanded configuration is shown.

3.5 Importance of calcium deposits

The results of the performed analyses show that the final deployment morphology of a TAVI stent is not uniform, but depends on the anatomy in which the stent is inserted. As it is known from the literature [John et al., 2010], the extent of aortic valve calcifications is related to post-procedural stent eccentricity. While conventional open-heart surgical techniques can account for calcium deposits and ensure optimal circular implantation of surgical valves, deployment of TAV devices against these deposits can result in non-concentric deployment of the valve stent, which can lead, as a consequence, to paravalvular regurgitation or altered blood kinematic.
For this reason it is believed that the association between the amount and the location of calcium deposits and the final shape of the deployed stent is an important parameter that has to be evaluated. The inclusion of calcifications as solid elements into the patient specific model can help to predict which is the optimal implantation depth and the correct valve position for each patient. Starting from different positions of the crimped device is possible to detect which of them leads to best performances. For example, a bioprosthesis implanted too low can result in severe paravalvular regurgitation. Furthermore, not only the depth of implantation plays a crucial role in the simulation outcome but also the prosthesis orientation can lead to different deformed shapes. In Figure 3.24a an asymmetrical configuration of the implanted stent, due to the calcific plaques, is observed. This inaccurate juxtaposition can be clearly seen from the frontal view. The stent configuration in the valvular area might cause hemodynamic problems. On the other hand, as depicted in the Figure 3.24b, the choice of a different implantation orientation lead to a better result in terms of stent eccentricity and, as a consequence, could decrease the potential area of paravalvular regurgitation. The calcific deposits displaced by the stent cause high stress concentration on the aortic root. As depicted in Figure 3.25, higher values of stresses are obtained on the inner wall due to the interaction with the calcifications that are pushed by the CoreValve stent. In this Figure a contour plot of the Von-Mises stress [1], superimposed on the deformed shape of the model, at the end of the last increment of the loading step, is displayed. These parameters can offer a better understanding to the surgeons.
However, finite element simulation may fail to reproduce the in-vivo behavior and thus provide clinicians inaccurate results. For this reason a validation study on the proposed method should be performed.

[1] The Von-Mises stress is a scalar quantity resuming the tensional state represented by the second-order stress tensor $\sigma_m = \sqrt{\frac{3}{2} S : S}$. $S = \sigma - pI$ is the deviatoric stress tensor where $p = tr(\sigma)$ is the pressure stress. In FEA regarding cardiovascular structures this quantity is often used as a stress measure, i.e. as an index concerting wall tensional state.

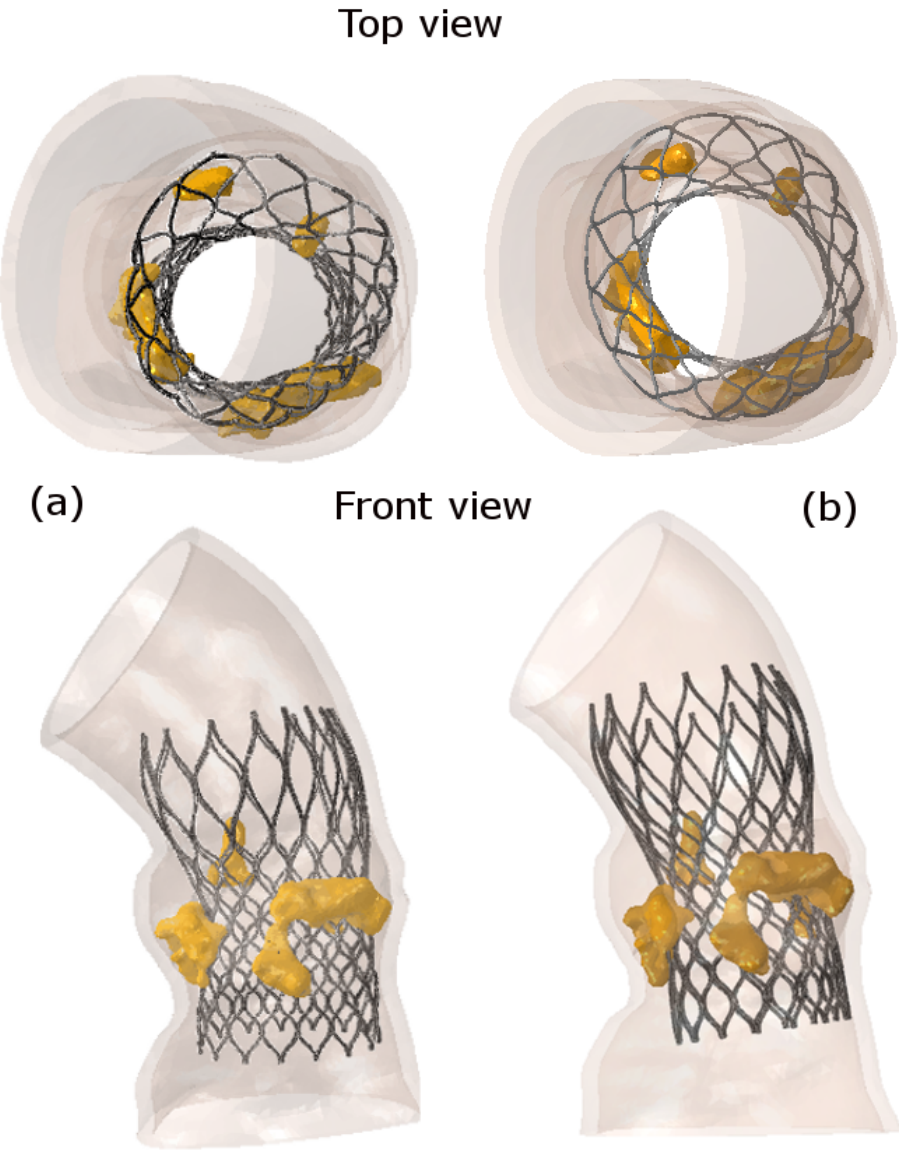

Figure 3.24: Predicted stent postoperative configuration when two different levels of orientation of implant are chosen. On the left, an irregular shape is reached from the stent. Changing prosthesis orientation a best result (right) can be achieved.

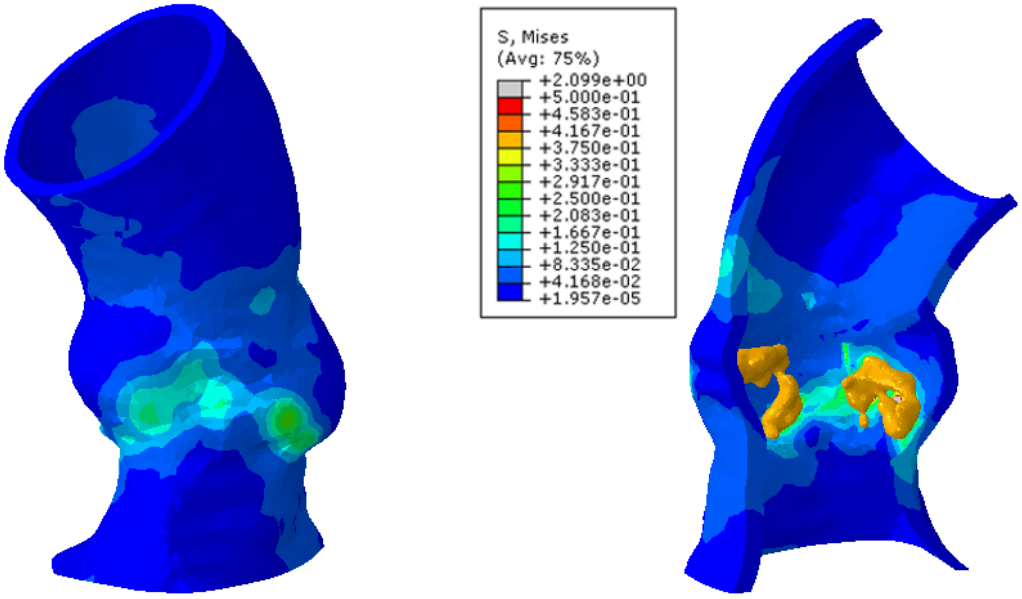

Figure 3.25: Von-Mises Stress distribution on aortic root after the CoreValve stent is deployed. Figure shows an high stress concentration region: maximum Von-Mises stress is recorded for the elements that interact with calcium. The stress values are calculated in MPa units. In the legend the 75% specifies the nodal averaging scheme.

Chapter 4

Validation of the patient specific finite element analysis

In Chapter 3 finite-element simulation of TAVI procedure, based on patient-specific aortic root models including native leaflets, calcifications and an accurate stent geometry, is addressed. However, to ensure reliability the whole procedure has to be validated. As a matter of fact, no model can be accepted unless it has passed the validation tests, since the procedure of validation is vital to ascertain the credibility of the model [Martis, 2006]. Many parameters in a finite element analysis are uncertain. This will inevitably account for some differences in the behavior of the real structure and the results of the analysis. Therefore, the finite element model validation consists in the verification that idealization premises and analysis conclusions are valid.
For the current study to have clinical relevance, validation of the results is necessary. Later in this chapter, the followed validation procedure will be explained in detail.

4.1 Proposed Validation Framework

To our knowledge, little has been written about validation of TAVI simulations.
Schultz et al. [2012] and Russ et al. [2014] proposed a framework to automatically estimate a patient-specific model of the aortic valve and compute implant deployment in which the undeployed device was placed according to the postoperative anatomy. Moreover the final aim of Russ' research team was to predict the movement of implants from any initial position and evaluate the difference in implantation depth before and after stent deployment in order to find the optimal initial placement of the prosthesis in relation to the aortic root. Also Grbic et al. compared the simulation results, obtained by respecting all steps of the clinical implantation such as implantation depth, with post-operative CT scans of patients who underwent a TAVI procedure. The same authors announced a commercial tool to bring TAVI simulations into the clinics too (FEops, 2014).
However, despite the proved feasibility and the success, other studies do not validate simulation results by performing computer-simulated implantation tested under blind conditions. In practice, the approach they adopted is to implant the simulated stent in the same position achieved during the real procedure and, after the virtual deployment, compare the resulting deformed stent model with the extracted one. If validation is performed according to what

can be found in literature, its results could be limited. Hence, in this dissertation, emphasis is put on the simulation of prosthesis deployment focusing on different implantation sites. By registering the 3D reconstruction of the implanted stent with the predictions of computer simulation, the shape that fits more to the implanted device is assessed. As a ground truth, the position achieved by the simulated device, in the best configuration, is finally compared with the information about the real implantation obtained from the intra-operative angiographic images with the aim of assessing the capabilities of the patient-specific computer simulation tool to predict post-implantation outcomes.
An overview of the proposed framework for the validation of TAVI simulation results is shown in Figure 4.1. The analysis-suitable patient-specific model is obtained by processing CT images and then is used as initial configuration for the device apposition. Different implantation sites are considered. The final configurations are explored to assess the success of the procedure: the computer simulation outcomes are compared with the device extracted from the post-operative CT and the best placement strategy is assessed. Even though post-operative CT is not included in the routine protocol of TAVI, post-TAVI CT images are available for the patient under examination. Afterward, results from the computational model are validated by measuring the position achieved from the device during the real procedure.

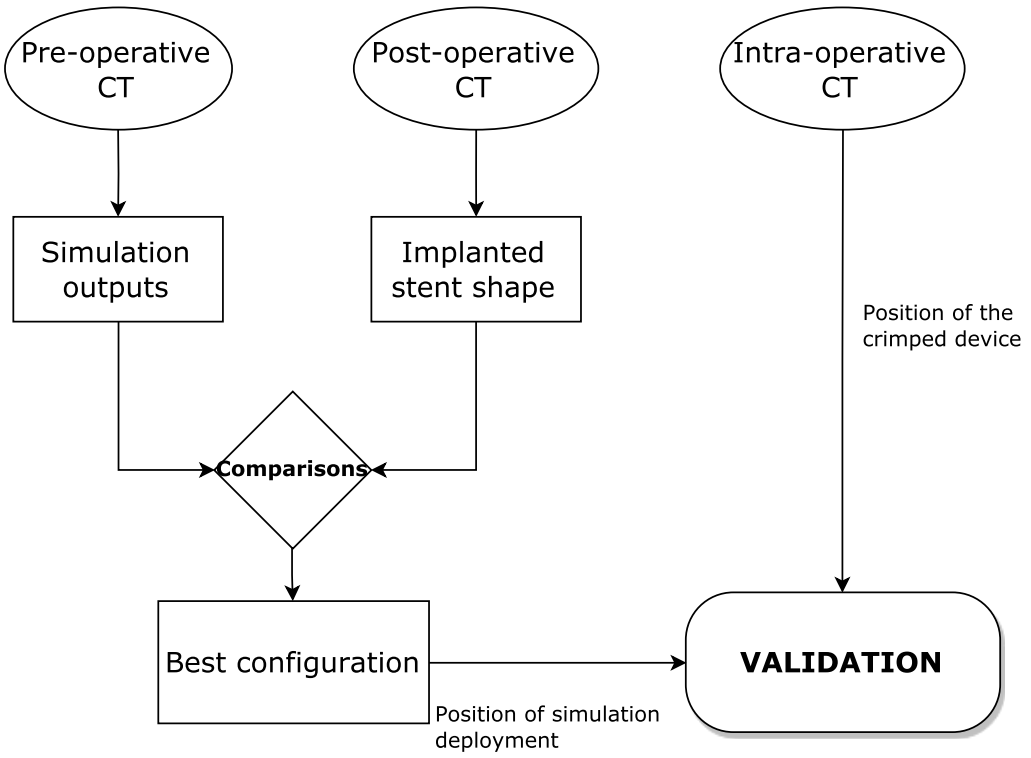

Figure 4.1: Validation framework for computer-based patient-specific simulations. The simulation outcomes are compared with the implanted stent and best configuration is assessed. Taking into account the position of the simulation deployment and the position of the crimped device, the proposed FEA method is validated.

The process of postoperative CT images acquisition, the methods to extract information about the postoperative stent shape and how that information is used to estimate similarities with the simulation results are discussed in detail below.

4.2 Implant deployment predictions vs post-operative configuration

Computational models of the implantation sites are reconstructed from pre-operative CT images as detailed in Chapter 3. Within these realistic geometries, TAVI with a CoreValve bioprosthesis (size 29 mm) is virtually simulated using finite element analysis.
Five simulations, positioning the crimped device in five different implantation sites are carried out. In the first simulation (referred as T0) the crimped device is positioned in proximity of the aortic annulus, which is detected by the nadirs of the sinuses. In the other cases either a distance of 5 mm (case T1) or 10 mm (case T2) between the aortic annulus and the stent inferior margin is set. When distance is equal to 5 mm, the crimped device is rotated by $\pm$ 10 degree with respect to the stent principal axis (known as R10 and R-10, respectively). In Figure 4.2 all configurations are depicted.

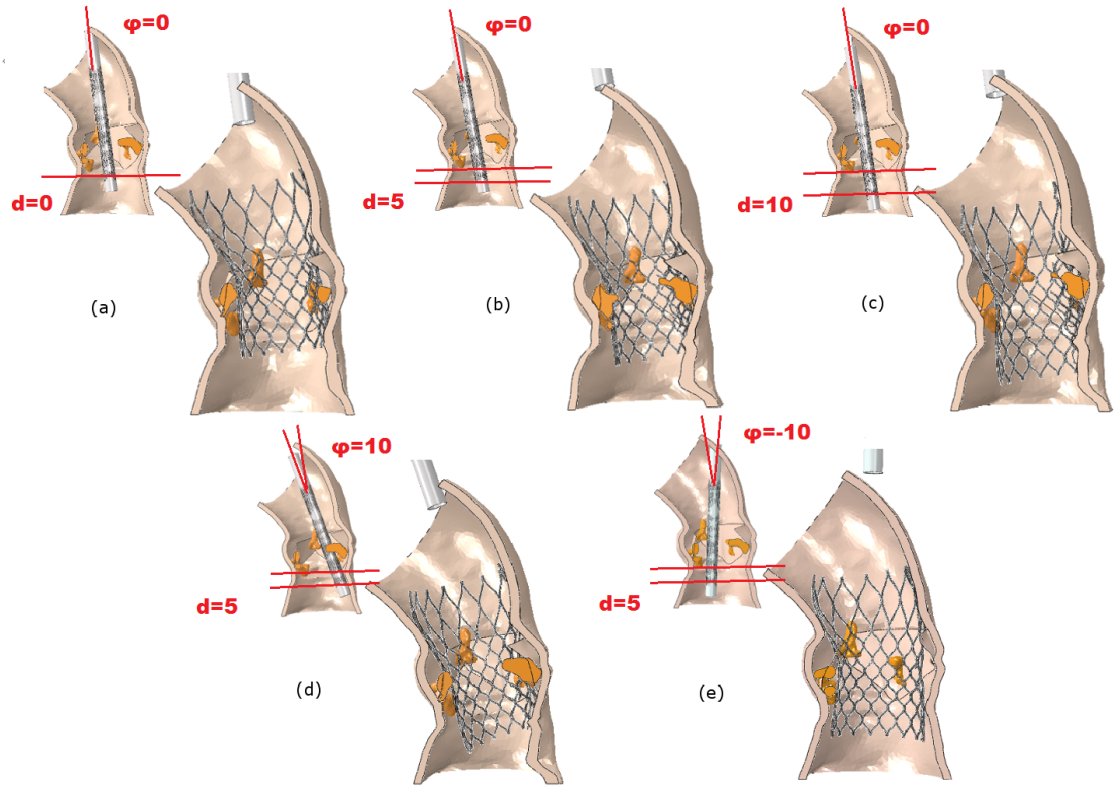

Figure 4.2: Different cases for stent apposition: a) T0 level, b) T1 level, c) T2 level, d) R10 level and e) R-10 level.

4.2.1 Post-operative CT

Since CT allows the acquisition of high-resolution volumetric data, it is a key instrument for showing accurate results of the procedure.
The 3D reconstruction of the implanted stent frame is obtained by processing DICOM images of the post-operative CT. OsiriX software and Itk-Snap 3.0 are used to extract a STL representation of the implanted stent. The pre-processing and segmentation study is independently performed by the two software and the best result, in terms of precision and accuracy of the extracted geometry, is considered for the following analysis.
With Itk-Snap a semi-automatic segmentation procedure of the object (i.e. the stent) is done. The performed steps are the following:

- definition of a Region of Interest (ROI);
- image pre-processing based on the intensity regions method to enhance image contrast;
- placement of the seeds within the region to be segmented that are the starting points of the evolution of the segmentation algorithm;
- setting of the evolution parameters;
- stopping of the evolution when desired.

The stent segmentation procedure performed with the software Oririx recalls the one already explained in Section 3.2.1.
Comparing the two extracted geometries, it has found that the segmentation computed by means of the Itk-Snap software has led to a more accurate result.

4.2.2 Methods for validation study

Post-operative clinical data are analyzed to prove reliability of the performed simulations.
For each configuration of implantation, the 3D reconstruction of the post-operative stent is overlapped and compared with the predictions of the computer simulation outcome. The result of this transformation (roto-translation) is made using the Abaqus software and the VMTK tool. Abaqus, using some functions of the 'Assembly' Module, is initially used to get manually close the two objects; later the VMTK software provides local displacements for a more accurate result. The following is the procedure in further detail:

- the geometry of the original stent and that referring to the simulation outcome are imported in Abaqus as STL files. The deformed shape of the stent, obtained at the end of the simulation procedure, comes from the ODB file which is imported at the last step of the simulation analysis.
- The Abaqus model now consist of two part: extracted stent and simulated one. In the modulus 'Assembly' an instance is translated and rotated to match the other one.
- The parts resulted by the submission of the job, have reached the desired overlapped position. At this step the extraction of the STL files of both stents is done.

- In the VMTK open-source collection an algorithm is included to register a surface to a reference surface using the ICP algorithm. The core of the algorithm is to match each vertex in one surface with the closest point on the other surface, then apply the transformation that modifies one surface to best match the other. It has noted that the ICP algorithm works better when the two surfaces are situated next to each other. For this reason the previous step with Abaqus is performed.
  The used VMTK instructions to register a surface to a reference surface are here reported:

```
vmtkicpregistration -ifile Original_TC.stl -ofile Original_translated.vtp
-rfile Stent_simulated.stl --pipe vmtksurfaceviewer
```

  Where the input file is represented by the surface of the stent extracted from the CT images processing procedure and the reference file is the stent obtained at the end of each simulation. Figure 4.3 depicts the registration result.

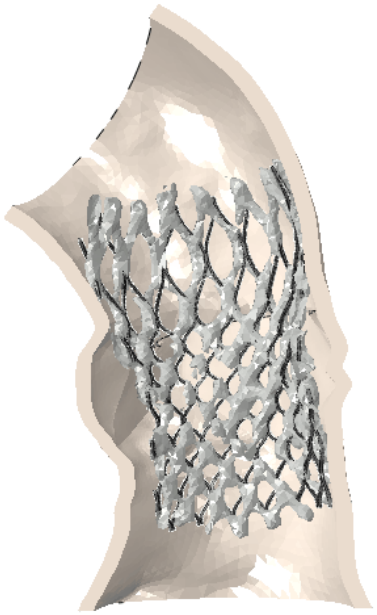

Figure 4.3: Deformed stent frame reconstructed from CT images (white) and deformed stent frame predicted from computer simulation (gray) are overlapped in the best possible way.

Once the best overlapping is obtained different quantitative analyses are performed in order to evaluate the quality of the alignments and, as a consequence, the similarities of the simulated stents to the extracted one.
The following quantities are measured:

- contour overlapping;
- distance map;

- mean distance and mismatching area;
- stent eccentricity.

In the successive paragraphs the analysis processes are explained in detail.

Contours overlapping

The algorithm implemented in Matlab is aimed at computing stents outer contours. The Matlab script works loading the nodes coordinates of both the simulated and the extracted stents. As depicted in the Figure 4.4, they are plotted in a planar configuration (yz plane) with the principal axis positioned horizontally. Figure 4.4a and 4.4b refer, respectively, to the extracted and the simulated frame-stent in the yz plane. After that, curve fitting of lateral contours, for both stents, is determined.

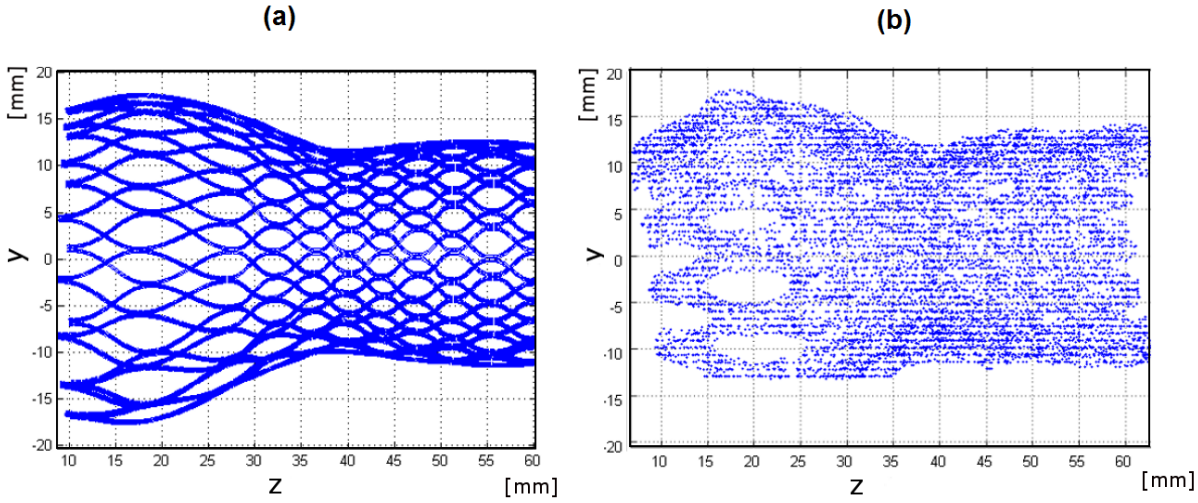

Figure 4.4: Extracted stent (a) and simulated device (b) are shown.

Distance map

To assess the accuracy of the results compared to the reality, the distance (in millimeters) between the corresponding points of the stents surfaces in the two configurations is quantitatively evaluated. The VMTK tool is used as follows:

```
vmtksurfacedistance -ifile Stent_simulated.stl
-rfile Original_translated.vtp -ofile File_dist.vtp
-distancearray DistanceArrayName --pipe vmtksurfaceviewer
```

Here the input file is represented by the stent surface resulting from the simulation process and the reference file refers to the original stent surface that is obtained in the registration step. The DistanceArrayName is the name of the array where the distance of the input surface to the reference surface is stored. Then, the output VTP file is opened with the ParaView software which allows the visualization of three-dimensional geometries showing the contour plot of the relative distance.

Mean distance and mismatching area

Mean distance and mismatching area on cross-sections at three different levels (L1, L2 and L3 as shown in Figure 4.5) are computed.

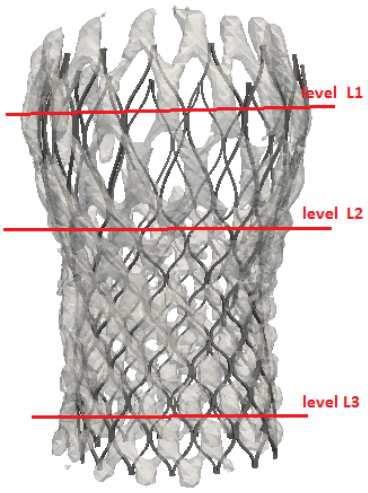

Figure 4.5: Measurements are taken considering three characteristic planes tagged as level L1, level L2 and level L3.

Matlab is used for this purpose: first a centerline of the stent structure is built. The construction of the centerline started with the selection of five points both in xz and in yz planes, manually picked in the middle of the stent. The centerline is then obtained by interpolating points with spline functions. The three planes associated to the transversal section are identified and the stent nodes lying in that planes are selected. An ellipse is then used to fit the obtained nodes. Afterwards, for each of the three levels the mean distance between the ellipse corresponding to the simulated stent and that related to the extracted one is calculated.
The algorithm implemented in Matlab allows also the calculation of the mismatching area (see Figure 4.6) to quantify the degree of misalignment between the two overlapped ellipses. Starting from the ellipses expressed in the parametric form, logical operators are used to get the union and the intersection areas of the polygons. At the end the mismatching area is computed by subtracting the intersection area from the union area.

Stent eccentricity

The native morphology of the aortic root and, in particular, the amount and position of calcifications may induce a non-circular shape to the implanted device. Stent eccentricity is measured to get an indication of the deformation affecting the stent after implantation. Also in this case, the same characteristic planes previously located are taken into account. The aim of this analysis is to assess if, for each of the three selected ellipses, there are no significant differences between eccentricities of the simulated stents and the extracted one.

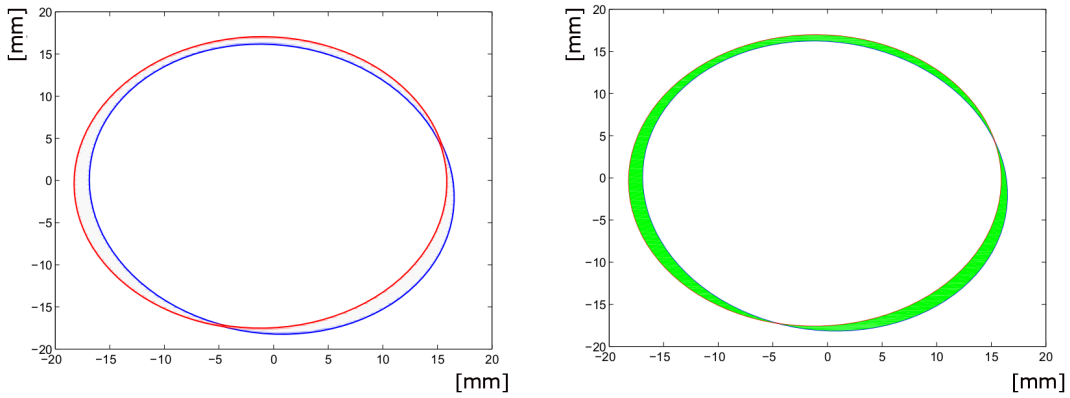

Figure 4.6: Plot of overlapped ellipses from simulated stent (blue) and extracted device (red). The figure on the right highlights the mismatching area.

4.2.3 Intra-operative imaging

As mentioned in Chapter 2, intraoperative angiography is the reference imaging technique for guiding TAVI procedure. Device positioning during TAVI has to be performed with respect to the native valve plane and, only the intra-operative images, combined with physician's ability, allow achieving the proper position.
Some technical data that characterize the angiographic examination are reported in Table 4.1.

Angiography machine	Toshiba
Hospital	ICSA, Milano
Format images	DICOM 512x512
Pixel spacing	[0.48/0.48]
Positioner primary angle	[2.0]
Positioner secondary angle	[0]

Table 4.1: Technical data of the angiographic examination.

Positioner primary and secondary angle describe the position of the image intensifier with respect to the supine patient. All these details refer to the case under consideration.
Information about the real implantation, such as depth of implantation and tilt angle of the device relative to the root axis, can be acquired analyzing the intra-operative angiographic images performed during the intervention. Synedra View Personal 3.4 is employed for this purpose. First of all, among all DICOM images only those with the crimped device are selected. Between all these available images showing the crimped device, the most recent is chosen because it is expected to be the final position achieved before the deployment starts.
As shown in Figure 4.7, by using the edit tool of Synedra the following measurements are extracted:

- **Depth of implantation** representing the distance of the distal margin of the stent from the aortic annulus. As displayed in Figure 4.7a the value 4.7 mm is obtained.

- **Tilt angle of the device relative to the root axis** (φ in Figure 4.7b) is calculated starting from the angle θ formed by the longitudinal axis of the device and the straight line joining the aortic annulus, resulting in 86.8 degrees. The complementary angle, φ=3.2 degrees, represents the tilt angle.

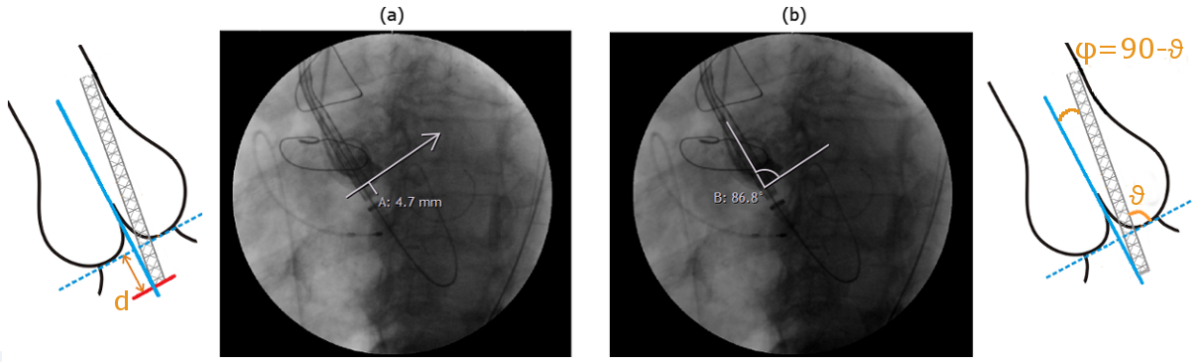

Figure 4.7: Extraction of information about the real delivery position. (a) and (b) show the measurements performed in an angiographic frame, using the Synedra tool.

4.3 Quantitative Results

4.3.1 Contours overlapping

Starting from the nodes of both the extracted and the simulated stents, lateral contours are extracted. The results are obtained through the implementation of a simple Matlab code. In Figure 4.8a the centerlines and lateral contours for the five different configurations are plotted. The analysis resulted in T1 configuration being the most similar to the real stent. Lateral contours and the manually selecting points, of the T1 configuration versus the extracted geometry, are depicted in Figure 4.8b.

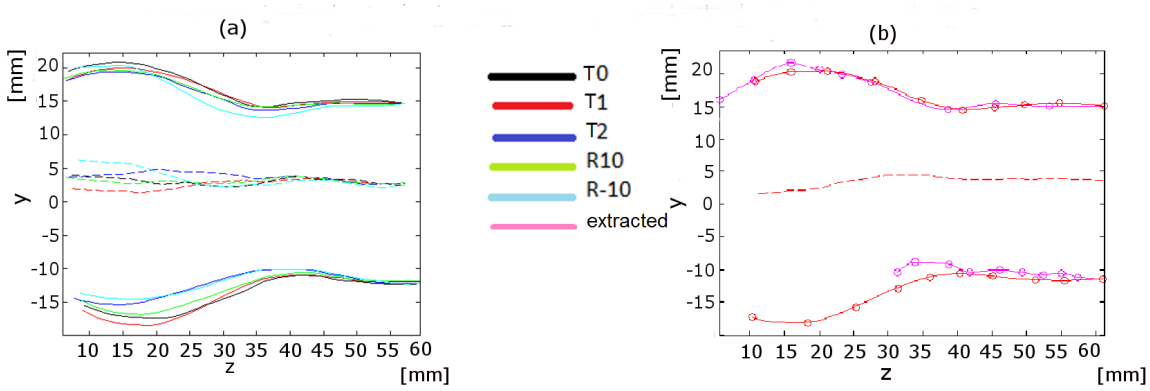

Figure 4.8: Overlapped contours are obtained. In the picture (a) all lateral contours and centerlines for the simulated stents are reported. On the right (b) results concerning T1 configuration are shown.

4.3.2 Distance map

In Figure 4.9 distribution of the point-wise distance into the simulated stents in comparison to the implanted device is shown: colors change, from blue to red, according to the relative distance.
In some cases the extraction of the entire surface of the device from post-operative CT is extremely hard to obtain. This is what occurred while working on this thesis work. Thus, only a partial extraction of the surface of the stent from post-operative CT has been performed by means of a segmentation operation. Hence, black-colored areas in the simulated stent are related to the corresponding missing zones of the implanted one. The Data Range is adjusted by setting the Minimum value to 0.0 and the Maximum value to 3.0 [mm]. The values between the minimum and maximum are then linearly interpolated into the color table. As shown in the Figure 4.9, higher values are obtained for the stent in R-10 configuration (worst case) while a greater degree of similarity is achieved by the T1 configuration (best case). The best configuration is highlighted by a green box while a red box surrounds the worst case.

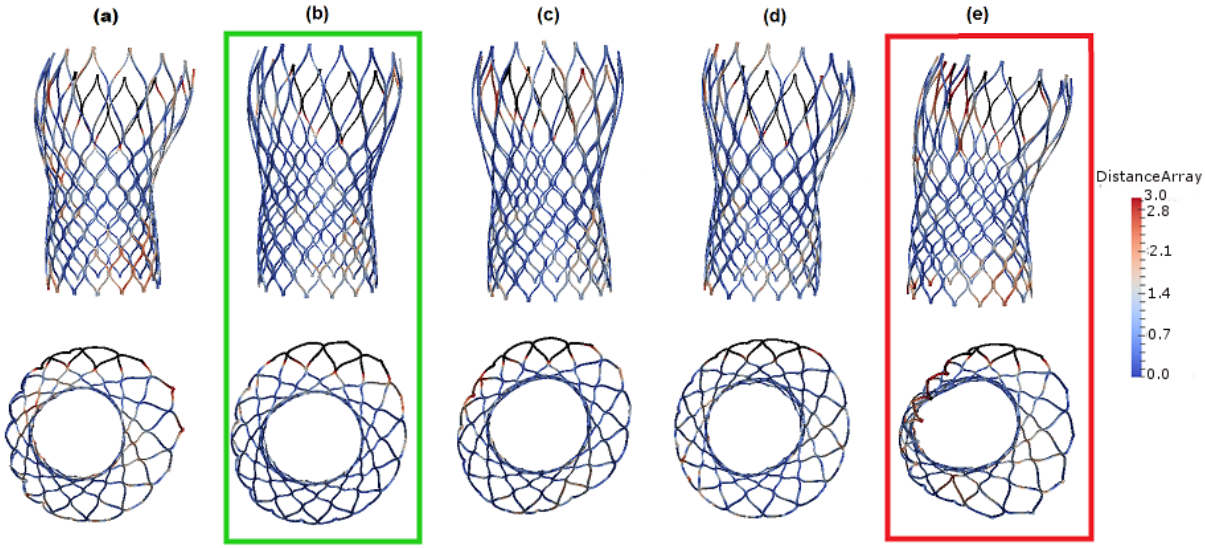

Figure 4.9: Distance map for all configurations is represented: a) T0; b) T1; c) T2; d) R10 and e) R-10. Distance between corresponding points increase from blue to the red zones. For each one of them top view and frontal view are displayed. Best configuration was highlighted by the green box, worst configuration by the red one.

4.3.3 Mean distance and mismatching area

As reported in Table 4.2, mean distance and mismatching area for all configurations are calculated. Results suggest that best configuration, both in terms of mean distance and mismatching area, is T1. Worst numerical outcomes derive from the configuration R-10. Best and worst cases are labeled, respectively, green and red.

Mean distance and mismatching area (in mm)

Apposition	Mean Distance				Mismatching Area			
	L1	L2	L3	mean	L1	L2	L3	mean
T0	0,61	1,45	1,165	1,075	65,65	106,77	99,55	90,66
T1	0,90	0,78	1,0	0.89	70,54	60,16	60,60	63.77
T2	1,28	1,082	1,0	1,12	177,06	50,01	69,73	98,93
R10	0,67	1,12	1,23	1,01	71,81	96,63	62,16	76,87
R-10	1,43	1,29	1,78	1,5	142,32	100,82	68,44	103,93

Table 4.2: Mean distance and mismatching area. Green line and red line refer, respectively, to the best and the worst case.

4.3.4 Stent eccentricity

Eccentricities of the ellipses for each of the three characteristic planes (L1, L2 and L3) are measured. This procedure is done for each implant configuration. Comparing the results between the simulated and the extracted stent, the eccentricities, with respect to L1, L2 and L3, between the implant configuration previously referred as T1 and the extracted one are the most similar. Results referring to the best case are reported in Figure 4.10.

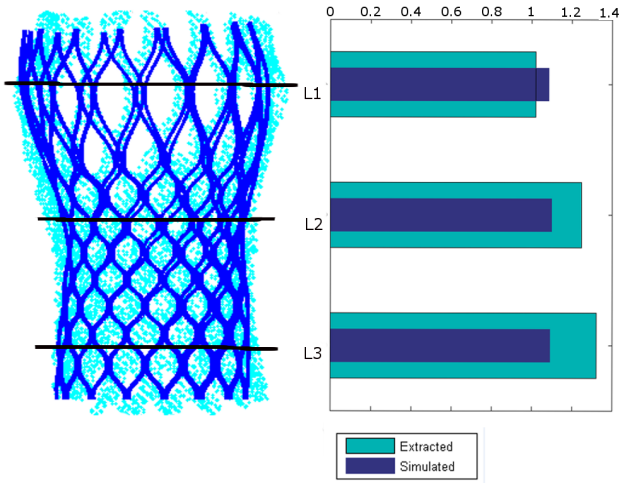

Figure 4.10: Bar plot showing differences between eccentricities. These results are performed considering T1 configuration.

4.4 Discussion

The validation consists in the evaluation of the outcome of the simulated procedure for a patient which has already undergone TAVI, comparing the expanded configuration within the aortic root of the real-implanted stent with that gained through the simulation.
Different stent deployment heights and implantation angles lead to different stent geometries

due to AV calcifications. In this study, the focus is on the impact of five different implantation sites. From the obtained numerical results it is assesses that the shape of the stent more fitting to the implanted device is that obtained by simulating prosthesis positioning in the intermediate configuration (known as T1) within the aortic root.
Intra-operative angiographic images used to performe TAVI are employed as support for the validation of the computer-based simulation of TAVI procedure. By measuring the position achieved from the device during the real procedure it is tested that the T1 configuration is very similar in terms of depth of implantation and tilt angle of the device relative to the root axis. Therefore, by implanting the simulated stent approximately in the same position achieved during the real procedure, the deformed configuration reached by the stent after the simulation procedure follows that of the device extracted from post-operative CT.
To the best of our knowledge, this is the first time a computational framework is validated using the proposed "blind-approach".

Chapter 5

Sensitivity analysis: mesh size and material model

Quantitative characterization of the aortic root structure and of the material properties are the foundation for finite element analysis methods to simulate TAVI procedures. The reliability of the results obtained through finite elements modeling can depend on the accuracy of the characterization and translation of these parameters into the model. Important parameters include aortic root tissue material properties and mesh refinement.

5.1 Mesh size analysis

The FEA works with a discretized model and, in the discretization process a continuum mathematical model is split into finite elements and continuous geometry is replaced by discrete nodes and elements. This process of discretization inevitably introduces errors in the mathematical model. The goal of a finite element simulation is to control and minimize the difference, i.e. the error, between the exact solution and the approximate one and to ensure that the error stays below some tolerance level that can vary depending on the analysis goal. Using the FEA method it is important to know that the accuracy of the solution is linked to the mesh size. As the mesh size decreases towards zero, the exact solution for the equations under study is going to be found. The main question when performing finite element simulations is how the results of the FEA vary according to the mesh size. In other terms, a mesh needs to be refined and the results to be examined in terms of their sensitivity to the refinement. The final aim is to generate meshes of adequate quality and, at the same time, to reach a balance between accuracy and computational time. Therefore, the use of patient specific simulations in the clinical practice involves the problem of computational time and model accuracy. The complexity and the accuracy of the model should not induce an impractical, long duration of computation in order to meet the clinical needs.
In this dissertation, for the mesh convergence study, mesh refinement on the aortic root is performed: three different meshes are used. The mesh sensitivity analysis is performed by considering the effects of the elements size on the Von-Mises Stress of the aortic root and on the deformed configuration reached by the stent after the simulation deployment.
For these purposes, starting from the mesh size used to perform all the previous analyses, a less refined mesh and a more refined one are considered. As showed in Table 5.1, the approximate

global size adopted to discretize the aortic root changes from 2 *mm* to 3.9 *mm* and 1.2 *mm* for the coarser and the finer mesh, respectively. Obviously, in the first case the mesh elements result increased in size (and decreased in number) while in the latter they result smaller (and increased in number).

Mesh refinement: approximate global size			
	Coarse Mesh	Original Mesh	Refined Mesh
Approximate size [mm]	2	3.9	1.2

Table 5.1: Approximate global sizes adopted to discretize the aortic root in the three different cases.

More in detail, taking into account the finer mesh the number of the aortic root elements is increased from 76559 to 200101. For the coarser mesh, it is decreased to 32232. In all cases, the number of the elements belonging to the leaflets is the same. The parameters of the mesh refinement related to the aortic valve are listed in Table 5.2. It is important to note that the mesh seeding in the junctions between root and leaflets needs to be the same in order to merge the two parts. It is assumed that the calcific blocks do not change the number of elements.

Mesh refinement: elements			
	Coarse Mesh	Original Mesh	Refined Mesh
Aortic root elements	32232	76559	200101
Leaflets elements	7700	7700	7700

Table 5.2: Number of elements for the different meshes are here reported.

With regard to the notation used in Chapter 4, the simulations are carried out with the undeployed stent positioned in the T1 configuration (i.e. 5 *mm* under the aortic annulus), which is resulted in being the real position of implantation. By following the procedure explained in Chapter 3, the predefined field, i.e. the tensional state of the crimped stent frame, is imported, the finite element model completed and the analyses submitted. In Table 5.3 the computational time for each of the three analyses is reported. After that, Von-Mises Stress related to the aortic root and the final shape that the deformed stent gains can be analyzed.

5.1.1 Final configuration of the deployed stent

The purpose of this section is to analyze if, by refining the mesh, the shape of the deformed stent undergoes significant changes.
For the sake of simplicity, in the following, the stent related to the coarse analysis is referred to as stent n°1, whereas the ones coming from the original and the refined analysis are labeled as n°2 and n°3, respectively. Using VMTK software and ICP algorithm embedded within it,

Mesh refinement: computational time			
	Coarse Mesh	Original Mesh	Refined Mesh
Time [hh:mm]	60:51	84:18	120:11

Table 5.3: Computation time for the three different analyses.

the registration between stents surfaces is performed. Once obtained the best overlapping, the software ParaView is used to assess qualitative and quantitative differences between stents (for more details see the procedure already explained in the Paragraph 4.2.2). Figure 5.1a gives a first qualitative representation. The three stents are superimposed and different colors are used to represent each of them: red for stent n°1, grey for stent n°2 and blue for n°3. Taking stent n°2 as reference surface, in Figure 5.1b-c the distribution of the point-wise distance of stents n°1 and n°3 from n°2 is reported. Colors are used to assess surfaces relative distances. For the Data Range, the Minimum value is set to 0.0 and the Maximum value to 1.0 [mm] for both the comparisons. The values between the minimum and maximum are mapped into the color bar with linear interpolation. The three planes associated with

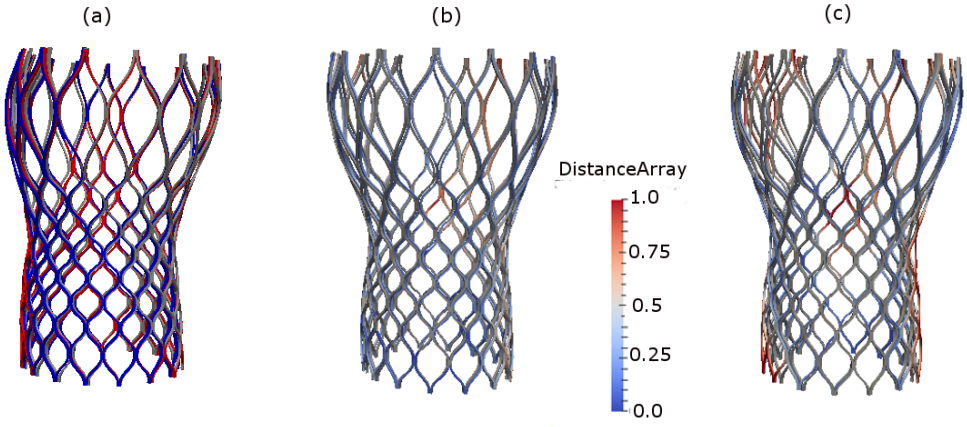

Figure 5.1: (a) Qualitative superimposition of the three stents. In (b) and (c) the contour plot of the relative distance is shown. The image on the center refers to the stent n°1 while the right image is relative to the stent n°3. In both these images the stent in gray is the stent n°2.

transversal sections, tagged as level L1, level L2 and level L3, are identified. For each of these characteristics planes the eccentricity is measured. This procedure is performed for each stent to assess whether, for each of the three levels, significant differences are found or not. In addition, a plot of the overlapped ellipses from stent n°1, stent n°2 and stent n°3 is computed. This procedure gives information about the degree of misalignment of the overlapped ellipses.

In Figure 5.2 all the data are plotted.

5.1.2 Von-Mises Stress on the aortic root

In this section the Von-Mises Stress of the aortic root, at the end of the analysis and in deformed configuration, is analyzed.
Element-based field output variables are written to the output database at the integration points. This means that extrapolation of the integration point stresses takes place within each element. The tensional state is investigated either from the qualitative and quantitative point of view. From a qualitative point of view, the contour plot indicating the stress distribution over the aortic root wall is evaluated. In Figure 5.3 contour plots of the Von-Mises stress for the three different models are shown. This picture is referred to the last frame of the expansion step. The values are calculated in MPa and the same color scale is used for all the three images.
Then, for each model, a text file, containing the Von-Mises Stress values that are computed during the analysis, is created. Matlab is used to calculate, for each of the three final configurations, the average of the Von-Mises stress of the elements. To avoid the results being affected by isolated peaks of the elements stress values, the average $\overline{\sigma}$ is calculated considering the lowest 95 % of the elements values. The obtained results are: $\overline{\sigma}_1$=47 kPa, $\overline{\sigma}_2$=42.5 kPa and $\overline{\sigma}_3$=36 kPa for models n°1, n°2 and n°3, respectively. The resulted mean stresses are then plotted against the number of elements. In Figure 5.4, the number of elements is reported on the X axis and the mean stresses on the Y axis. The number of elements are normalized by the value of the maximum number of elements (i.e. the elements of the finer mesh). The stress values are reported in kPa units.

5.1.3 Discussion of the obtained results

In this section a sensitivity study to explore the potentiality of how different mesh sizes affect the simulation outcomes is conducted.
Results of the analysis of mesh convergence allow to validate the original mesh size used for the all the previous simulations since it offers a good compromise between accuracy requirements on the one hand and computational time on the other hand.
It can be found that the mesh refinement has a larger effect on the stress distribution rather than on the overall deformation of the stent. More specifically, since the obtained values for the mean Von-Mises stress are $\overline{\sigma}$=47 kPa, $\overline{\sigma}$=42,5 and $\overline{\sigma}$=36 kPa for the coarser, the original and the the more refined model, an increase of 23% is observed between the coarse model and the refined one. While the differences in stress between the original and the finest mesh are roughly 9%. No significant differences in stent eccentricities are detected. Therefore, if the main goal of the research is the sole evaluation of the stent deployed shape, also a coarser mesh can be used; otherwise the original mesh size has to be used. The use of a coarser mesh implies a reduction of analysis computational time. The more refined mesh is not strictly necessary for the sake of the topic under study.

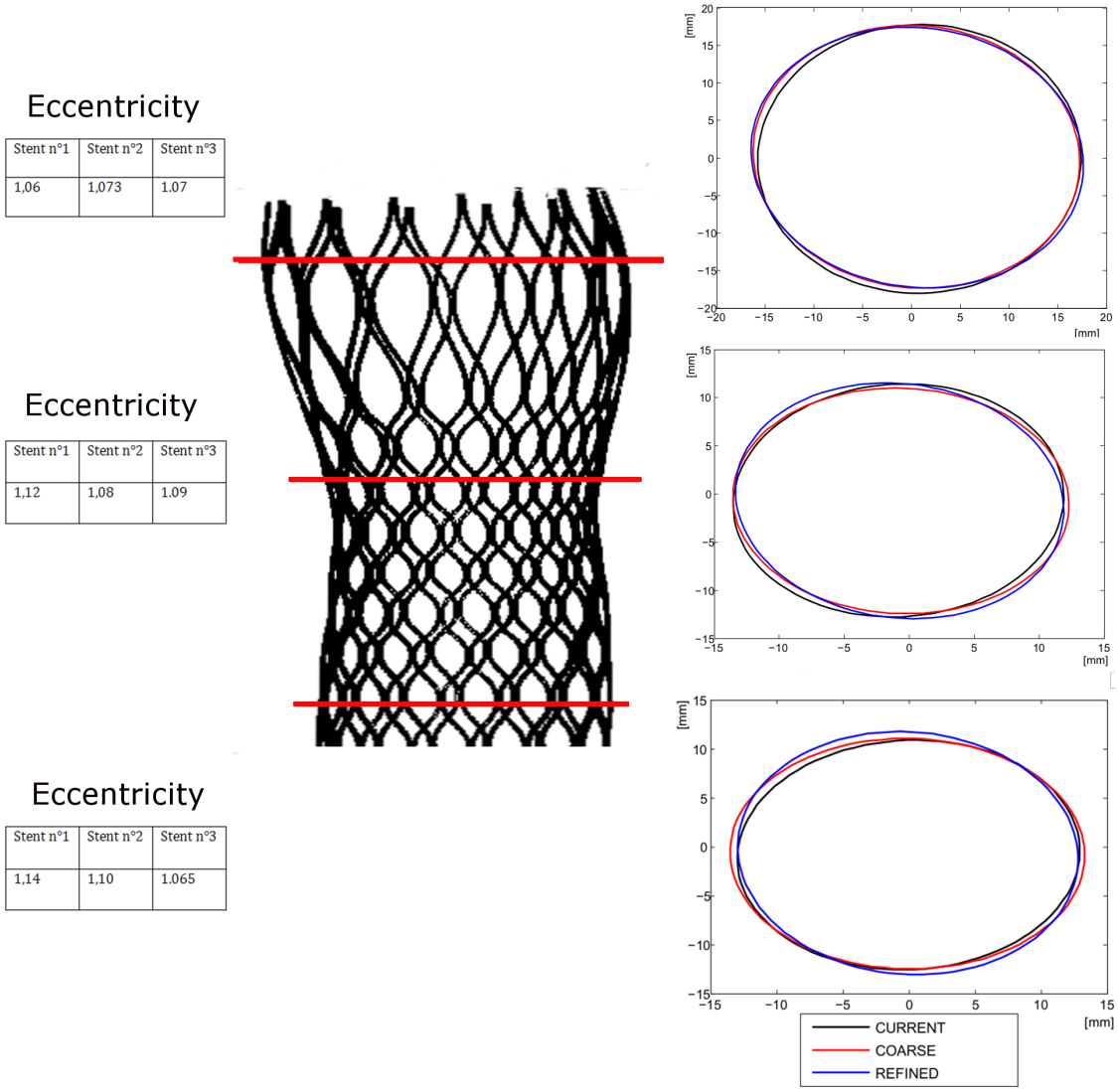

Figure 5.2: L1, L2 and L3 are the characteristic levels. On the right site the plot of the overlapped ellipses is presented: red, black and blue are used for stent n°1, stent n°2 and stent n°3, respectively. For each ellipse the eccentricity is determined (left side).

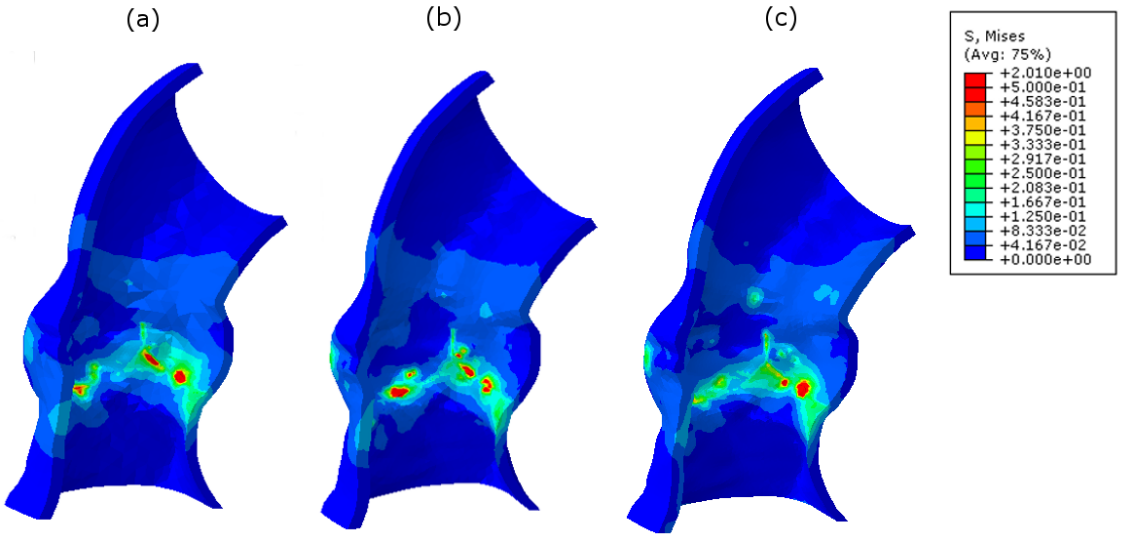

Figure 5.3: The analysis results show the Von-Mises Stress distribution on the aortic root. Figure (a), (b) and (c) refers, respectively, to the coarse, the original and the refined mesh.

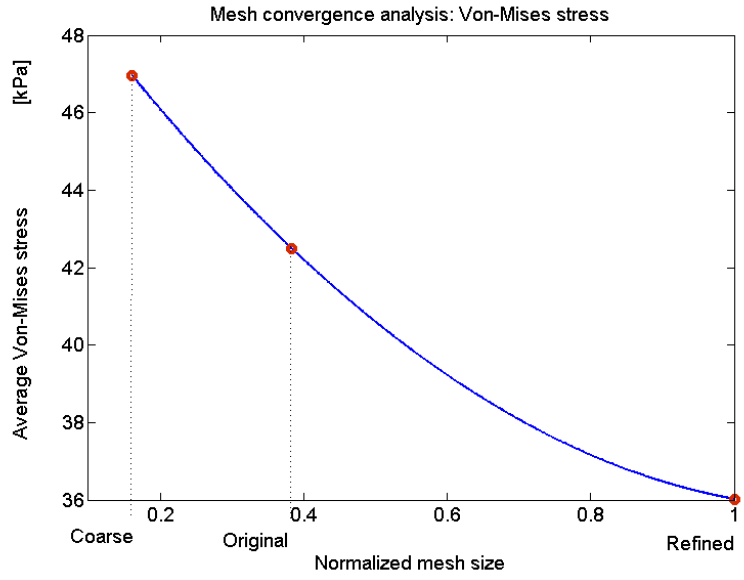

Figure 5.4: Mises Von-Mises Stress plotted against the number of mesh elements.

5.2 Aortic root material model

When reviewing the sensitivity of the analysis, an important issue refers to the variation of the material properties. In this case the attention is paid on the the aortic root constitutive model.
A great number of studies agree that constitutive models based on the theory of nonlinear hyperelasticity are required for biological soft tissues in TAVI simulation. For example, Capelli et al. [2012] and Gunning et al. [2014] base their formulation on a Mooney-Rivlin constitutive model while Russ et al. [2013] compares the simulation outcome testing rigid, linear-elastic and hyper-elastic isotropic materials. In this dissertation, the analyses previously performed are based on a elastic isotropic material law. The purpose of this section is to propose an analysis based on a hyperelastic material model for the soft tissue of the aortic root and to assess if simulation outcomes may be relate to the material properties.
A hyperelastic material is still an elastic material but the difference to linear elastic material is that in hyperelasticity the stress-strain relationship derives from a strain energy density function and not from a constant factor. So, the description of the strain energy density is more complex compared to linear elastic material, where the stress is just a linear function of strain. In Figure 5.5 the stress-strain curves for both elastic and non-elastic material model are reported. The deformation of hyperelastic materials remains elastic up to large strain values. Several hyperelastic strain energy potentials such as the polynomial model, including particular cases (the reduced polynomial, neo-Hookean, Mooney-Rivlin, and Yeoh forms), the Ogden form, the Arruda-Boyce form, the Van der Waals form and the Marlow form are available.

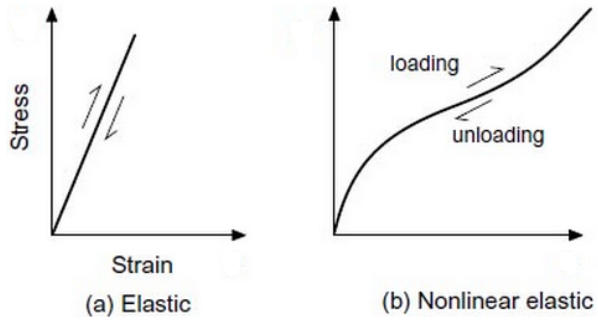

Figure 5.5: Stress-strain curves for the linear elastic model (a) and non-linear elastic model.

The strain energy potential function for the reduced polynomial model is:

$$U = \sum_{i=1}^{N} C_{i0}(\overline{I}_1 - 3)^i + \sum_{i=1}^{N} \frac{1}{D_i}(J^{el} - 1)^{2i} \tag{5.1}$$

where U is the strain energy potential, which defines the strain energy stored in the material per unit of reference volume as a function of the strain at that point in the material. C_{i0}, D_i are material parameters and N determines the order of the strain energy potential. J^{el} is the elastic volume ratio and $\overline{I}_1$ is the first invariant of the deviatoric strain. This quantity is

defined as:

$$\overline{I}_1 = \overline{\lambda}_1^2 + \overline{\lambda}_2^2 + \overline{\lambda}_3^2 \tag{5.2}$$

with λ_i the deviatoric stretches:

$$\overline{\lambda}_i = J^{-1/3}\lambda_i \tag{5.3}$$

Here J is the total volume ratio and λ_i the principal stretches. The initial shear modulus and bulk modulus are given by:

$$\mu_0 = 2C_{i0}, \qquad K_0 = \frac{2}{D_1} \tag{5.4}$$

The material is assumed to be incompressible and the D_i values, that determine the compressibility of the material, are set to zero. Abaqus/Explicit does not allow to assume that the material is fully incompressible because the program has no mechanism for imposing such a constraint at each material calculation point. If, as in this case, no value is given for the material compressibility in the hyperelastic model, by default Abaqus/Explicit assumes values corrisponding to a Poisson's ratio of 0.475. After choosing a six-order strain energy potential function, the identification of constitutive parameters is performed according to [Morganti et al., 2014]. An homogeneous mechanical behavior is assumed for the whole aortic root. In Table 5.4 the adopted parameters are reported. Since in this study the focus is on the aortic

Material constants for the aortic root [kPa]

C_{10}	C_{20}	C_{30}	C_{40}	C_{50}	C_{60}
21.3601	591.752	1925.0067	1012.0336	669.1259	603.9645

Table 5.4: Material constants relative to the aortic root are here reported. A six-order function is chosen to fit experimental data. The values are calculated in *kPa*.

root behavior, a simplified material model for the aortic leaflets is used. The same elastic linear isotropic material previously used is adopted.

5.2.1 Performed tests

Two different approaches are adopted to reproduce the material behavior of the aortic root:

- linear-elastic (LE) isotropic material;
- reduced polynomial hyperelastic (HE) isotropic material (see Equation 5.1).

The simulation is carried out starting from the T1 configuration. The model taken as reference model refers to the T1 configuration with the aortic root exhibiting a linear elastic behavior. Accordingly to Section 3.2.6, analysis results shall allow the investigation of the deformation of the self-expanding stent and the Von-Mises stress on the aortic root. The latter is related to the stent-calcifications-aortic valve interaction.
Taking into consideration the final shape of the stent, the two stents, coming from the output files, are superimposed and the contour plot of the relative distance is computed by using the software ParaView. In the following, the stent coming from the Model with a LE aortic root material model is called stent O while that referring to the HE aortic root material model is

named as stent H. In Figure 5.6 the distribution of the pointwise distance into the stent H in comparison to the stent O is graphically shown. The values between the minimum (0 mm) and maximum (2.48 mm) are linearly interpolated into the color table.
Figure 5.7 refers to the differences in eccentricities between the stent of the original model and this new one. Also in this case the three characteristics planes L1, L2 and L3 are considered.

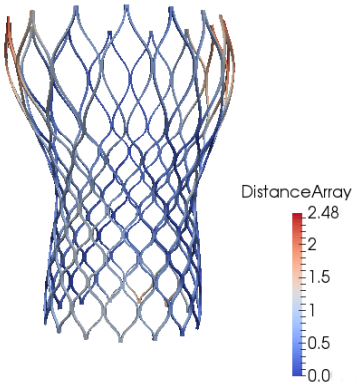

Figure 5.6: The contour plot of the relative distance into the stent H in comparison to the stent O is shown.

In Figure 5.8 Von-Mises Stress distribution on aortic root after the CoreValve stent deployment is displayed. The same color scale is used for both the configurations. It is possible to observe that the adopted HE material model produces reduced stress values on the aortic root with respect to the LE material model. Matlab is used to calculate the average of the lowest 95 % of the Von-Mises stress of the elements both for the aortic root characterized by hyperelastic properties. Comparing the average Von-Mises stress values for both the considered model, the following values are obtained: $\overline{\sigma}_{LE}$=42.5 kPa (LE aortic root) and $\overline{\sigma}_{HE}$= 13.2 kPa (HE aortic root).

5.2.2 Discussion of the obtained results

The use of different constitutive models can affect the simulation outcomes. As reported in literature, the use of hyper-elastic material models can improve simulation accuracy [Russ et al., 2013].
Considerating Figures 5.6 and 5.7, it is worthwhile to note that there are no significant differences between the two stents with exception to the upper extremity. This result is surely related to the material laws employed. In the central part of the stent, where the solid calcific blocks are located, the shape is quite identical because the plaques strongly influence the final shape of the deployed stent. Instead, in the case under consideration, no relevant calcifications are observed in close proximity to the sinotubular junction and the expansion of the stent is solely related to the aortic root material behavior. It is possible to assume that, when the amount of calcification is relevant and located at the height of the aortic annulus, also a simplified material model can be adopted. Indeed, the TAV leaflets are mounted on the central part of the device and is the degree of expansion and circularity is this zone to determine

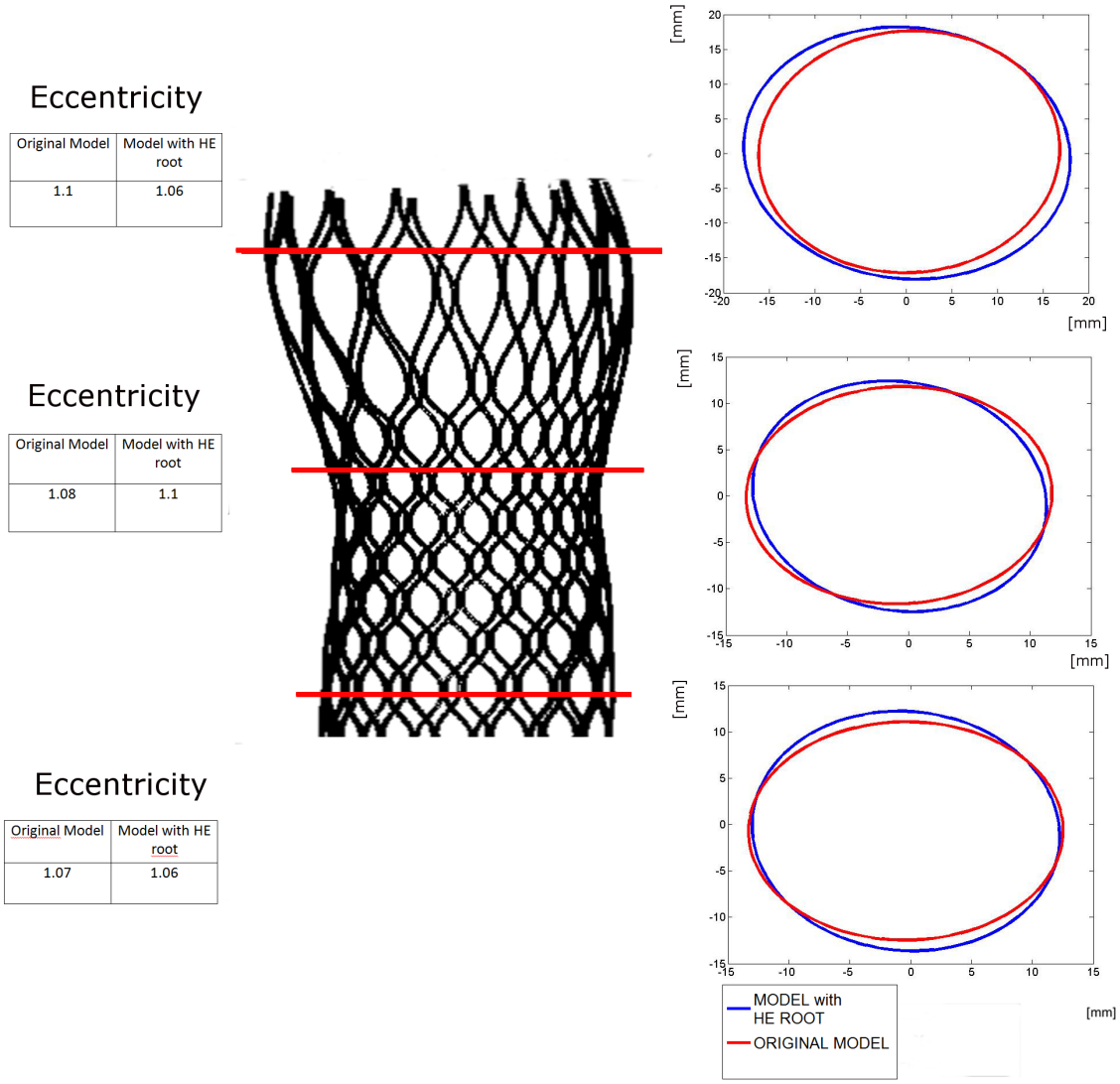

Figure 5.7: L1, L2 and L3 are the characteristic levels. On the right site the plot of the overlapped ellipses is presented: red and blue are used for the stent O and the stent H, respectively. For each ellipse the eccentricity is determined (left side).

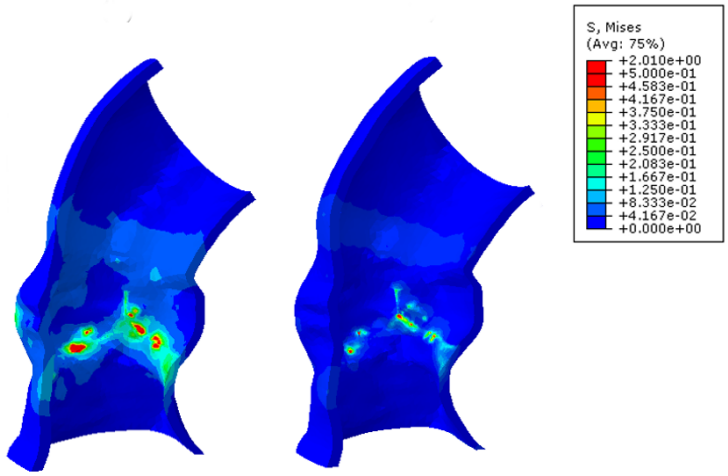

Figure 5.8: The analysis results show the Von-Mises Stress distribution on the aortic root. Figure on the left refers to the original Model where LE material model is employed. On the right side the aortic root characterized by the HE material model is depicted.

the overall performance of the implanted device. On the other hand, when the patient under exam shows only a moderate stenosis or the blocks are disposed on the ascending part of the aortic root, a more accurate constitutive model needs to be taken into account. Concerning the Von-Mises stress on the aortic wall, the obtained results (see Figure 5.8) accord to the literature. Actually, the material constitutive law tells how the strain is related to the stress. It can be easily deducted that, different material models for the aortic root lead to different values of the Von-Mises stress. However, it should be pointed out that, independently of the quantitative results, the distribution of the higher stress values is the same in both models. A qualitative insight of the higher stress concentration regions can be obtained also with a simplified model.

Chapter 6

Conclusions and future perspectives

In the last years TAVI emerged as a valuable alternative to classical surgery for severe AS, especially for old and high-risk patients. Given the growing cohort of aging patients with degenerative valvular disease, this novel treatment is increasingly executed. It requires a meticulous preparation, which is heavily dependent on accurate and high quality imaging techniques. Inaccurate pre-operative assessment can severely impair the success of the procedure [Clayton et al., 2014]. In this scenario, advanced computational models could play a crucial role for precise planning and outcomes assessment and may significantly improve percutaneous valve implantation techniques.
This thesis work is developed from a specific clinical case, referred to the TAVI procedure. Starting from clinical examinations, a set of variables that could provide information about the final configuration of the implanted stent in relation to the patient specific geometry are investigated.
After processing of CT pre-operative data, the simulation of the deployment of the CoreValve bioprosthesis was performed. Calcifications are supposed to have a crucial importance on the stent expansion. Thus, they were treated as solid mesh elements and attached to the valve leaflets. Leaflets and calcifications were properly constrained in order to move together during the valve opening. Results of the analyses indicate that the inclusion of leaflets and calcium deposits into the aortic valve model is important, because they heavily affect the post-operative configuration of the device and, as a consequence, the performance of the implanted valve. After that, different implantation sites are considered. The post-implantation 3D geometry of the physical model, imaged with a CT-scan, was then compared to the deformed configuration predicted by the virtual models and best-configuration was assessed. Afterward, results from the computational model are validated by measuring the position achieved from the device during the real procedure.
Moreover, a sensitivity study was conducted to assess the impact of the mesh size with respect to the capability of the mesh generation to capture the stent deployed final shape and predict aortic wall stresses. Three different simulations with three different aortic root meshes were performed. Mesh convergence analysis indicates that the mesh used for all the simulations represents a good balance between computation time and accuracy. If the main goal of the research is to solely evaluate the stent deployed shape in relation to the anatomical geometry, also a coarser mesh could be used; otherwise the original mesh size has to be used. The use of a coarser mesh implies a reduction of analysis computational time. An additional study was conducted on the constitutive model to realistically represent the aortic wall soft tissue: the

previously adopted linear elastic material model was compared with an hyperelastic material model.
With the present study, a step forward in the direction of creating a computational tool capable of supporting TAVI pre-operative surgical planning has been done. In this study, in effect, the validity of the proposed simulation strategy to predict post-operative implant geometry using pre-, post- and intra-operative data is demonstrated.
As a conclusion, it is possible to say that finite element analysis can be a valid method to investigate several aspects of stenting procedures. Although limited to only one patient, this study represents a further step towards the use of realistic computer-based simulations for virtual planning of TAVI procedures. Such an approach can pave the way to safer and more effective procedures tailored to the patient-specific characteristics. This is particularly important as more patients may be eligible for TAVI procedure in the future.

6.1 Limitations

The major limitation of this study is the inclusion of only a single patient. This drawback is related to the small number of patients who can underwent post-operative CT. In fact, CT imaging is associated with the administration of iodinated contrast which can cause problems to the patients affected by renal impairment.
Even though our data for the use of the developed computational models to reproduce TAVI are encouraging, this small sample still means that computational simulations will not be used routinely in clinical practice. Moreover, there is the need to test the proposed validation framework on a greater number of patients who underwent TAVI, with different stent models, for more conclusive results.
Although the diastolic pressure characterizing the reconstructed geometry has to be taken into account, in the present model, the inclusion of a prestress state on the aortic wall is still neglected. Other limitation of the work regards the material properties of the aortic valve. Native tissues are anisotropic but, at present, this property is not included in the proposed model.

6.2 Future developments

The engineering analysis could provide additional information to help clinicians evaluate complicated cases and choose the best treatment possible.
This work could be a starting point for future research in several directions. First of all, simulation and validation of the proposed FE computational approach from a larger patient group, using additional stent models, are required to obtain more conclusive results. The inclusion of prosthetic leaflets and the evaluation of the paravalvular area could be also investigated. In fact, measurements of coaptation area could indicate whether the simulated surgical intervention fails or not.
Preliminary tests were conducted regarding the following topics:

- During simulation step, the common approach is to assume that the initial input geometry of the model is in a stress-free state. But, when in vivo imaging is applied the

resulting images and therefore reconstructed 3D geometries represent a configuration under in vivo load such as, e.g. blood pressure. Therefore, the geometry of the patient based on this anatomy should not be taken as a stress-free reference configuration. For this reason, the aim is to introduce aortic root wall prestress that was not considered in the original modeling framework. In most cases [Gee et al., 2009, Lu et al., 2007], papers implementing this strategy based their analyses on the Inverse Design (ID) method, that aims at solving the inverse elastostatic problem. Some FE studies [Gee et al., 2009, Grytz and Downs, 2013] suggested the use of the Modified Updated Lagrangian Formulation (MULF) method that is based on a multiplicative split of the deformation gradient in order to produce a displacement-free prestressed/prestrained state.
With the present work an approach to circumvent difficulties by prescribing a state of prestress to the arterial tissue is proposed. In fact, Matlab is used to compute a percentage of reduction of aortic root diameter to translate the reference configuration into a pressure-free configuration. The simulation procedure involves a loading step (to gain the pressurized state of the aortic wall) as well as a deployment step and is still under development.

- An important area of improvement is which material model better describes the aortic root tissue. Literature refers that an isotropic, linear elastic or hyperelastic material model is not entirely reflective of the anisotropic and hyperelastic nature of valve tissues. The works of Auricchio et al. [2012] and Wang et al. [2012] represent the first TAVI simulations that use the Holzapfel-Gasser-Odgen (HGO) anisotropic and hyperelastic model [Holzapfel and Gasser, 2001, Gasser et al., 2006]. Also in the studies of Nolan et al. [2014] and Wang et al. [2015] the HGO model was adopted to characterize the mechanical behavior of the human heart and arterial tissues.
  In this dissertation, the aortic root is divided into sets of elements and local coordinate systems are defined for each of these sets to define fiber orientations. In this way, fibers can be included in the original model. Abaqus does not allow to import any initial state field from a previous analysis whenever anisotropy is involved in the model. Therefore, a two-step simulation has to be conducted: firstly, the device has to be crimped, then the deployment phase can be performed.
  No numerical results involving the aforementioned anisotropic material model are presented in this thesis work, since its complete implementation and testing in the context of TAVI simulations is still a work in progress.

A further extremely relevant perspective for the future is the translation of this computational framework into the clinical practice.

Bibliography

F. Auricchio and R.L. Taylor. Shape-memory alloys: modelling and numerical simulations of the finite-strain superelastic behavior. *Computer Methods in Applied Mechanics and Engineering*, 1997.

F. Auricchio, M. Conti, S. Morganti, and A. Reali. Simulation of transcatheter aortic valve implantation: a patient-specific finite element approach. *Computer Methods in Biomechanics and Biomedical Engineering*, 2012.

J.J. Bax, V. Delgado, V. Bapat, H. Baumgartner, J.P. Collet, and R. Erbel. Open issues in transcatheter aortic valve implantation. part 1: patient selection and treatment strategy for transcatheter aortic valve implantation. *European Heart Journal*, 2014.

M.M. Black, I.C. Howard, X. Huang, and E.A. Patterson. A three-dimensional analysis of a bioprosthetic heart valve. *J Biomech.*, 1990.

C. Capelli, A.M. Taylor, F. Migliavacca, P. Bonhoeffer, and S. Schievano. Patient-specific reconstructed anatomies and computer simulations are fundamental for selecting medical device treatment: application to a new percutaneous pulmonary valve. *Philos Transact A Math Phys Eng Sci.*, 2010.

C. Capelli, G.M. Bosi, E. Cerri, J. Nordmeyer, T. Odenwald, P. Bonhoeffer, F. Migliavacca, A.M. Taylor, and S. Schievano. Patient-specific simulations of transcatheter aortic valve stent implantation. *Med Biol Eng Comput.*, 2012.

P. T. L. Chiam and C.E. Ruiz. Percutaneous transcatheter aortic valve implantation: Evolution of the technology. *American Heart Journal, vol. 157, no. 2, pp. 229-42*, 2009.

B. Clayton, G. Morgan-Hughes, and C. Roobottom. Transcatheter aortic valve insertion (tavi): a review. *The British Journal of Radiology*, 2014.

R.W. Clough. Original formulation of the finite element method. *Elsevier Science Publishers B.V*, 1990.

H. Cribier, A.and Eltchaninoff, A. Bash, N. Borenstein, C. Tron, F. Bauer, G. Derumeaux, F. Anselme, F. Laborde, and M.B. Leon. Percutaneous transcatheter implantation of an aortic valve prosthesis for calcific aortic stenosis: first human case description. *Circulation*, 2002.

H.A. Dwyer, P.B. Matthews, A. Azadani, N. Jaussaud, L. Ge, T.S. Guy, and E.E. Tseng. Computational fluid dynamics simulation of transcatheter aortic valve degeneration. *Interact Cardiovasc Thorac Surg.*, 2009.

T.C. Gasser, R.W. Ogden, and G.A. Holzapfel. Hyperelastic modelling of arterial layers with distributed collagen fibre orientations. *Journal of the royal society interface*, 2006.

M.W. Gee, C. Reeps, H.H. Eckstein, and W.A. Wall. Prestressing in finite deformation abdominal aortic aneurysm simulation. *J Biomech.*, 2009.

M. Gessat, R. Hopf, T. Pollok, and C. Russ. Image-based mechanical analysis of stent deformation: Concept and exemplary implementation for aortic valve stents. *Biomedical Engineering IEEE*, 2013.

P.L. Gould, A. Cataloglu, and R.E. Clark. Mathematical modelling of human aortic valve leaflets. *Appl. Math. Modelling*, 1976.

K.J. Grande, Cochran R.P., Reinhall P.G., and Kunzelman K.S. Stress variations in the human aortic root and valve: The role of anatomic asymmetry. *Annals of Biomedical Engineering*, 1998.

S. Grbic, T. Mansi, R. Ionasec, I. Voigt, H. Houle, M. John, M. Schoebinger, N. Navab, and Comaniciu D. Image-based computational models for tavi planning: From ct images to implant deployment. *Springer-Verlag*, 2013.

R. Grytz and J.C. Downs. A forward incremental prestressing method with application to inverse parameter estimations and eye-specific simulations of posterior scleral shells. *Comput Methods Biomech Biomed Engin.*, 2013.

P.S. Gunning, T.J. Vaughan, and L.M. McNamara. Simulation of self expanding transcatheter aortic valve in a realistic aortic root: Implications of deployment geometry on leaflet deformation. *Annals of Biomedical Engineering*, 2014.

G.A. Holzapfel and T.C. Gasser. A viscoelastic model for fiber-reinforced composites at finite strains: continuum basis, computational aspects and applications. *Comput. Meth. Appl. Mech. Eng*, 2001.

X. Huang, M.M. Black, I.C. Howard, and E.A. Patterson. A two-dimensional finite element analysis of a bioprosthetic heart valve. *J Biomech.*, 1990.

B. Iung, A. Cachier, G. Baron, D. Messika-Zeitoun, F. Delahaye, P. Tornos, C. Gohlke-Barwolf, E. Boersma, P. Ravaud, and A. Vahanian. Decision-making in elderly patients with severe aortic stenosis: why are so many denied surgery? *Eur Heart J.*, 2005.

D. John, L. Buellesfeld, S. Yuecel, R. Mueller, G. Latsios, H. Beucher, U. Gerckens, and E. Grube. Correlation of device landing zone calcification and acute procedural success in patients undergoing transcatheter aortic valve implantations with the self-expanding corevalve prosthesis. *JACC Cardiovasc Interv.*, 2010.

S.V. Lichtenstein, A. Cheung, J. Ye, C.R. Thompson, R.G. Carere, S. Pasupati, and J.G. Webb. Transapical transcatheter aortic valve implantation in humans - initial clinical experience. *Interventional Cardiology*, 2006.

H.M. Loree, A.J. Grodzinsky, S.Y. Park, L.J. Gibson, and R.T. Lee. Static circumferential tangential modulus of human atherosclerotic tissue. *J Biomech.*, 1994.

J. Lu, X. Zhou, and M.L. Raghavan. Inverse elastostatic stress analysis in pre-deformed biological structures: Demonstration using abdominal aortic aneurysms. *J Biomech.*, 2007.

G. Marom, R. Haj-Ali, E. Raanani, H.J. Schafers, and M. Rosenfeld. A fluid-structure interaction model of the aortic valve with coaptation and compliant aortic root. *Med. Biol. Eng. Comput.*, 2012.

M. S. Martis. Validation of simulation based models: A theoretical outlook. *The Electronic Journal of Business Research Methods*, 2006.

S. Morganti, M. Conti, M. Aiello, A. Valentini, A. Mazzola, A. Reali, and F. Auricchio. Simulation of transcatheter aortic valve implantation through patient-specific finite element analysis: Two clinical cases. *Journal of Biomechanics*, 2014.

K. Nieman, O. Gaemperli, P. Lancellotti, and S. Plein. *Advanced Cardiac Imaging: Techniques and Applications.* 2015.

V.T. Nkomo, J.M. Gardin, T.N. Skelton, J.S. Gottdiener, C.G. Scott, and M. Enriquez-Sarano. Burden of valvular heart diseases: a population-based study. *Lancet*, 2006.

D.R. Nolan, A.L. Gower, M. Destrade, R.W. Ogden, and McGarry J.P. A robust anisotropic hyperelastic formulation for the modelling of soft tissue. *J Mech Behav Biomed Mater.*, 2014.

J. Ozkan. European perspectives in cardiology. *Circulation*, 2013.

C. Russ, R. Hopf, S. Hirsch, S. Sundermann, V. Falk, G. Szekely, and M. Gessat. Simulation of transcatheter aortic valve implantation under consideration of leaflet calcification. *IEEE Eng Med Biol Soc.*, 2013.

C. Russ, R. Hopf, S.H. Sundermann, S. Born, S. Hirsch, V. Falk, G. Szekely, and M. Gessat. Computational stent placement in transcatheter aortic valve implantation. *Springer International Publishing*, 2014.

S. Schievano, A.M. Taylor, C. Capelli, P. Lurz, J. Nordmeyer, F. Migliavacca, and Bonhoeffer P. Patient specific finite element analysis results in more accurate prediction of stent fractures: application to percutaneous pulmonary valve implantation. *J Biomech.*, 2010.

C. Schultz, P. Mortier, and G. De Santis. Towards simulation-based pre-operative planning of transcatheter aortic valve replacement. *Journal of the American College of Cardiology*, 2012.

F. Sturla, E. Votta, M. Stevanella, C.A. Conti, and A. Redaelli. Impact of modeling fluid-structure interaction in the computational analysis of aortic root biomechanics. *Med. Eng. Phys.*, 2013.

W. Sun, K. Li, and E. Sirois. Simulated elliptical bioprosthetic valve deformation: Implications for asymmetric transcatheter valve deployment. *Journal of Biomechanics*, 2010.

W. Sun, C. Martin, and T. Pham. Computational modeling of cardiac valve function and intervention. *Annu. Rev. Biomed.*, 2014.

F. P. P. Tan, Xu X.Y., R. Torii, N. B. Wood, N. Delahunty, M. Mullen, N. Moat, and R. Mohiaddin. Comparison of aortic flow patterns before and after transcatheter aortic valve implantation. *Cardiovascular Engineering and Technology*, 2011.

A. Vahanian, O. Alfieri, F. Andreotti, M.J. Antunes, G. Baron-Esquivias, H. Baumgartner, M. Borger, T.P. Carrel, M. De Bonis, A. Evangelista, V. Falk, B. Iung, P. Lancellotti, L. Pierard, S. Price, H.J. Shafers, G. Schuler, J. Stepinska, K. Swedberg, J. Takkenberg, U.O. Von Oppell, S. Windecker, J.L. Zamorano, and M. Zempala. Guidelines on the management of valvular heart disease. *European Heart Journal*, 2012.

T. Walther, T. Dewey, M.A. Borger, J. Kempfert, A. Linke, R Becht, V. Falk, G. Schuler, Mohr F.W., and M. Mack. Transapical aortic valve implantation: Step by step. *Ann Thorac Surg*, 2009.

Q. Wang, E. Sirois, and W. Sun. Patient-specific modeling of biomechanical interaction in transcatheter aortic valve deployment. *J Biomech*, 2012.

Q. Wang, S. Kodali, C. Primiano, and W. Sun. Simulations of transcatheter aortic valve implantation: implications for aortic root rupture. *Biomechanics and Modeling in Mechanobiology*, 2015.